UNIVERSITY OF CALIFORNIA,
IRVINE

How do warming temperatures and disease affect abalone? Examining digestive physiology and withering syndrome in *Haliotis*

DISSERTATION

submitted in partial satisfaction of the requirements
for the degree of

DOCTOR OF PHILOSOPHY

in Ecology and Evolutionary Biology

by

Alyssa Rita Frederick (Braciszewski)

Dissertation Committee:
Professor Donovan P. German, Chair
Professor Cascade Sorte
Professor Timothy Bradley

2019

DEDICATION

To my child, Augustine Lewis Braciszewski,
may we see the oceans heal in your lifetime.

To all the people dedicating their life's work
to conserving and preserving our planet.

To my beloved snails, for their ultimate sacrifices for this work.

TABLE OF CONTENTS

LIST OF FIGURES

LIST OF TABLES

ACKNOWLEDGMENTS

The work presented here was conducted primarily on the occupied and unceded land of the Tongva and Acjachemen Nations. Animals were collected from the occupied and unceded land of the Pomo Nation and from Aotearoa's coastal seas. I have benefitted and continue to benefit from access to this land and its resources, and the denial of these Nations from their traditional territories.

Many thanks to my advisor, Dr. Donovan P. German, for his guidance over the last six years. Donovan provided me with exceptional guidance during this PhD journey. He gave me the confidence to explore areas of research in which I had no experience or preexisting knowledge, providing just the right amount of independence for me to build confidence in my abilities as a researcher while growing towards end goals. He has been a trusting, kind, and encouraging mentor who helped me grow as a scientist and in my capacity to create accepting environments for all researchers who come after me. I was able to bring my whole self to my work, and I thank him or his advising and work.

The other members of the German Lab have served as mentors during my dissertation work. Dr. Joseph Heras and Michelle Herrera helped me learn bioinformatics and data analysis. I am especially thankful to Dr. Beck A. Wehrle who served as an advisor, mentor, chocolate provider, and team leader in my absence. I also thank Dr. Andres Carrillo for sharing his time and expertise in everything related to animal care and maintenance – this work could not have been done without that help. A stellar team of undergraduates helped with experiments, sample analysis and animal care including Caitlyn Catabay, Ariana Min Lee, A. Harits Abdurrohman, Priscilla San Juan, Austin Gonzales, Calahan Dineen, Daniel Rankins, Emily Vuu, Helen On, Jordon Stone, Jose Daniel Bastian Salgado, Maggie Van, Michael Pimentel, Myguel Angelo M. Del Mundo, Alex Luu, David Perez, Lauren Strope, Quang Nguyen-Phuc, Nandeye Quintero, Avneet Kaur, and Cai Kunheng. A special thanks to the first two, who independently ran experiments or analyses. A special thanks to colleagues Laura Elsberry and Evelyn Valdez-Ward, who all provided emotional support and inspiration. With the additional of Louise Sider, I appreciate the help of these three in watching my dogs so I could do field work.

Thank you to my collaborators, including Dr. Douglas Eernisse, Dr. Carolyn Friedman, Dr. Kendall Clements. Doug was instrumental in learning more about invertebrate anatomy, physiology, and phylogenetics. Carolyn provided experimental samples and advice for Chapter 2, and Kendall advised on experimental design and data collection for Chapter 3. Other tissue samples were provided by Dr. Jim Moore, Dr. John Hyde, Bruce Marshall from Te Papa, and Nancy Caruso (Get Inspired1). I'd also like to thank the entire Victoria University Coastal Ecology Laboratory at the Victoria University of Wellington, for providing me space to conduct experiments and collecting animals and algae for this work. This includes Dr. Jeff Shima, John Ven der Sman, Daniel McNaughtan, and Dan Crossett. A special thanks to the abalone fishers, especially Ashley Peterson and Dr. Ben Perlman, who provided tissue samples from their red abalone harvests. Thank you to Doug Bush at The Cultured Abalone Farm for your support of this work by providing animals for experiments. I appreciate the willingness of Dr. Norman Ragg to discuss abalone/pāua physiology, and for bringing me to Cawthron for a visit. Thank you to Charles L. Powell II for supplying information on the fossil distribution of abalone.

I thank my committee members, Drs. Cascade Sorte and Tim Bradley, for their extensive feedback in improving my experiments, data collection, and presentation. I also thank my advancement committee, with the additions of Drs. Katrine Whiteson and J. J. Emerson, for providing their diverse inputs into these studies.

Thank you to the mentors that have supported me in my pursuit of applying my scientific knowledge to management, policy, and activism. These mentors include Dr. Audrey D. Thévenon (National Academy of Science), Dr. Melissa Neuman (NOAA), Susan Wang (NOAA), and Dr. Stephen Allison (UCI).

Thank you to Patrick and Augustine Braciszewski, and to Dolce and Rocco, the best support team anyone could ask for.

Samples from both *Haliotis fulgens* individuals were collected under permit SC-4786, MAB-95 broodstock collecting permit, and commercial fishing license 1028617285. Other tissue samples were sub-sampled from museum specimens or the abalone tissue archive at CDFW Shellfish Health Lab. *Haliotis sorenseni* samples were archived under the authority of federal ESA (Endangered Species Act) permit #14344, and specific permission was granted to use tissue and extracted DNA for this research. My tuition and stipend were supported by the National Science Foundation Graduate Research Fellowship under Grant No. DGE-1321846. Any opinion, findings, and conclusions or recommendations expressed in this material are those of the authors(s) and do not necessarily reflect the views of the National Science Foundation. This work was also funded by: the American Malacological Society Melbourne R. Carriker Student Research Award, the Society for Integrative and Comparative Biology Grant in Aid of Research, UCI OCEANS Graduate Student Fellowship, Southern California Academy of Sciences Research Grant, and Conchologists of America Academic Grant, UCI Undergraduate Research Opportunity Program grants, UCI's Newkirk Center for Science and Society Graduate Research Fellowship, National Geographic Young Explorers Grant, Western Society of Malacologists Research Grant, Sea and Sage Audubon Society Bloom-Hays Research Grant, and the UCI Microbiome Pilot Project Award. I'd also like to acknowledge the following scholarship funders: UCI Public Impact, Grover C. Stephens Memorial Fellowship, and ARCS.

CURRICULUM VITAE

Alyssa R. Frederick (Braciszewski)

EDUCATION

2019 Ph.D., Ecology and Evolutionary Biology, School of Biological Sciences, University of California, Irvine, CA
Advisor: Dr. Donovan P. German

2018 M.S. Ecology and Evolutionary Biology, School of Biological Sciences, University of California, Irvine, CA
Advisor: Dr. Donovan P. German

2013 Fulbright Fellow, Victoria University of Wellington, New Zealand
Advisor: Dr. Simon Davy

2012 B.S. Marine Biology, American University, Washington, D.C.
Advisor: Dr. Kiho Kim

RESEARCH INTERESTS

- Human impacts on coastal ecosystems and resources
- Climate change impacts on fishery species biology and physiology
- Interface of society, environmental change, and policy
- Integrating multiple knowledge systems and science fields into robust models
- Communicating complex scientific data with diverse audiences and stakeholders

PUBLICATIONS

(2) Santos, A.*****, **A.R. Frederick***, B. Higgins, A. Carrillo, A. Carter, K.M. Dickson, D.P. German, and M.H. Horn. (2018) Egg cannibalism in fishes: the beach-spawning *Leuresthes tenuis* eats and digests its own eggs. *Journal of Fish Biology* 93: 282-289.
*****These authors contributed equally to this work.

(1) MacAvoy, S.E., **A. Braciszewski**, E. Tengi, and D.W. Fong. (2016) Trophic plasticity among spring versus cave populations of *Gammarus minus:* examining functional niches using stable isotopes and C/N ratios. *Ecological Research* 31: 589.

FELLOWSHIPS AND HONORS

2019 *Christine Mirzayan Science and Technology Policy Fellow,* National Academies of

Science, Engineering, and Medicine (Washington, D.C.)

2018 *UCI Public Impact Fellowship*, University of California, Irvine

2018 *Grover C. Stephens Memorial Fellowship Award*, University of California, Irvine

2017 *Student Journalism Internship,* Society for Integrative and Comparative Biology

2016 *Achievement Rewards for College Scientists (ARCS) Foundation Scholarship*, ARCS Orange County

2015-16 *Climate Action Training Program*, University of California, Irvine

2014-18 *Graduate Research Fellowship*, National Science Foundation

2014 *National Defense Science and Engineering Graduate Fellowship*, U.S. Dept. of Defense (Offered but declined for NSF GRF)

2014 *Graduate Recruitment Fellowship*, University of California, Irvine (The name of this fellowship has been modified here since the School Biological Sciences changed its name.)

2013 *Fulbright Scholarship*, Fulbright New Zealand

2013 *Victoria Fulbright Master's Scholarship*, Victoria University of Wellington, New Zealand

2013 *Kathleen Stewart Postgraduate Award*, Victoria University of Wellington, New Zealand

2008–12 *Presidential (tuition) Scholarship*, University Honors Program, American University

RESEARCH FUNDING

2017 *Microbiome Pilot Project Award*, University of California, Irvine

2017 *Bloom-Hays Research Grant,* Sea and Sage Audubon Society

2017 *Research Grant,* Western Society of Malacologists

2017 *Young Explorers Grant*, National Geographic

2016 *Graduate Student Fellowship*, Newkirk Center for Science and Society, University of California, Irvine

2016 *Academic Grant*, Conchologists of America

2016 *Research Grant*, Southern California Academy of Sciences

2016 *UCI OCEANS Graduate Student Fellowship*, University of California, Irvine

2016 *Grant-in-Aid of Research*, Society for Integrative and Comparative Biology

2015 *Melbourne R. Carriker Student Research Award*, American Malacological Society

2011 *Scholars & Artists Research Fellowship*, American University, Washington, D.C.

2011 *Dean's Undergraduate Research Award*, American University, Washington, D.C.

PROFESSIONAL EXPERIENCE

2019 Postdoctoral Researcher, Bodega Marine Lab, University of California, Davis

2019 Christine Mirzayan Science and Technology Policy Fellow*,* National Academies of Science, Engineering, and Medicine, Washington, D.C.

2019 Teaching Assistant: Foundation for Physiology and Exercise Sciences, University of California, Irvine

2016 Graduate Research Intern, NOAA National Marine Fisheries Service, Long Beach

2014-5 Teaching Assistant: Human Physiology Laboratory, University of California, Irvine
2015 Teaching Assistant: From Organisms to Ecosystems Discussion, University of California, Irvine
2014 Teaching Assistant: Genetics Discussion, University of California, Irvine
2013 Teaching Assistant: Introductory Marine Biology, Victoria University of Wellington, New Zealand

PROFESSIONAL SERVICE & OUTREACH

2017-18 Associate Editor, Journal of Science Policy and Governance
2017-18 Associated Graduate Students Council Member, University of California, Irvine
2017-18 Abalone Outreach, Crystal Cove State Park
2014-18 Targeted Instruction Generating Excitement about Research and Science (TIGERS)
2017 UC Student Lobbying Converence and Lobby Day, Sacramento, CA
2016-17 Graduate Representative, Ecology and Evolution Department, University of California, Irvine
2014-16 Events Coordinator, Orange County Society for Conservation Biology, Irvine, CA
2014-15 Crystal Cove German Lab Outreach
2013-18 Remutaka Forest Trust volunteer
2010-12 Student Representative, Sustainability Project Team, American University, Washington, D.C.
2015- Peer Review: Comparative Biochemistry and Physiology - B Biochemistry; Hydrobiologia

PUBLIC SCIENCE COMMUNICATION

(2017-present) "Turn of the Tide" Podcast Creator/Director and Co-Host.
Frederick, A. (2019) "Bat wing muscles specialize for different temperature ranges." Authored press release for *SICB*.
Frederick, A., and S. Mana`oakamai Johnson. (2018) "Climate Change Is Strengthening Typhoons, Hurricanes and Cyclones. The US Isn't Paying Attention." Union of Concerned Scientists Blog.
Frederick, A. (2018) "New immunotherapy technique can specifically target tumor cells, UCI study reports." Authored press release for *UCI News*.
Frederick, A. (2018) "Augmenting Reality to Make Science More Inclusive" *Society for Integrative and Comparative Biology Student Journalism*.
Cat, L.A., A. Frederick, M. Herrera, E. Valdez-Ward (2018) "Diverse ecosystems require diverse ecologists" Rapid Ecology.
Interviewed in: Kuo, M. (2018) "Celebrating women in science" *Science* Careers.
Frederick, A.R. (2017) "From abalone to advocacy." Working Life piece in *Science* 357: 6349. (
Interviewed in: Kuo, M. (2017) "What to know before starting our Ph.D. program" *Science* Careers.
Frederick, A., A. Oetmen, R. Delaney, J. Goldberg (2011) "Repopulating Pinta." Production team for film for Galapagos Conservancy.

INVITED PRESENTATIONS

"Women in Science Alumni Panel" (2019) American University, Women in Science club panel on careers in science.

"There and Back Again: Turning Field Failures into Successes" (2018) Western Society of Naturalists, annual meeting opening plenary panelist. Tacoma, WA, USA.

"From Abalone to Advocacy: Science to support climate change resiliency, community engagement, and coastal management" (2018) Invited seminar, Cawthron Institute**,** Nelson, New Zealand.

"Hydrothermal Vents" (2017) Physiology of Extreme Environments, Course E155 course, guest lecture, University of California, Irvine.

"Contacting your elected officials; expert panel on D.C. climate policy" (2017) Climate Solutions course guest lecture, UC Irvine.

"Abalone decline through the ages: Overfishing, climate change, and disease, oh my!" (2017) Brews and Brains at UC Irvine.

Panel discussion on science and policy. (2017) AGS Student Policy Symposium. Irvine, CA.

CONTRIBUTED ABSTRACTS

Frederick, A.R., C. Catabay, K. D. Clements, B. A. Wehrle, and D. P. German. (2019) "Will abalone survive climate change? Comparative digestive physiology and the effect of temperature stress on abalone across the Pacific Ocean" Society for Integrative and Comparative Biology, Tampa, FL. [oral]

Frederick, A.R., M. Neuman, S. Wang, and D. P. German. (2018) "A Snail's Pace: Can policy and physiological research protect abalone/pāua from climate change?" Pacific Climate Change Conference, Wellington, New Zealand. [oral]

Frederick, A.R., K. I. Ramin and S. D. Allison. (2018) "Training tomorrow's climate leaders: University of California Irvine's Climate Action Training Program." Pacific Climate Change Conference, Wellington, New Zealand. [oral]

Frederick, A.R., C. S. Freidman and D. P. German. (2018) "Withering-syndrome induced gene expression changes in pinto abalone, *Haliotis kamtschatkana*." Society for Integrative and Comparative Biology, San Francisco, CA. [oral]

Frederick, A.R. and D. P. German. (2017) "Differential disease resistance patterns in eastern Pacific Haliotids." Euromal: 8th European Congress of Malacological Studies. Polish Malacological Society, Kraków, Poland. [oral, Awarded 2nd Best PhD Student Presentation]

Frederick, A.R. (2017) A Snail's Pace: "Can policy save ecosystems in the face of global climate change?" University of California Student Lobbying Conference, Sacramento, CA. [oral]

Braciszewski, A.R., M. Neuman, S. Wang, and D. P. German. (2017) "Climate change and the recovery of Endangered Black Abalone." ARCS Award Symposium, Irvine, CA. [poster]

Braciszewski, A.R. and D. P. German. (2017) "Relatedness and differential disease resistance in Eastern Pacific Haliotids." Society for Integrative and Comparative Biology, New Orleans, LA. [oral]

Braciszewski, A.R. and D. P. German. (2016) "Relatedness and differential disease expression in abalone (genus *Haliotis*)." American Malacological Society and Western Malacological

Society Joint Meeting, Ensenada, Baja California, Mexico. [oral]

Braciszewski, A.R. and D. P. German. (2016) "Relatedness and differential disease resistance in California Haliotids." Southern California Academy of Sciences Meeting, Los Angeles, CA. [poster]

Braciszewski, A.R., A. Carrillo, M.H. Horn, A. Carter, and D.P. German. (2015) "How do you like your eggs? Cannibalism and digestibility in the California grunion, *Leuresthes tenuis* (Teleostei: Atherinopsidae)." Society for Integrative and Comparative Biology, West Palm Beach, FL. [oral]

Braciszewski, A.R., A. Carrillo, M.H. Horn, A. Carter, and D.P. German. (2014) "How do you like your eggs? Cannibalism and digestibility in the California grunion, *Leuresthes tenuis* (Teleostei: Atherinopsidae)." American Physiological Society Intersociety Meeting, San Diego, CA. [poster]

Braciszewski, A.R., A. Carrillo, M.H. Horn, A. Carter, and D.P. German. (2014) "How do you like your eggs? Cannibalism and digestibility in the California grunion, *Leuresthes tenuis* (Teleostei: Atherinopsidae)." Comparative Biology Southwest Organismal Biology Meeting, Irvine, CA. [poster]

Frederick, A.R., and K. Kim. (2012) "Measuring Base Line Health of Mangrove Forests as an Indicator of Nutrient Pollution in Guam Using Stable Nitrogen Isotope Analysis." Benthic Ecology Meeting, Norfolk, VA. [poster]

Frederick, A.R., K. Kim, D.M. Baker, and M.L. Fogel. (2011) "Quantifying Mutualism in Tropical Reef Corals." Carnegie Institution of Washington, Geophysical Laboratory. Washington, D.C. [oral]

Frederick, A.R., K. Kim, D.M. Baker, and M.L. Fogel. (2011) "Quantifying Mutualism in Tropical Reef Corals." American University Honors Symposium & American University Robyn Rafferty Mathias Student Research Conference. Washington, D.C. [oral]

ABSTRACT OF THE DISSERTATION

How do warming temperatures and disease affect abalone?
Examining digestive physiology and withering syndrome in *Haliotis*

By

Alyssa Rita Frederick (Braciszewski)

Doctor of Philosophy in Ecology and Evolutionary Biology

University of California, Irvine, 2019

Professor Donovan P. German, Chair

The physiological underpinnings of many marine host-pathogen systems are poorly understood, and even less is known about how climate change will affect the physiology of these systems. In the abalone and *Rickettsiales*-like organism (RLO) system, the RLO infects abalone digestive tissues and leads to extreme starvation and a characteristic "withering" of the gastropod foot. The withering syndrome-causing RLO (WS-RLO) has led to large declines in most abalone species on the northeastern Pacific coast, but disease resistance levels are species-specific and dependent on environmental temperature.

In order to clarify differential susceptibility in species whose geographic ranges overlap substantially (such as the highly susceptible Black Abalone and relatively resistant Green Abalone), I estimated the phylogenetic relationships of northeastern Pacific *Haliotis* species using concatenated data from two mitochondrial and two nuclear regions. The most susceptible species form a monophyletic grouping apart from the other northeastern Pacific taxa, implying that WS susceptibility could be a derived trait that traces back to the last common ancestor of

this hypothesized clade, and that patterns of WS resistance and susceptibility have a quite deep evolutionary basis.

I then determined differences in gene expression in the digestive gland, the site of infection, in infected and uninfected Pinto Abalone over seven months. Pinto Abalone showed changes in gene expression at seven months post-infection, compared to naïve conspecifics. Differentially expressed gene groups were identified that likely correspond to advanced disease state and to general stress response of being held in captivity.

The third chapter examined the effects of heat stress on metabolic rate, digestibility, and digestive enzyme activities in Red Abalone and Pāua. Metabolic rates were significantly elevated in heat treatment animals. Digestibility did not significantly change, but this may be balanced by changes in transit time and total intake. Digestive enzyme activities changed independently, with amylase remaining the same, maltase increasing, and trypsin decreasing.

In summary, WS susceptibility follows a phylogenetic pattern. Genes associated with immune and hunger are upregulated, but protein transport and reproduction are downregulated in infected Pinto Abalone guts. Heat stress leads to metabolic rate increases, digestibility decreases, and digestive enzyme changes in abalone.

INTRODUCTION

Digestion and nutrient acquisition are the most fundamental ways in which animals interact with their environment. It is therefore surprising (and ironic – gastropod means "stomach-foot") that there is no synthesis of this information for gastropods. In fact, for many invertebrate groups, aside from arthropods, digestion is largely understudied. Yet, digestive processes in invertebrates are impacted by climate change (Stumpp et al. 2013), disease (Crosson et al. 2014), and interaction of the two (Burge et al. 2014). Without a better understanding of the "normal" function of these systems, we cannot hope to predict how the interaction of climate change, disease, and physiological factors interact.

Physiological models and a general gastropod digestive system

The physiology and anatomy of all digestive systems has been likened to three different ideal chemical reactors (Penry and Jumars 1987). Batch reactors are single-opening blind sacs. Plug-flow reactors (PFRs) are tubes that allow passage of a bolus of material generally in a unidirectional manner. Continuous-flow stirred tank reactors (CSTR) act an intermediary between the two, where there is a stop in movement of a bolus, churning, and exit of material (through a different point than the entrance) determined by particle size (Karasov and Douglas 2013).

Gastropod digestive systems include CSTRs (the digestive gland) and PFRs (intestines). Primitive molluscs probably fed on fine particulate matter using a scraping radula (Morton 1979). However, once the food enters the rest of the digestive system, the application of these digestive models becomes difficult. The ancestral state of digestion in these animals is thought to be intracellular based on the characteristics of basal molluscs (Morton 1979), so food particulates must have been small enough to be phagocytized by cells of the digestive tract. A system which

relies primarily on intracellular digestion cannot be classified as a batch reactor or PFR as readily as an extracellular digestion system. Digesta movement was probably achieved by ciliary movement through the gut in these ancient species, and this movement follows the PFR model. However, we cannot apply one model or even one combination of models to all gastropod groups, as modern gastropods feed on a diverse array of foods and have a diversity of digestive strategies to meet this long menu (Morton 1979).

Gastropod digestive tracts

The buccal region houses salivary glands and a scraping radula, which are characteristic of gastropods (Martin et al. 2011). The buccal region is one of the most complex parts of the digestive system in gastropods. It contains a scraping radula, a series of hard plates that scrape food further into the buccal region. Despite the commonality of these features, radular and odontophore form (structure upon which the radula acts inside the buccal cavity) diversity is extremely high. The number of teeth and their strength and shape vary widely across different taxa and diet types. For instance, among Neogastropods, some carnivorous taxa have few sharp teeth for cutting tissue. In other lineages the radula is highly modified into a few harpooning teeth that inject prey with a venom (see below, *Conoidea*) (Morton 1979). Recently, limpet teeth were shown to be stronger than spider silk, the previously held strongest natural substance. The strength of the teeth, made of goethite, even approaches that of manmade materials (e.g., steel), and is thought to be an adaptation for scraping algae off of hard rocks (Barber et al. 2015).

Once ingested, food then enters the esophagus through the buccal region (Martin et al. 2011). The esophagus itself is divided into the three regions, and the cellular types and morphology of each region vary across different molluscan and gastropod groups (Lobo-da-Cunha et al. 2010; Martin et al. 2010; Martin et al. 2011). The posterior end of the esophagus can

store food and is sometimes labelled a crop, but this is not a universal structure, even within closely related groups (Lobo-da-Cunha et al. 2010). The esophagus travels to an organ, collectively called the stomach and/or digestive gland, that aids in digestion of the food, but there is debate about the function and anatomy of this organ. There is usually an acidic stomach with a style, which is a crystalline rod that stores digestive enzymes in the stomach. This is the ancestral state of molluscan digestion, where a protostyle develops and contains amylase to aid in digestion (Morton 1952; Morton 1979). In derived prosobranchs and bivalves, the style is a more advanced crystalline structure (Morton 1979). The style also contains lipases in lamellibranchs (George 1952), yet little is known about the presence of lipases in gastropod styles. Gastropods also possess a somewhat uniquely ciliated stomach. Ridges and valleys within the tract are ciliated, and act as a sorting mechanism as they do in the labial palps of other molluscs such as bivalves. The finer material that can enter the deeper valleys moves into the digestive gland, while the larger indigestible material, or pseudofeces, is moved past the digestive gland and into the intestine before being excreted (Morton 1979).

In some lineages, it is difficult to differentiate the stomach from the esophagus or digestive gland, an organ which contains both secretory and absorptive tissue (Nybakken 1996; Martin et al. 2011). The digestive gland consists of highly branched glandular tissue. Digestion in this region is interestingly intracellular, although some digestion from extracellular enzymes in the esophagus and stomach have already occurred before reaching the digestive gland. The cells of the digestive gland start as crypt cells that are relatively undifferentiated and have a few cilia. As these cells move towards the ridges of the gland, they differentiate into actively absorbing cells that phagocytize material (Morton 1979). After leaving these organs, digesta exits the body through the intestine, where absorption via amoebocytes occurs. In some lineages

of gastropods and related molluscs, amoebocytes are uniquely implicated in transport in the intestinal tract (Morton 1982; Degnan et al. 1995). They have been shown to have intracellular amylase, protease, and lipase activity in bivalves, although their primary function may actually be in waste removal (reviewed in (Morton 1982)). The function of amoebocytes in immune and circulatory systems of molluscs is fairly well-documented (reviewed in (Morton 1982)). There appears to be systematic amoeboid activity in the digestive systems of gastropods and the function and mechanisms of this relationship remain largely understudied.

Vetigastropod digestive anatomy

Vetigastropods are representative of primitive gastropods in their digestive anatomy. The clade comprises keyhole limpets (*Diodora, Fissurella, Megatebennus,* and *Megathura*) and abalone (genus *Haliotis*). The mouth of these organisms contains a radula and a radula sac, with salivary glands and buccal pouches (Nybakken 1996). Digesta enters the esophagus, which can be divided into three regions. The anterior region stretches from the end of the buccal cavity to the esophageal pouches, which define the middle section. The posterior section extends beyond the pouches until the beginning of the crop or stomach. The narrow posterior region contains ridges that can be affected in disease states. The esophagus consists of ciliated columnar cells (Bevelander 1988), which may help the digesta move through the esophagus. Some species contain a crop, which is used to store food before it enters the stomach (Bevelander 1988). The digestive tract then spirals through the digestive gland, a blind sac that houses the primary site of digestion.

The digestive gland contains both secretory and absorptive cells, and movement of food particles is largely attributed to ciliated cells (Bevelander 1988). The movement of food through

the gland and onward into the intestine is poorly understood, but insights from other mollusk groups may be useful for directing future research.

Before reaching the anus, the intestine actually passes through the heart ventricle (Nybakken 1996). This is a remarkable trait of the primitive gastropods, and may be an ancestral trait as it is shared with other mollusk groups, like bivalves (Morton 1982). The function of the intestine passing through cardiac tissue is unclear, but it may create some peristaltic movement, as the digestive tract of gastropods is not muscular in the same way that it is in humans and other vertebrates (Morton 1951).

Abalone guts and withering syndrome

A Rickettsiales-like organism (newly deemed cXc for *candidatus* Xenohaliotis californiensis) is a bacterial parasite that infects abalone digestive tissues, which leads to starvation and a characteristic degradation of the gastropod foot (a disease called withering syndrome, or WS) (Crosson et al. 2014). The infection moves to the digestive gland and results in glycogen reserve depletion and metabolism of muscle tissue, which results in the "withering" symptom. The digestive gland tissue undergoes metaplasia (the functional changing of tissue type) from secretive and absorptive cells to ciliated tubules, disabling the process of digestion in highly infected individuals (Friedman et al. 2000; Friedman et al. 2003; Braid et al. 2005; Crosson et al. 2014). Behavioral and other physiological functions are disrupted by the disease, which leads to decreased feeding and excretion, decreased metabolism, and lower energy availability (Gonzalez et al. 2012). The disease appears to be modulated, in part by temperature, wherein we see abalone exposed to high temperatures generally showing marked increases in infection intensity and disease (Braid et al. 2005; Rogers-Bennett et al. 2010; Moore et al. 2011).

First identified in Black Abalone following an El Niño event (Vanblaricom et al. 1993), the RLO has been found globally in all abalone species examined. Curiously, not all species express WS at environmentally relevant temperatures (Crosson et al. 2014). For instance, WS affected Black Abalone so severely that this disease is listed as a main contributing factor to the federal classification of Black Abalone (*Haliotis cracherodii*) as "Endangered." WS also contributed to the listing of White Abalone (*H. sorenseni*), but historic overfishing and low wild population densities posed a bigger threat to White Abalone. Like these, Red Abalone (*H. rufescens*) is quite susceptible to WS (Moore et al. 2000), whereas Green and Pink Abalone are relatively highly resistant to the disease in the wild (Álvarez Tinajero et al. 2002; Moore et al. 2009). High temperatures can enhance WS in more resistant animals (Garcia-Esquivel et al. 2007).

WS resistance, therefore, varies by species and is dependent on temperature. The ultimate **goal** of this dissertation is to develop a detailed understanding of the abalone digestive system and the potential mechanisms involved in WS disease progression in the *Haliotis* genus, and to determine the physiological effects of temperature on the gut. To do this, I employed genetic, transcriptomic, and comparative physiology methodologies.

To compare WS susceptibility or resistance across species, it is important to consider the evolutionary history of the *Haliotis* taxa. However, fine scale phylogenies do not exist for comparing the California taxa. Most published abalone phylogenies are individual gene trees (Lee and Vacquier 1992; Lee et al. 1995; Lee and Vacquier 1995; Yang et al. 2000; Coleman and Vacquier 2002; Galindo et al. 2002), which may be useful for studying gene evolution and specific selection pressures (a good example being egg-sperm proteins in abalone (Lee and Vacquier 1992; Lee et al. 1995; Yang et al. 2000; Swanson et al. 2001; Galindo et al. 2003;

Aagaard et al. 2010)). However, single gene trees do not necessarily accurately reflect interspecific relationships, as gene trees are subject to complications from gene duplications, horizontal gene transfer, and individual selection pressures and strengths (Page and Charleston 1997). The first chapter of my dissertation aims to delineate differential WS susceptibility across California species, I will use the methodology outlined by Kim, et al (2014) to create a robust phylogeny of the California *Haliotis* taxa using a multiple gene tree with two mitochondrial and two nuclear genetic markers.

In addition to this limited understanding of relatedness among Californian taxa, there is limited information on how the abalone gut functions and responds on the cellular and molecular level to RLO-infection. The WS-RLO was first characterized in 2000, and is identifiable by specific histological changes in the abalone gut, and a unique 16s rDNA sequence of the bacterial taxon (Friedman et al. 2000). Since then, few studies have looked at the physiological response of the abalone digestive system (the site of infection) to the WS-RLO. One study found that infected abalone experienced reduction in growth, food intake, and metabolism (Gonzalez et al. 2012). Another demonstrated body mass decline, foot atrophy, higher mortality, and decreased glycogen stores in the foot muscle and digestive gland (Braid et al. 2005). Metaplasia in gut tissue has also been demonstrated, with infected animals losing functional digestive tissue (Friedman et al. 2003). Apart from these macro-level observations, the critical digestive functional changes that occur during WS-RLO infection, especially during sub-lethal stages of the disease, have not been studied. The second chapter of my thesis fills part of this knowledge gap by examining Pinto Abalone (*H. kamtschatkana*) transcriptomics in control and experimental animals before and during WS-RLO infection.

Even with this transcriptomic-level comparison, our understanding of WS impacts on abalone digestive function is far from complete. Much of this stems from the fact that the fundamental, basic knowledge of how abalone guts function is limited. Enzyme function in abalone guts is poorly studied; often the gut is homogenized as if it is a single organ without compartmentalized function (Bansemer et al. 2016a; Bansemer et al. 2016b), even though there is clear visual evidence for compartmentalization of abalone gut function. Digestive enzyme activity levels, which indicate an animal's ability to digest specific substrates, are often measured at temperatures (e.g., 37°C) irrelevant to any abalone species (Picos-Garcia et al. 2000; Garcia-Carreno et al. 2003; Garcia-Esquivel and Felbeck 2006). Other studies focused on detecting the basic presence or absence of enzymes in abalone guts, and others conducted feeding trials comparing growth and digestibility of artificial feeds (Britz et al. 1996; Knauer et al. 1996; Hernandez-Santoyo et al. 1998; Picos-Garcia et al. 2000; Garcia-Esquivel and Felbeck 2009). However, there are no detailed comparative investigations of gut physiology in abalone (and none at all on wild animals), and as a result, most of the available literature details the efficacy of different commercial feeds on growth in farmed animals. While this may be useful for aquaculture's immediate needs to grow larger animals for human consumption, it does little to improve our understanding of the nutritional physiology of abalone, and particularly what they do in nature.

Beyond the lack of a basic understanding of abalone nutritional physiology, there are no studies detailing the effect of heat stress on individual aspects (specific enzyme function, microbiome shifts, digestive efficiency) of digestive function, which is surprising given the centrality of these processes in digestive tract function in the face of WS. In addition to limited data on function, it is unknown whether abalone digestion can keep pace with the higher

metabolic demands of heat stress. Episodes of unusual heat and El Niño events are occurring with increasing frequency, creating concern for the future of these species. Furthermore, New Zealand's abalone (*Haliotis iris*, known locally by the Māori name pāua,) are smaller at the northern (and warmest) end of their biogeographic range (Dr. Norman Ragg, Cawthron Institute, pers. comm.). As both Red Abalone in California and Pāua are commercially farmed, and there is some evidence that temperature impacts gut function of at least some abalone species (Hooper et al. 2014), the final chapter of my thesis aims to conduct a rigorous comparative digestive physiology study between these two species, using both wild and captive animals, and to determine the effects of temperature on their physiology.

The research topics outlined above constitute the research chapters of my thesis. The first chapter assesses relatedness in the northeastern Pacific *Haliotis* species. In this work, a phylogenetic hypothesis was constructed and WS susceptibility for each species was overlaid on the tree. The second chapter examines gene expression changes in naïve and exposed Pinto Abalone, *H. kamtschatkana*. This chapter used mRNA expression to examine exactly how withering syndrome impacts biological processes in the gut of abalone. Lastly, the third chapter documents the healthy gut function of two abalone species, *H. rufescens* and *H. iris*, and the impact of temperature stress on digestive physiology (metabolism, digestibility, and enzyme function). This work is critical for furthering our understanding of abalone physiology and gut function. It has strong implications for conservation, fisheries, and aquaculture, as these management groups face serious challenges in maintaining the health and persistence of abalone species across the globe in the face of climate change and disease pressures.

Chapter 1

Defining species relationships and disease resistance patterns in northeastern Pacific abalone

INTRODUCTION

Abalone have extremely high cultural value in California and use of their meat and shells dates back thousands of years (Reviewed in (Leighton 2000)). In 2018, California's recreational fisheries for all species were closed for the first time in history, as the recreational red abalone fishery—the last remaining open fishery—was closed when populations declined due to the disappearance of kelp forests (Catton et al. 2016a; CDFW 2019). The decline of the kelp forests in the northeastern Pacific was caused by the combination of a 2011 algal bloom, the 2013 seastar wasting disease that led to the 2014 proliferation of purple sea urchins (a kelp predator and competitor of abalone), and the 2015-2017 El Niño and "warm blob" warming events (Catton et al. 2016b). Historic abalone population declines were attributed to commercial overharvesting, which was prohibited starting in 1997. In the mid-1980s, however, declines for Black Abalone (*Haliotis cracherodii*) were also attributed to a disease called withering syndrome (WS) (Altstatt et al. 1996).

WS resistance or susceptibility varies by species, temperature stress, and the interaction of species and temperature stress. That is, increased temperature can lead to the disease state in all species, but the degree of temperature stress that is needed to lead to the disease state may vary by species. The seven northeastern Pacific abalone species are often infected with a Rickettsiales-like organism (RLO) bacterial parasite that infects their digestive tissues, and leads to starvation and a characteristic degradation of the gastropod foot (i.e., WS) (Crosson et al.

2014). First identified in *Haliotis cracherodii* (Leach, 1814) following an El Niño event (Vanblaricom et al. 1993), the RLO has been found infecting all species in the northeastern Pacific. Curiously, not all species express WS with the same intensity at environmentally relevant temperatures (Crosson et al. 2014). In this chapter, more resistant species are denoted with an (R) and highly susceptible species are denoted with (S), while one species that is understudied denoted with (U) (See Table 1.1). For instance, WS has affected *H. cracherodii* (S) so severely that this disease is listed as the main contributing factor (along with historic overfishing and habitat decline) to the federal classification of *H. cracherodii* (S) as "Endangered" (Altstatt et al. 1996; Butler et al. 2009; Register 2009; Neuman et al. 2010). WS has also contributed to the listing of *Haliotis sorenseni* (S) (Bartsch, 1940) as Endangered, although overfishing was more important in the historic decline of this species (Hobday and Tegner 2000). *H. sorenseni* (S) adults appear to be more susceptible to infection (become affected more easily) and less resistant to fighting off the disease once infected (Boots and Bowers 1999; Crosson et al. 2014). Like *H. cracherodii* (S) and *H. sorenseni* (S), *Haliotis rufescens* (S) (Swainson, 1822) is often affected by WS (Moore et al. 2000; Braid et al. 2005), although the population declines of *H. rufescens* (S) have not been as extreme as those seen in wild populations of *H. cracherodii* (S) and *H. sorenseni* (S). On the other hand, Green Abalone, *Haliotis fulgens* (R) (Philippi, 1845), and Pink Abalone, *Haliotis corrugata* (R) (W. Wood, 1828), are more resistant to WS infection and experience less WS-associated mortality (Álvarez Tinajero et al. 2002; Vilchis et al. 2005; Moore et al. 2009; Crosson et al. 2014). Still, experimentally high temperatures (Garcia-Esquivel et al. 2007) and temperature variability (Ben-Horin et al. 2013) can increase disease severity in *H. fulgens* (R) held in captivity. Pinto Abalone, *Haliotis kamtschatkana* (S) (Jonas, 1845), have also been tested for WS resistance and

susceptibility, however the thermal regime under which the animals were held caused significant distress and mortality, thus making it difficult to discern patterns of disease resistance at environmentally relevant temperatures (Crosson and Friedman 2018).

Additionally, abalone species of the northeast Pacific occupy different habitats with distinct temperature regimes, spanning depths from intertidal to about 60 meters, and ranging in latitude from southern Baja California to Alaska. Because each species occupies a specific range of latitude and depth (though there is substantial overlap between some species), they also experience distinct wild temperature regimes (Table 1.1). For example, *Haliotis fulgens* (R) and *H. corrugata* (R) occupy intertidal habitat in the southernmost portion of any northeastern Pacific abalone ranges, and they experience temperatures in their normal habitat from 14-27°C and 12-23°C, respectively. *H. sorenseni* has substantial overlap in its range with these two species, yet it is only found in deeper water below 20 meters, and experiences water temperatures in the wild of about 6-12°C (Figure 1.1, Table 1.1). These differences in habitat temperature have led to a common explanation for the differential WS resistance patterns, which is that *H. fulgens* (R) and *H. corrugata* (R) are more tolerant to diseases because they naturally inhabit warmer waters (Figure 1.1, Table 1.1) and they are, therefore, more capable of tolerating higher temperatures than the more susceptible abalone species (Crosson and Friedman 2018).

Evidence suggesting that differences in WS resistance can not be explained solely by geographic distribution (and corresponding habitat temperature) comes from the distribution of and disease history of Black Abalone, *H. cracherodii* (S). Once very abundant in the rocky intertidal zones of southern California and on the Pacific coast of Baja California, Mexico (i.e., the Californian warm temperate marine biogeographic province) (Leighton 2000; Wildlife 2016-2017), *H. cracherodii* (S) historic natural latitudinal and depth ranges overlap substantially with

those of *H. fulgens* (R) and *H. corrugata* (R) (Figure 1.1). Hence, though the natural temperature range for *H. cracherodii* (12-25°C) overlaps substantially with those of *H. fulgens* (R) (12-27°C) and *H. corrugata* (R) (12-13°C), *H. fulgens* (R) and *H. corrugata* (R) are considered to experience low WS severity while *H. cracherodii* (S) experiences high WS severity. In fact, WS declines are one of the main reasons expressed for the significant population declines of *H. cracherodii* that led to the species being added to the Endangered Species list. Therefore, geographical and depth ranges, and corresponding habitat temperature cannot be the sole explanation for the observed differences in how susceptible different abalone species are to WS. An evolutionary explanation, for example, for patterns of WS resistance and susceptibility would predict that the susceptible species all belong to a clade that is more susceptible to WS, for instance, as seen for Wolbachia infection in beetles (Kajtoch et al. 2019). In plants, too, disease susceptibility and pathogen spread are strongly related to phylogenetic history (Gilbert and Parker 2016). The goal of this chapter is to test this alternative hypothesis to the range/depth/temperature explanation for WS resistance patterns, that resistance and susceptibility instead have an evolutionary explanation. Understanding the evolutionary pattern of WS resistance would enable better understanding of the mechanisms inside the gut (the site of RLO infection) that differ between susceptible and resistant species.

Before investigating the proximal mechanisms of susceptibility or resistance to WS (i.e., the "*how*" questions), it is important to explore the "*why*" aspects of susceptibility or resistance by considering the evolutionary histories of the organisms. If WS susceptibility is found in only one lineage, then it is a shared character of that lineage. Alternatively, WS resistance being found in more distantly related taxa would indicate that susceptibility is a shared ancestral trait that has been lost in some lineages. Most published abalone phylogenies are individual gene trees (Lee

et al. 1995; Lee and Vacquier 1995; Yang et al. 2000; Swanson et al. 2001; Galindo et al. 2002; Aagaard et al. 2010), which elucidate gene evolution and specific selection pressures (a good example being egg-sperm proteins in abalone (Lee and Vacquier 1992; Lee et al. 1995; Yang et al. 2000; Swanson et al. 2001; Galindo et al. 2003; Aagaard et al. 2010). However, single gene trees do not necessarily reflect accurate interspecific relationships (Page and Charleston 1997), which could lead to errors of character state optimization when mapping patterns of susceptibility or resistance in a genus. Other existing phylogenies consider the broad diversity of *Haliotis* (Brown 1993; Degnan et al. 2006; Streit et al. 2006), but do not include all of the northeastern Pacific taxa. These broader phylogenies, while including more taxa than in this study and showing broader evolutionary patterns of the *Haliotis* genus, do not completely successfully resolve relationships among the species of interest for WS (Lee and Vacquier 1995; Coleman and Vacquier 2002; Gruenthal and Burton 2005). This makes it difficult to understand the evolution of WS susceptibility or resistance, as the most complete phylogenetic analysis to date (Estes et al. 2005) produced one polytomy within the northeastern Pacific taxa. A robust phylogenetic analysis that resolves polytomies among the affected taxa would enable an understanding of these resistance and susceptibility patterns from an evolutionary context.

The goal of this chapter was to explore whether different gene sampling within the northeastern Pacific taxa might better resolve these species relationships to determine whether there are phylogenetic patterns in WS susceptibility and resistance. This study tests the hypothesis that the most vulnerable species to WS share some sort of susceptibility that is due to common ancestry, which is lacking in more resistant species. This hypothesis would be consistent with a result that supports the monophyly of susceptible species, even if this would not directly implicate a specific host vulnerability mechanism. Likewise, we could reject the

hypothesis if we reject the monophyly of the grouping of susceptible species. To test this hypothesis, two mitochondrial regions (16S ribosomal DNA and cytochrome *b*) and two nuclear regions (Histone 3 and internally transcribed spacer 1, 5.8S ribosomal DNA, and internal transcribed spacer 2 of the ribosomal gene cluster) were sequenced and aligned. These combined gene regions were used to estimate a phylogeny of the northeastern Pacific *Haliotis* taxa to examine the relationships among these *Haliotis* species. By mapping resistance and susceptibility traits onto the phylogenetic results, this study also determines whether WS susceptibility or resistance are traits with shared or divergent evolutionary histories.

MATERIALS AND METHODS

Foot muscle tissue was acquired from abalone samples collected between 1996 and 2018 for seven species from the northeastern Pacific (*Haliotis corrugata, H. cracherodii, H. fulgens, H. kamtschatkana, H. rufescens, H. sorenseni,* and *Haliotis walallensis* (Stearns, 1899) and one from New Zealand, *Haliotis iris* (Gmelin, 1791) (Table 1.2). Tissue samples from the Californian taxa (except *H. fulgens*) were acquired from the UC Davis Bodega Marine Laboratory. Epipodial clippings of *H. fulgens* were acquired from freshly harvested, live animals from Catalina Island, from Nancy Caruso of Get Inspired! Inc. Tissue from *H. iris* came from Te Papa Tongarewa Museum of New Zealand, after the animals were freshly collected in 2015 (Table 1.2). Before DNA extraction, tissues were stored in molecular-grade ethanol at 4°C.

Total DNA was extracted from the foot muscle using a DNeasy Blood and Tissue extraction kit (Qiagen, Valencia, CA, USA) following the manufacturer's instructions. 10-25mg of tissue was blotted dry of ethanol and cut into small pieces before proceeding with protocol. Extracted DNA was stored in the elution Buffer AE from the DNeasy protocol (10mM Tris-Cl,

0.5mM EDTA, pH 9.0) at 4°C until ready to be used for PCR reactions. Spectrophotometry (Synergy H1, BioTek, Winooski, VT, USA) was used to quantify DNA concentration for each sample.

Following the methodology outlined by (Kim et al. 2014), polymerase chain reactions (PCR) were conducted to amplify sequences for two mitochondrial genes (16S rDNA and *cytochrome b*) and two nuclear genes (*h3* and a region spanning *its1* and *its2*). The concatenated sequence of all four gene regions was 2,171 bp with the following breakdown per gene. 545 bp of the 16S ribosomal DNA (16S) gene and 705 bp of the cytochrome *b* (cyt *b*) gene were obtained. The latter codes for a protein involved in transmembrane electron transfer in respiration (Degliesposti et al. 1993). A 342 bp region of the H3 (Histone 3) gene and a 579 bp portion of the internal transcribed spacer region 1, *5.8s* rRNA, and internal transcribed spacer region 2 (hereafter ITS1-5.8S-ITS2) were obtained. Each PCR cycle consisted of an initial denaturation at 95°C for 2-3 min, followed by 35 cycles of: denaturation at 95°C for 30 sec, annealing (temperatures adjusted for each primer set) for 30-60 sec, extension at 72°C for 60-90 s. The final extension step was at 72°C for 5 min. For 16S, an annealing temperature of 61°C was used (except for *Haliotis sorenseni, H. iris,* and *H. fulgens*, for which 59°C was used) with the following primers (Kim et al. 2014): 16SrDNAF 5′-CGC CTG TTT ATC AAA AAC AT-3′, 16SrDNAR 5′-CCG GTC TGA ACT CAG ATC ACG T-3′. For cyt *b*, an annealing temperature of 60°C was used with the following self-designed primers (Primer-BLAST, NCBI): cytbF3 5′-GTG CTC ACG TTG AGT TAG CTT-3′, cytbR2 5′-TAA ACA CAC GCC CAA TCC CT-3′. For *H. fulgens*, an annealing temperature of 57°C was used with a custom reverse primer that overlapped with cytbR2 but was more specific for *H. fulgens*: cytbR1 5′-GCC CAA TCC CTT CAA ATG GC-3′. Likewise, for *H. sorenseni*, primers designed to be specific to that species

were used, and both overlapped with primers used the other taxa: cytbF1 5′-GGG GTT GTG TCT TGT TGT GC-3′ and cytbR3 5′-AGA ACA GTA AAC ACA CGC CCA-3′. For H3, a 60°C annealing temperature was used with the following designed primers: H3F 5′-ATG GCT CGT ACC AAG CAG AC-3′ and H3R 5′-TCC TTG GGC ATG ATG GTG AC-3′. For ITS1-5.8S-ITS2, the following primers (Coleman and Vacquier 2002) were used for all individuals unless specified, with an annealing temperature of 63°C: ABA-FOR 5′-TCG ATG AAG AGC GCA GCC-3′ and Hal-REV 5′-AGT CTC GTC TGA TCT GAG GTC-3′. Primers Hal-FOR 5′-TGA ACC TGC GGA AGG ATC ATT AAC G-3′, G-FOR 5′-GGG ATC CGT TTC CGT AGG TGA ACC TGC-3′, and G-REV 5′-GGG ATC CAT ATG CTT AAG TTC AGC GGG T -3′ were also used (Coleman and Vacquier 2002), with details on variations as follows: one *H. walallensis* sample was sequenced with primer sets Hal-FOR/Hal-REV and G-FOR/G-REV with an annealing temperature of 56°C. *H. cracherodii* was sequenced using primer set Hal-FOR/Hal-REV.

PCR products were visually inspected on 1% agarose gels, and then cleaned with a PCR NucleoSpin Gel and PCR Cleanup kit (Macherey-Nagel, Bethlehem, PA, USA). Occasionally samples with faint extra bands were gel-extracted, both procedures following the manufacturer's protocol. Cleaned samples were sent to Eton Bioscience (San Diego, CA, USA) for Sanger sequencing. Sequences from one *Haliotis discus* (Reeve, 1846) individual were extracted from the genome (Nam et al. 2017) using Blast 2.2.31. Sequences were aligned for each gene using CodonCode Aligner (v4.2.7) (CodonCode Corporation, Dedham, MA, USA), and trimmed to the size of the shortest fragment. An open reading frame was determined for H3 using ORFfinder (NCBI), and analysis was partitioned by codon for H3. All novel sequences were deposited on GenBank (NCBI, accession numbers in Table 1.3).

Phylogenetic relationships were generated using a mixed-model, partitioned Bayesian method as implemented in the software package Mr. Bayes version 3.2.6 (Ronquist et al. 2012). Analyses were conducted on concatenated sequences of all genes, partitioned by gene, as well as separate analyses for each nuclear or mitochondrial marker. Ten million generations of Markov Chain Monte Carlo (MCMC) sampling were performed using a random starting topology with trees sampled every 200 generations, with 25,000 early runs counted as burnin. The retained 50,002 trees were used to construct a 50 % majority rule consensus tree. The percentage of times that a particular node was recovered in the analysis is interpreted as the posterior probability of the occurrence of that node. Phylogenetic trees were created using FigTree (v1.4.2) and rooted with *H. iris* (New Zealand) because all gene-trees or phylogenies to date show *H. iris* as an outgroup to a clade containing northeastern Pacific taxa (Lee and Vacquier 1995; Coleman and Vacquier 2002; Estes et al. 2005; Geiger and Owen 2012).

RESULTS

The phylogenetic hypothesis for the *Haliotis* species examined is presented in Figure 1.2, based on analysis of a combined data set of sequences of 16S*,* cyt *b,* H3*,* and ITS1-5.8S-ITS2 genes. Most nodes in the tree are supported with $P \geq 0.99$ Bayesian posterior probabilities, and the species-differentiating node with the lowest support has $P=0.69$. Three main branches emerge in the northeastern Pacific taxa. This tree provides a phylogenetic estimate that includes all seven species native to the northeastern Pacific plus one from Japan, *Haliotis discus* (R). In our result, *H. fulgens* (R) is sister to the rest of the included northeastern Pacific taxa. The monophyly of the other ingroup species besides *H. fulgens* (R) is strongly supported ($P=0.94$), as is its internal split into two monophyletic subgroups (each supported with $P=0.84$). In one of these subgroups, *H.*

discus is the sister taxon of *H. corrugata* (R). In the other subgroup that is sister to the *H. discus* and *H. corrugata* (R) clade, *H. cracherodii* (S) is the sister taxon to a well-supported ($P \geq 0.99$) grouping of *H. rufescens* (S), *H. walallensis* (U), *H. kamtschatkana* (S), and *H. sorenseni* (S). This subgroup consisting of five taxa includes all four northeastern Pacific taxa (*H. rufescens* (S), *H. kamtschatkana* (S), and *H. sorenseni* (S)) that are known to be more susceptive to WS, in addition to *H. walallensis* (U), which hasn't been studied well for WS susceptibility (Table 1.1). The resistant taxa, *H. fulgens* (R), *H. corrugata* (R), and the Japanese *H. discus* (R), all fall outside of this subgroup.

Single gene tree hypotheses are presented in Figure 1.3, and each gene appears to provide somewhat different topologies for the relationships amongst the *Haliotis* taxa. For instance, the two mitochondrial genes support the presence of a clade that includes the susceptible northeastern Pacific *Haliotis* taxa, with *H. cracherodii* (S) variously placed as sister to this group. The 16S gene tree is largely compatible with the patterns in the combined gene tree, is the only gene tree that strongly supports the basal position of *H. fulgens* (R) within the ingroup, and is the only result that that supports the monophyly of the susceptible clade. This suggests that 16S may be the individual gene data set contributing the strongest signal to the combined-gene result. The Cyt *b* analysis also supports the monophyly of the northeastern Pacific susceptible clade (Figure 1.3-B), with *H. cracherodii* (S) being the only susceptible species alone falling outside of this otherwise "susceptible" clade. Conversely, trees for the nuclear genes (H3 and ITS1-5.8S-ITS2) result in multiple polytomies and unresolved relationships, indicating that the inclusion of these nuclear markers has contributed relatively little to the resolution of species relationships within northeastern Pacific *Haliotis*. However, ITS1-5.8S-ITS2 supports a

subgroup that contains all resistance species, grouping these species separately from all susceptible species.

DISCUSSION

The commonly held explanation for different patterns in WS susceptibility has been that *Haliotis fulgens* (R) and *H. corrugata* (R) are more resistant to WS due to their high thermal tolerance (e.g., (Crosson and Friedman 2018). Perhaps this explanation emerged from the observation that WS appears to be modulated, in part by temperature, with abalone exposed to high temperatures generally showing marked increases in infection intensity and disease (Braid et al. 2005; Rogers-Bennett et al. 2010; Moore et al. 2011). However, the thermal range of susceptible *H. cracherodii* (S) (Figure 1, Table 1.1) lends evidence against this hypothesis. The sea temperature range of *H. fulgens* (R) and *H. corrugata* (R) habitat is 14-27°C and 12-23°C, respectively (Dahlhoff and Somero 1993b). *H. cracherodii* (S) is the species of abalone that is perhaps most susceptible to WS (as suggested by it being the only species led to near-extinction by the disease), with a temperature range in the wild of 12-25°C (Dahlhoff and Somero 1993b). This contradicts the thermal-tolerance hypothesis because it overlaps completely with the temperature range of more resistant species (*H. fulgens* (R) and *H. corrugata* (R)).

Instead, the phylogenetic tree presented here (Figure 1.2) shows support for the hypothesis that the common ancestor of the more susceptible taxa is separate and more recent than the common ancestor shared with the more resistant species (P=0.94; more resistant species shown in grey in Figure 1.2). Estes *et al*. (2005) presented results that included support, as in this phylogeny, where we found a monophyly of a northeastern Pacific cluster of species (*Haliotis*

rufescens (S), *H. walallensis* (S), *H. kamtschatkana* (S), and *H. sorenseni* (S)), and with other northeastern Pacific species (*H. fulgens* (R) and *H. corrugata* (R)) intermixed with a northwestern Pacific species (*H. discus* (R)). This latter finding, that these two NE Pacific species are both highly WS resistant yet more related to a distant species, makes it ambiguous whether the radiation of all northeastern Pacific species might have occurred only in western North America or perhaps involved up to two or more longer range trans-Pacific invasions, in either direction. The phylogenetic result in Estes *et al*. (2005) is consistent with our hypothesis, but is partially unresolved at the northeastern Pacific taxa level. The results presented here lend more support to the monophyly of the susceptible clade that Estes *et al*. (2005) demonstrated, but further taxon sampling of the northwestern Pacific taxa might improve the resolution and possibly support particular northwestern Pacific taxa as potentially susceptible to WS. Additionally, further work should consider using a more proximal outgroup, as *H. iris* is a distant outgroup.

Biogeography of *Haliotis*

Understanding physiological patterns in an evolutionary context requires a robust phylogenetic analysis of the affected taxa. In both Estes *et al*. (2005) and this current study, the nesting of *Haliotis sorenseni* (S) within a clade consisting of *H. rufescens* (S), *H. kamtschatkana* (S), and *H. walallensis* (U) (Figure 1.2) is interesting when considering current geographic ranges (Figure 1.1). *H. rufescens* (S), *H. kamtschatkana* (S), and *H. walallensis* (U) all have ranges extending further into the north than the southern species (Figure 1.1), yet *H. sorenseni* (S) is limited to more southern latitudes despite being more closely related to species whose ranges extend further north. Abalone are distributed nearly world-wide on rocky shores, which has led to three hypotheses explaining their biogeography (Geiger and Groves 1999; Geiger and

Owen 2012). What all three have in common is that ancient haliotids likely spread to California from eastern Asia, and results to date suggest that the entire North Pacific abalone fauna could be part of a monophyletic diversification event. The origin and diversification of the impressively large-bodied North Pacific species appears to be a much more recent phenomenon, with no fossil species similar to extant ones predating the late Miocene (summarized by (Geiger and Owen 2012)). Estes *et al*. (2005) have attributed much of the diversification and body size increases to the rise of productive kelp forests that occurred in the cooling of the Miocene North Pacific. These authors further emphasized the potential role of the sea urchin- and abalone-eating sea otter in providing kelp with an opportunity to avoid a more ubiquitous investment in chemical defense against grazers (Estes and Steinberg 1988; Steinberg 1989), instead maximizing rapid growth and as a consequence providing ample food resources for the grazers that do escape otter predation.

Robustness of phylogenetic sampling

A future expanded study is still needed to determine whether the species-level relationships we found between all seven *Haliotis* taxa native to California will remain robust. Our phylogeny is still preliminary because it is in need of more complete taxon- and gene-sampling, but provides intriguing support for our hypothesis that the WS resistant species (*H. fulgens* (R) and *H. corrugata* (R) of California, and *H. discus* (R) of Japan) are outgroup species of the other northeastern Pacific *Haliotis* taxa (Figure 1.2). In a test of how to best resolve phylogenetic patterns, an analytical comparison compared two methods – one using 26 genes selected for their similarity to the strongest phylogenetic hypothesis and another choosing genes at random from a pool of 830 genes for the genus *Primulina*. When selecting specific genes, only 8 genes were needed to resolve the phylogeny compared to 175 needed when genes were chosen

at random (Ai and Kang 2015). The authors recommend choosing single genes that are well known to differentiate between at least some of the species to be included in the full phylogenetic inference. 16S was used in other closely related Pacific abalone species (Estes et al. 2005) and was used to differentiate species relationships in the 6 species studied (An et al. 2005), including *H. discus,* which was used in this study, so it was chosen as a target gene for this study. The results of this study show that 16S provides some differentiation between the species used in this study, though it is more useful for identifying species than estimate phylogenetic distance between the species (Figure 1.3-A). Cytochrome b (cyt *b*) was chosen for this study because it had been examined as a genetic marker for the same species involved in this study (Gruenthal and Burton 2005). In this study, cyt *b* was perhaps the most useful gene for phylogenetic reconstruction, as it provided the clearest phylogenetic differentiation between the species of interest (Figure 1.3-B). In this study, H3 was chosen as a gene of interest because of its use in gastropod phylogenies (Colgan et al. 2000). With closely related species of abalone, however, this gene (sequenced by codon) mostly helps with differentiating between species, without providing much context for how those species are related to one another (Figure 1.3-C). Likewise, ITS1-5.8S-ITS2 was chosen because it is one of the few genes that had been used in phylogenetic reconstruction of *Haliotis* (Estes et al. 2005). Although ITS1-5.8S-ITS2 is presumed to be a neutrally evolving region and therefore not extremely useful for comparing closely related species, in *Haliotis*, sequencing of region has instead led to congruent trees with that of a rapidly evolving gene, sperm protein lysin (Lee et al. 1995; Coleman and Vacquier 2002). ITS1-5.8S-ITS2 was chosen for this study as a substitute for sperm protein lysin for this reason. The latter gene region would not amplify for all species on the northeastern Pacific, thought future work creating a more robust analysis would use more advanced techniques to

include this gene region in analysis. In this study, ITS1-5.8S-ITS2, like H3, was useful for grouping individuals of the same species together, but did not provide great phylogenetic resolution of species relationships for most species included (Figure 1.3-D).

Based on the conclusions and suggestions of (Ai and Kang 2015) to choose genes for a phylogeny that have been used in some of the species of interest, 16S, cyt *b*, H3, and ITS1-5.8S-ITS2 were chosen. However, only cyt *b* provided strong data for differentiating between species. Therefore, future analysis would consider addition genes and perhaps substituting other genes in place of 16S, H2, and ITS1-5.8S-ITS2 that provide better phylogenetic clarity.

Susceptibility and resistance

The data support a hypothesis of monophyly of susceptible species. This study does not test for host vulnerability or pathogen specificity mechanisms. Future research priorities should determine if a mechanism of infection, the spread of the WS-RLO disease organism, or some other host-pathogen specificity mechanism evolved to target the supported clade of abalone species that are highly susceptible to WS. Alternatively, the common ancestor of this clade could have lost whatever cellular mechanism(s) or host-pathogen compatibility differences that confer higher WS resistance under environmentally relevant temperatures. A physiological comparison of the disease state in species from these two groups would help elucidate the evolutionary pattern of disease resistance.

To our knowledge, only Crosson and Friedman (Crosson and Friedman 2018) have attempted to test the hypothesis that temperature tolerance explains WS susceptibility or resistance, or they are the only authors to previously propose a mechanistic link between temperature tolerance and the physiology of disease resistance in these species. The authors examined differences in WS susceptibility and resistance in *Haliotis kamtschatkana* (S)*, H.*

rufescens (S), and *H. corrugata* (R) (Crosson and Friedman 2018). Apart from this study, there is still little or no information about disease severity and its impact on otherwise healthy digestive function (the site of infection) in species at environmentally relevant temperatures, limiting our understanding of how these species physiologically respond to disease in their natural ranges. Crosson and Friedman (Crosson and Friedman 2018) determined that WS susceptibility was inversely related to sequence divergence, relative to *H. sorenseni* (S). This was determined using mitochondrial cytochrome oxidase subunit I (COI) sequences, which is congruent with our findings that *H. sorenseni* (S) is nested within a clade of other species that are more susceptible to withering syndrome.

The WS-RLO was first characterized by Friedman *et al*. (Friedman et al. 2000) and, since then, a handful of studies have looked at some outcomes of the WS-RLO in the abalone digestive system (the site of infection). Infected abalone experience reduction in growth, food intake, and metabolism (Gonzalez et al. 2012). They also experience body mass decline, foot atrophy, higher mortality, and decreased glycogen stores in the foot muscle and digestive gland (Braid et al. 2005). Metaplasia in gut tissue has also been demonstrated, with infected animals losing functional digestive tissue (Friedman et al. 2003). Apart from these macro-level observations, the functional digestive changes that occur during WS-RLO infection (i.e. digestive enzyme function, digestibility of nutrients and organic matter), especially during sub-lethal stages of the disease, have not been well studied. Understanding the cellular-level and gene-expression level physiological responses to WS-RLO, and especially a comparison of these functions in more resistant species (e.g., *Haliotis fulgens* and *H. corrugata*) versus susceptible species in the Northeast Pacific clade (e.g., *H. rufescens*), is crucial for understanding disease susceptibility/resistance. Our phylogenetic estimate based on the concatenated data set (Figure

1.2) suggests that evolutionary history plays a role in the species differences in susceptibility to this disease, and highlights the need for further investigations into the specificities of this mechanism (or mechanisms) that allow for differential susceptibility across abalone species. To that end, even within one species (*H. rufescens* (S)), populations show variation in gene expression related to oxygen uptake, metabolism, and biomineralization that is related to acidification stress (De Wit and Palumbi 2013).

Compliance with Ethical Standards

Ethical Approval

Samples from both *Haliotis fulgens* individuals were collected under permit SC-4786, MAB-95 broodstock collecting permit, and commercial fishing license 1028617285. Other tissue samples were sub-sampled from museum specimens or the abalone tissue archive at CDFW Shellfish Health Lab. *Haliotis sorenseni* samples were archived under the authority of federal ESA (Endangered Species Act) permit #14344, and specific permission was granted to use tissue and extracted DNA for this study. *Haliotis cracherodii* individuals were collected before the species was added to the ESA (before 2003), and therefore use of their tissue and DNA does not require a federal ESA permit.

Data accessibility

GenBank accession numbers MH395932 to MH395937, MH395940 to MH395958, MH427176 to MH427200, MH443009 to MH443058.

Figure 1.1 Map of historical abalone distribution along the northeast Pacific coastline, with depths (inlay) and ranges of each species. Ranges of temperatures experienced by each species (Leighton 2000; Wildlife 2016-2017)(Bird 2018). The habitats of *H. rufescens*, *H. cracherodii*, and *H. sorenseni* are limited to cold upwelling areas in the southern portion of their ranges. In the southern portion of its range, *H. kamtschatkana* are strictly subtidal, occurring up to 40m but are most common between 20-30m (Geiger and Owen 2012).

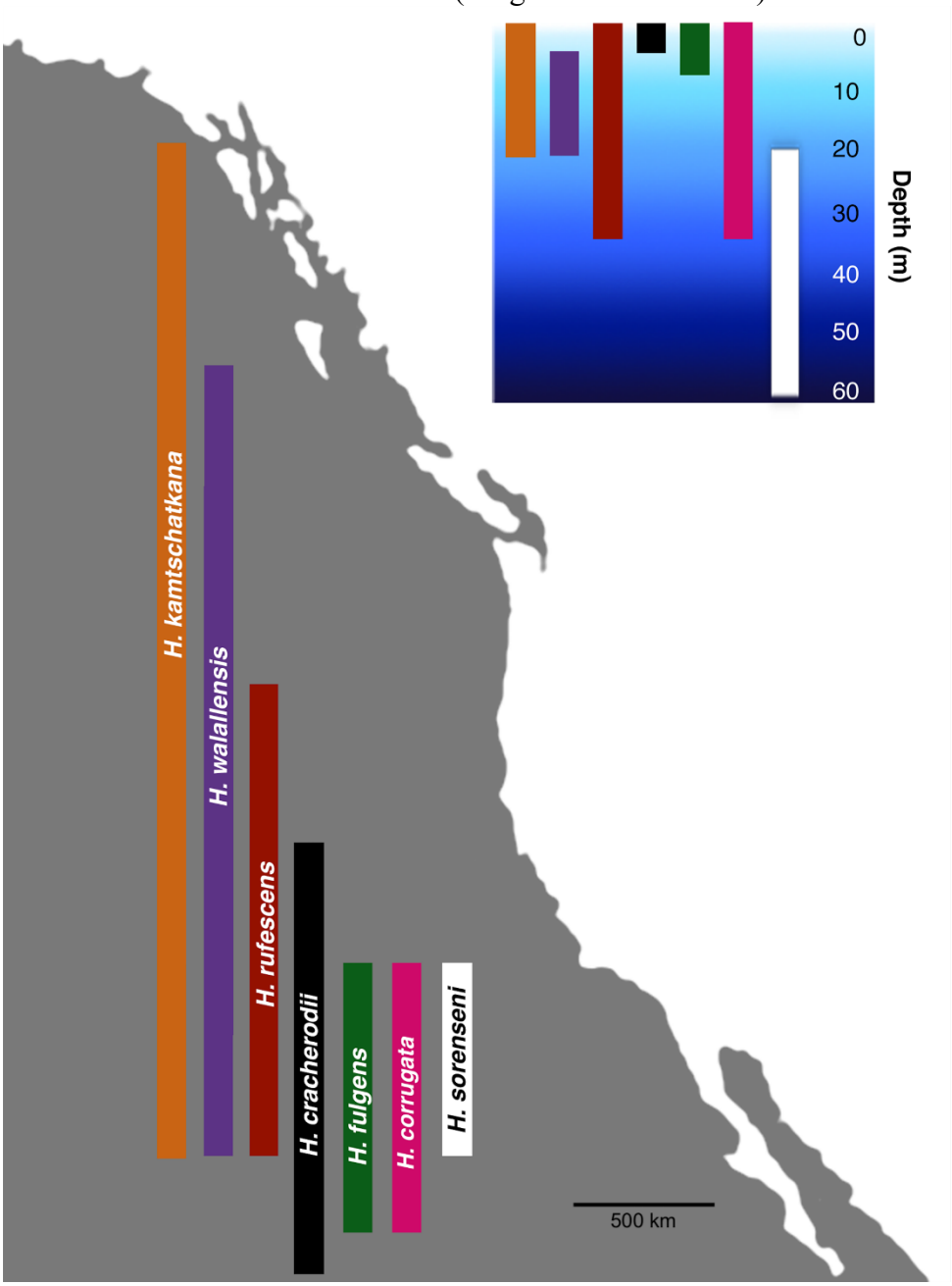

Figure 1.2 Bayesian phylogenetic hypothesis for the *Haliotis* species in this study based on sequences of 16S, cyt *b,* H3, ITS1-5.8S-ITS2genes. Ten million generations of MCMC were performed with trees sampled every 200 generations and 15% of early runs counted as burnin. The percentage of times that a particular node was recovered is listed as the Bayesian posterior probability, with ** signifying $P \geq 0.99$. Species with relatively high WS resistance capabilities are in light grey. Numbers next to species names indicate number of individuals.

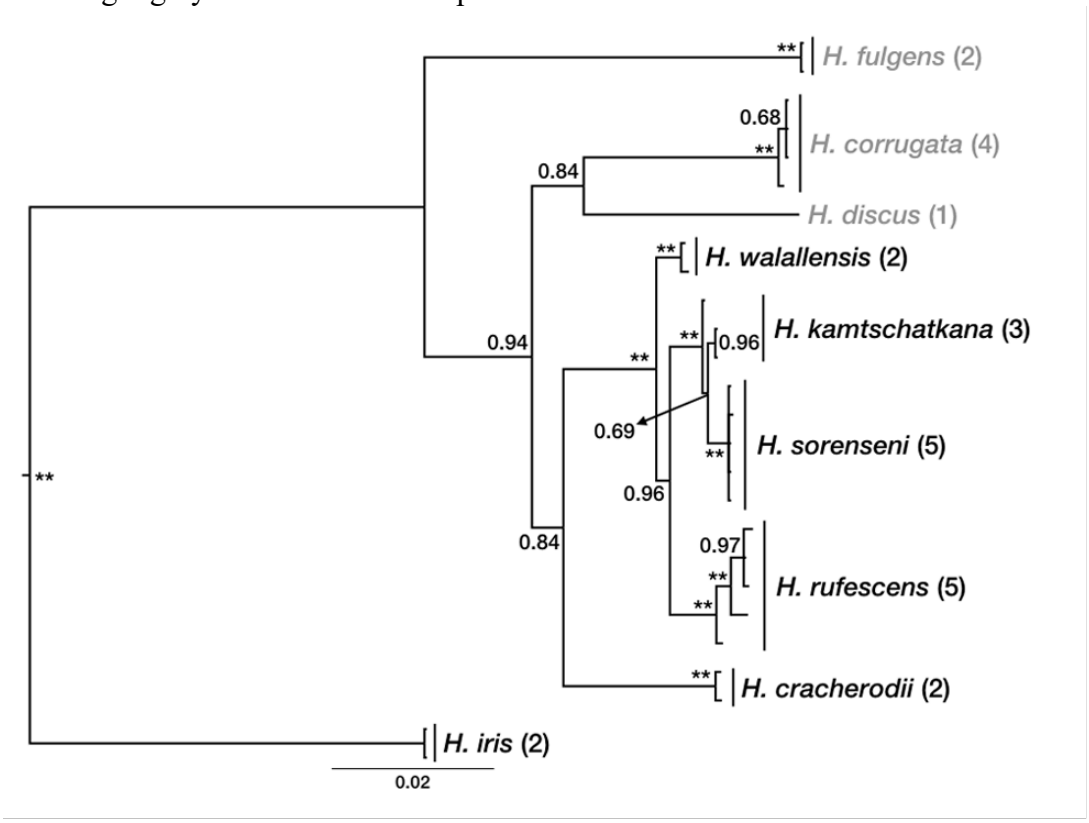

Figure 1.3 Bayesian phylogenetic hypothesis for each gene tree in the *Haliotis* species in this study. 3A- 16S gene tree. 3B- cyt *b* gene tree. 3C- H3 gene tree. 3D- ITS1-5.8S-ITS2 gene tree. The percentage of times that a particular node was recovered is listed as the Bayesian posterior probability, with ** signifying $P \geq 0.99$. Species with relatively high WS resistance capabilities are in light grey. Numbers next to species names indicate number of individuals.

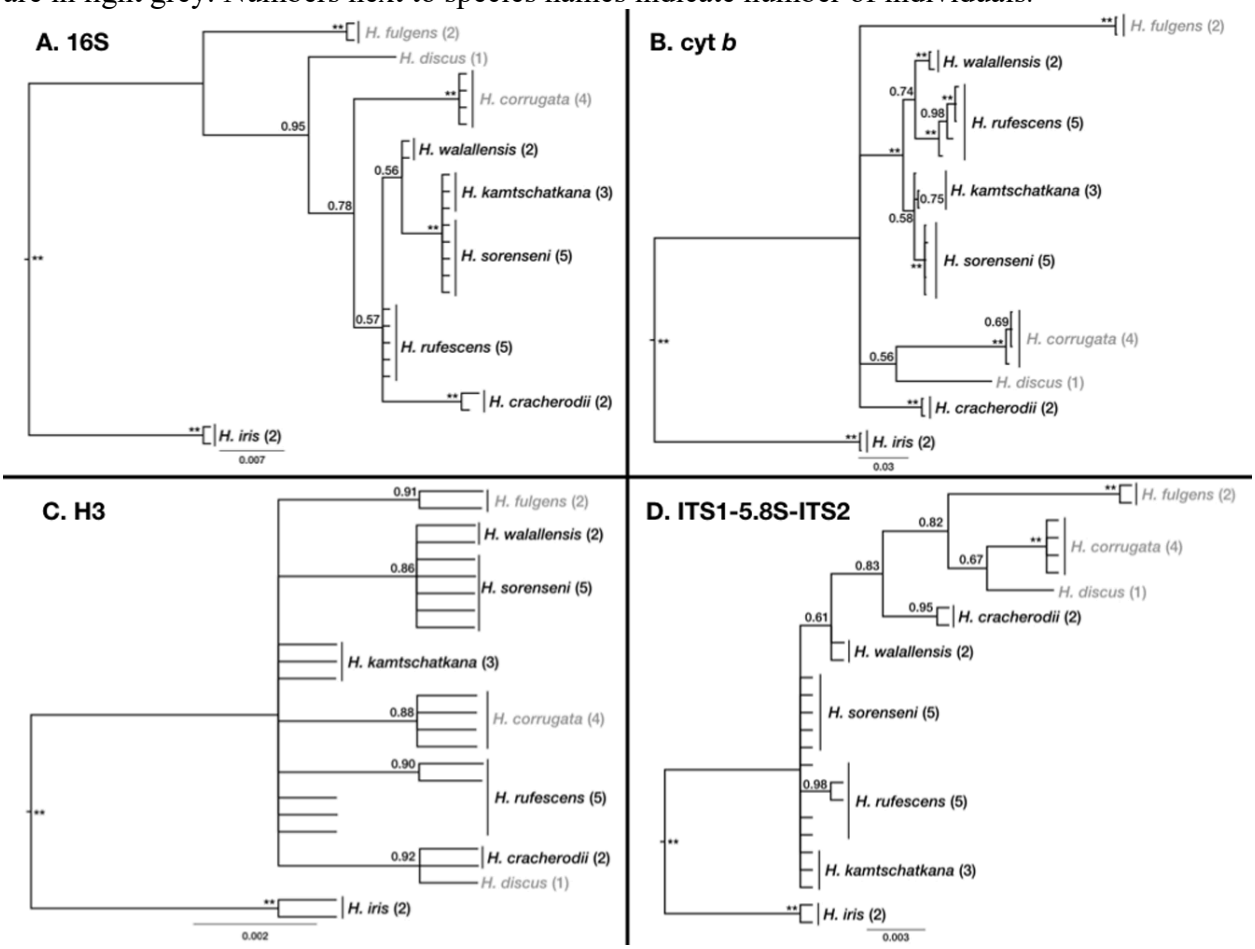

Table 1.1 Geographic ranges and wild temperature ranges of northeastern Pacific abalone taxa (Dahlhoff and Somero 1993b; Hobday and Tegner 2000; Leighton 2000; Wildlife 2016-2017; Owen and Raffety 2017) (Bird 2018). Qualitative assessment of relative WS susceptibility in northeastern Pacific abalone taxa (Crosson et al. 2014; Crosson and Friedman 2018).

Species	**Depth (m)**	**Wild range temperature (°C)**	**WS Severity**
Haliotis fulgens	Intertidal, 0-9	14-27	Low
H. corrugata	Intertidal, 0-36	12-23	Low
H. sorenseni	20-60	6-12*	High
H. walallensis	6-21	4-12*	Understudied
H. rufescens	Intertidal, 0-10 (N); 10-35 (S)	8-18	High/medium
H. kamtschatkana	Intertidal, 0-21	4-14	High
H. cracherodii	Intertidal, 0-6	12-25	High

*Based on known depth and range, what is known about other abalone species, these temperatures were estimated.

Table 1.2 Sampling dates and sources for foot muscle tissues of each animal. The gene sequences from the one *Haliotis discus* individual included in the tree were from a full genome (Nam et al. 2017).

Species	Animal ID	Date collected	Source
Haliotis rufescens (n=5)	SF07-3-1	5 Feb 2007	Van Damme, CA
	SF07-25-133	18 Jul 2007	Farallones Island, CA
	SF07-48-7	26 Apr 2003	Soberanes Pt., CA
	SF10-15-1	14 May 2010	Bodega Head, CA
	SF07-32-18	25 Aug 2007	San Miguel Island, CA
Haliotis corrugata (n=4)	SF08-6-3	2000	T. McCormick Broodstock
	SF02-24	pre-1997	Hatchery Raised 1993, Proteus
	SF04-36-1	20 Aug 2004	Cape Cortes, Santa Catalina Island
	SF08-6-2	2000	T. McCormick Broodstock
Haliotis walallensis (n=2)	SF06-18-15	Nov 2003	Van Damme, CA
	SF08-48-1	unknown	Oregon
Haliotis kamtschatkana (n=3)	SF15-52-2	17 Aug 2015	Van Damme, CA
	SF15-52-3	17 Aug 2015	Van Damme, CA
	SF15-52-4	17 Aug 2015	Van Damme, CA
Haliotis cracherodii (n=2)	SF03-34-2	1996	Ano Nuevo Island (S of San Francisco), CA
	SF03-31-30	pre-2003	Carmel, CA
Haliotis sorenseni (n=5)	SF08-25-2	2004	Santa Cruz Island (via Tom McCormick and BML)
	SF08-25-3	7 Nov 2000	Farnsworth (via Tom McCormick and BML)
	SF03-20-1	8 Nov 2000	Farnsworth (via CIMRI)
	SF08-25-1	28 Mar 2000	Farnsworth (via Tom McCormick and BML)
	SF05-37-1	7 Nov 2000	Farnsworth (via Tom McCormick)
Haliotis iris (n=2)	M.318749 (6)	3 Oct 2015	40° 39.82' S, 172° 24.17' E, New Zealand, South Island, Punapaua, W of Collingwood, M Young
	M.318749 (7)	3 Oct 2015	40° 39.82' S, 172° 24.17' E, New Zealand, South Island, Punapaua, W of Collingwood, M Young
Haliotis fulgens (n=2)	Cat-G01	13-14 Jan 2018	Catalina Island
	Cat-G03	13-14 Jan 2018	Catalina Island

Table 1.3 Isolate and GenBank accession numbers for each gene region of each individual (isolate) sequenced for phylogenetic analysis.

		Gene region			
Species	**Isolate**	**16S**	**cyt *b***	**H3**	**ITS1-5.8S-ITS2**
Haliotis rufescens (n=5)	SF07-3-1	MH395949	MH427191	MH443024	MH443049
	SF07-25-133	MH395950	MH427192	MH443025	MH443050
	SF07-48-7	MH395951	MH427193	MH443026	MH443051
	SF10-15-1	MH395952	MH427194	MH443027	MH443052
	SF07-32-18	MH395953	MH427195	MH443028	MH443053
Haliotis corrugata (n=4)	SF08-6-3	MH395945	MH427187	MH443020	MH443045
	SF02-24	MH395946	MH427188	MH443021	MH443046
	SF04-36-1	MH395947	MH427189	MH443022	MH443047
	SF08-6-2	MH395948	MH427190	MH443023	MH443048
Haliotis walallensis (n=2)	SF06-18-15	MH395936	MH427180	MH443013	MH443038
	SF08-48-1	MH395937	MH427181	MH443014	MH443039
Haliotis kamtschatkana (n=3)	SF15-52-2	MH395942	MH427184	MH443017	MH443042
	SF15-52-3	MH395943	MH427185	MH443018	MH443043
	SF15-52-4	MH395944	MH427186	MH443019	MH443044
Haliotis cracherodii (n=2)	SF03-34-2	MH395932	MH427176	MH443009	MH443034
	SF03-31-30	MH395933	MH427177	MH443010	MH443035
Haliotis sorenseni (n=5)	SF08-25-2	MH395955	MH427197	MH443030	MH443055
	SF08-25-3	MH395956	MH427198	MH443031	MH443056
	SF03-20-1	MH395957	MH427199	MH443032	MH443057
	SF08-25-1	MH395958	MH427200	MH443033	MH443058
	SF05-37-1	MH395954	MH427196	MH443029	MH443054
Haliotis iris (n=2)	M.318749 (6)	MH395940	MH427182	MH443015	MH443040
	M.318749 (7)	MH395941	MH427183	MH443016	MH443041
Haliotis fulgens (n=2)	Cat-G01	MH395934	MH427178	MH443011	MH443036
	Cat-G03	MH395935	MH427179	MH443012	MH443037

Chapter 2

Withering-syndrome induced gene expression changes and a de-novo transcriptome for Pinto Abalone, *Haliotis kamtschatkana*

INTRODUCTION

Withering syndrome

Beginning in 1985, populations of Black Abalone (*Haliotis cracherodii*) began to crash along the California coastline, especially in the Channel Islands. These extreme declines in abalone numbers are attributed to the emergence of a new disease, withering syndrome (Lafferty and Kuris 1993). It was later discovered that a Rickettsiales-like organism (RLO), a bacterial parasite, infects abalone digestive tissues and leads to starvation and a characteristic degradation of the gastropod foot (a disease called withering syndrome, or WS) (Crosson et al. 2014). First histopathology analyses of the disease state in Black Abalone showed that bacteria formed inclusions throughout the digestive system, from the esophagus to the intestine. The most profound changes in the tissue occur in the digestive gland, where inclusions lead to metaplasia—the changing of secretory cells (which would otherwise secrete enzymes) to absorptive cells—and massive morphological changes of diverticula (Gardner et al. 1995). The resultant pedal atrophy was attributed to lack of nutrition from the changes to enzyme secretory cells (Gardner et al. 1995), but digestive enzyme activity was not measured in the infected guts. The bacteria that is responsible for withering syndrome, WS-RLO, was first characterized in 2000, and is identifiable by some of the aforementioned histological changes in the abalone gut, as well as a unique 16s rDNA sequence of the bacterial taxon (Friedman et al. 2000). A variant of the WS-RLO, referred to as RLOv, has been measured in abalone as well. The RLOv and WS-

RLO are both suspected to be the same bacteria species, *Candidatus* Xenohaliotis californiensis, but the RLOv is a separate variant because it is infected with a phage hyperparasite that results in some distinct morphological differences from the standard WS-RLO (Friedman and Crosson 2012). Black Abalone infected with RLOv tend to have lower mortality and lower host responses to the disease than animals infected with the WS-RLO, presumably because the phage dampens the effects of the RLO (Friedman et al. 2014a).

A few studies have more holistically examined the physiological response of the abalone digestive system (the site of infection) to the WS-RLO. Infected abalone experience reduction in growth, food intake, and metabolism (Gonzalez et al. 2012). Body mass decline, foot atrophy, higher mortality, and decreased glycogen stores in the foot muscle and digestive gland also appear as symptoms of the advanced stages of WS, and exposure to higher temperatures leads to significantly greater transmission of the RLO to other abalone (Braid et al. 2005). In addition, elevated temperatures led to higher pathogenicity in Red Abalone (*H. rufescens*) infected with the RLO (Moore et al. 2000). Thus, the disease appears to be modulated in part by elevated temperatures, in response to which we see some abalone species showing marked increases in infection intensity and disease (Moore et al. 2000; Braid et al. 2005; Rogers-Bennett et al. 2010; Moore et al. 2011). Interestingly, some abalone are able to repair some of the metaplastic damage if treated with oxytetracycline, which kills the RLO (Friedman et al. 2003).

Apart from the aforementioned morphological changes to the digestive system, the functional physiological changes (such as changes in gene expression (McDowell et al. 2014)) that occur during WS-RLO infection, especially during sub-lethal stages of the disease, have not been extensively studied. For example, although it is known that the secretory tissue undergoes metaplasia, the degree to which this affects gene expression, and the related physiological

processes encoded by those genes, in abalone digestive tissue is unknown. In this chapter, I used transcriptomics to examine the gene expression patterns in unexposed and infected Pinto Abalone (*H. kamtschatkana*) before and during WS-RLO infection.

Pinto Abalone are one of the species from the northeastern Pacific that are particularly susceptible (low resistance) to WS (See chapter 1; (Crosson and Friedman 2018)), making them an ideal test species for this study. Pinto Abalone, as of April 2019, were listed as an Endangered species in the state of Washington (Carson and Ulrich 2019) and WS was identified as a major threat to the species, making it even more critical that we understand how this disease impacts their physiology. In other species, such a Black Abalone, WS has had even more severe impacts on populations. For example, WS is listed as a main contributing factor to the federal classification of Black Abalone as "Endangered." All abalone species in California are culturally, economically, and ecologically important, so understanding the mechanisms that underly WS is essential to conserving these species and preserving this legacy.

Transcriptomics and disease states

All -omics tools, paired with other physiological measurements such as digestive function, disease load, and survival, contribute to a holistic understanding of the disease state and how it impairs physiological function. This can be especially useful when attempting to understand the complex interactions between host, pathogen, and environment (Gomez-Chiarri et al. 2015). For example, transcriptomic tools have been used to identify immune-related changes and function in response to pathogen challenges in bivalves, as well as the interaction of environmental impacts on disease resistance pathways (Gomez-Chiarri et al. 2015).

Transcriptome analysis during infection can also highlight organ-specific changes caused by disease. For instance, spring viremia of carp virus (SVCS) infections leads to differential gene expression changes in the brain and spleen of zebrafish, and these expression changes are associated with inflammation and metabolic pathways (Wang et al. 2017). These differentially expressed genes can have function or identity assigned to them, which would significantly improve understanding of the very fine ways in which pathogens alter host physiology, or pathways by which hosts respond to infectious agents. For example, an analysis of the transcriptomic response in grass carp intestines to *Aeromonas hydrophila* (a bacterial parasite) demonstrated that the intestinal tissue responded to infection with a large upregulation of immune-related pathways compared to other tissues (Song et al. 2017).

This study aims to determine the differentially expression genetic patterns in Pinto Abalone during a 7-month WS challenge, to form this basis of knowledge for comparing other species' responses to WS-RLO infections.

METHODS

Infection experiment of Pinto Abalone

Pinto Abalone (n=144) were divided into two treatment systems at University of Washington, with 4 replicates per system and 18 animals per replicate (Figure 2.1). Water was passed through UV light and filtration before reaching a head tank. The two treatments have separate head tanks, which contained either uninfected red abalone (control), or RLO-infected red abalone as a source of the WS-RLO pathogen. WS-RLO is shed in the infected Red Abalone feces (Crosson et al. 2014) and animals downstream were exposed to the bacteria. In a sampling scheme designed to emphasize early immune responses post-exposure to the WS-RLO, two animals every replicate were sampled at t=0 and post-exposure at 24 hours, 3 days, 7 days, 6

weeks, 3 months, and 7months. During each sampling, animals were dissected and post-esophageal (PE) and digestive gland (DG) tissue samples were taken and frozen in RNAlater and stored at -80°C.

WS-RLO infection intensity of pinto abalone (extraction and qPCR parameters)

DNA was extracted by the Freidman lab from post-esophageal tissues bordering the digestive gland, as outlined in (Friedman et al. 2014a). A QiaAmp DNA Stool Mini Kit (Qiagen Inc., Valencia, CA, USA) was used with modifications and parameters following (Friedman et al. 2014b). DNA was stored at -20°C until qPCR analysis. qPCR techniques followed those developed in (Friedman et al. 2014b) and used in (Friedman et al. 2014a). 25 µl reactions contained 12.5 µl 2x Immomix (Bioline USA Inc., Taunton, MA, USA), 320 nM of each primer, 200 nM of probe (Biosearch Technologies, Inc., Novato, CA, USA), 0.6 mg/µl BSA, 2 µl of DNA template, and sterile water to bring the final volume to 25 µl per reaction. Primers for the WS-RLO were WSN1 F (AGT TTA CTG AAG GCA AGT AGC AGA) and WSN1 R (TCT AAC TTG GAC TCA TTC AAA AGC) (Friedman et al. 2014b). An initial denaturation incubation lasted 5 minutes at 95°C, followed by 41 cycles of 95°C for 15 seconds and 60°C for 60 seconds. Samples were run in duplicates with a plasmid-based standard curve of known copy numbers for the WS-RLO and RLOv (Friedman et al. 2014a).

RNA extraction, cDNA preparation, and sequencing

To identify the genes being differentially expressed between the control and infected individuals, RNA was extracted from the 20-50 mg of digestive gland (DG) tissue per sample for RNAseq (Garcia et al. 2012; Briscoe et al. 2013). Total RNA was extracted from DG tissue

using Trizol (Life Technologies, Grand Island, NY) at UCI. Samples were checked with a spectrophotometer at the UCI Genomics High Throughput Facility for Total RNA quality and concentration. A TruSeq RNA sample prep kit (Illumina) was used to prepare individual cDNA libraries (Briscoe et al. 2013) for 20 samples, according to the manufacturers instructions. Re-purification was performed using Agencourt AMPure XP magnetic beads (Beckman Coulter Genomics). Quantification of the cDNA pool was performed with a Qubit 2.0 Flourometer, and cDNA was control-checked with an Agilent Bioanalyzer 2100. The cDNA was then normalized to 10 nM and run paired-end 100 bp runs on a HiSeq 4000 (Illumina, San Diego, CA) at the UCI Genomics High-Throughput Facility.

Raw data files were filtered and trimmed following Garcia et al. (Garcia et al. 2012). A de novo transcriptome was assembled using transcripts from 3 individuals, a control from the pre-exposure group, a control from the 7-month group, and an infected animal from the 7-month group. Transcript assembly was performed using oases v0.2.08 (Schulz et al. 2012) in conjunction with velvet v1.2.08 (Zerbino and Birney 2008) and annotated with Trinotate. Blast2GO v5.2.5 was also used, according to the standard gene ontology annotation pipeline, to annotate DEGs. However, it provided less detail than the Trinotate analysis and was not further considered in this study. After assembly and annotation, Reads Per Kilobase per Million (RPKM) were estimated to differential expression of digestive gland genes in animals exposed to the WS-RLO and healthy, naïve animals. Unique genes being expressed differentially between the two groups ($P<0.001$) with at least a 4-fold difference were compared using heat maps generated in R (https://www.r-project.org/). Differential gene expression data was obtained for 7 pre-exposure animals, 2 animals exposed to the RLO for 24 hours, 3 animals exposed to the RLO

for 3 months, 4 animals exposed to the RLO for 7 months, and 3 naïve animals in the experiment set-up after 7 months.

Gene Prediction with Augustus

Because large numbers of the DEG's in Groups 1 and 3a were unable to be identified or assigned a functional annotation, I mapped these gene fragments to the Red Abalone (*H. rufescens*) genome from (Masonbrink et al. 2019) using Blast v2.2.30. This allows for at least the identification of what genes are in the same neighborhood as the unidentified DEGs, and thus, future work can reveal what these genes are. Red Abalone genomic scaffolds where the DEG's aligned with a greater than 90% identity were pulled from the genome. Both the genomic Red Abalone scaffold sequences and their corresponding Pinto Abalone cDNA sequences were uploaded to Augustus v3.3.3, a gene prediction tool (Stanke et al. 2008). Any neighboring or overlapping sequences predicted by Augustus were run through NCBI Nucleotide Blast database.

RESULTS

RNA extraction, cDNA preparation, and Pinto Abalone transcriptome assembly

A final de novo transcriptome was assembled from 130,209 transcripts after trimming. Data from three individuals was used to construct the reference transcriptome, a pre-exposure animal, and 7-month control animal, and a 7-month experimental animal. Sixty eight genes were differentially expressed (p=0.001) between pre-exposure, 24-hour exposed, 3-month exposed, 7-month exposed, and 7-month control individuals included in the analysis (see Figure 2.3). Annotations were derived using Trinotate through searches of NCBI BlastP, NCBI BlastX, and

EMBL EggNOG databases. Gene ontologies were derived using NCBI Blast and EMBL pfam databases. Eighteen of the total 68 DEGs were identified with either annotation or gene ontologies, or both (see Table 2.2).

WS-RLO infection intensity of pinto abalone

Quantitative PCR (qPCR) data was analyzed for number of copies of DNA per reaction. Data was analyzed in duplicate samples. Average copies/reaction and standard deviations are shown in Table 2.1. Both WS-RLO bacterial genes and RLOv copies/reaction were measured for select samples. Two of the control animals at 7 months that were used for the final transcriptome analysis showed no WS-RLO or RLOv copies/reaction, confirming no contamination of control Pinto Abalone with RLO. Data for all 4 exposed animals at 7 months, and the one animal exposed at 3 months, are included and confirm WS-RLO and RLOv infection in all exposed animals at advanced timepoints (Figure 2.2). This confirms that only the exposed animals were infected with the RLO, while control animals remain naïve throughout the experiment.

Patterns of gene expression in Pinto Abalone exposed to WS-RLO

Sixty-eight genes (0.05% of the total number of transcripts sequenced) were differentially expressed with $p<0.001$, and at least a 4-fold difference in expression. Heat map analysis was implemented to look for patterns in gene expression differences between treatment groups in n=17 animals, across 7 months of infection. Heat map clustering (Figure 2.3) showed four main transcript clusters (Table 2.2). In Group 1, pre-exposure animals and exposed animals at 7 months post-infection show downregulation of transcripts relative to control animals at 7 months, and infected animals at 24 hours post-infection and 3 months post-infection. Group 2 DEGs shows upregulation in the majority of pre-exposure, 24-hour infected, 3-month infected, and 7-month control animals, but variation with some individuals in each group showing relative

downregulation of the transcripts in that cluster. All individuals in the 7-month infected group show downregulation in these Group 2 DEGs. In Group 3, there appear to be two different patterns of DEG regulation, one with strong upregulation of transcripts in the 7-month infected animals, and to a lesser degree, the 3-month infected individual. The other sub-cluster within Group 3 shows upregulation of transcripts in 7-month infected animals, and some upregulation in the majority of the 7-month control animals. The fourth major cluster shows upregulation in a majority of the pre-exposure animals (though with some DEGs showing equal up- and down-regulation averaged across individuals) and in the 24-hour infected animals, but downregulation in the rest of the individuals.

DEG's were divided by lineage into 6 groups (Groups 1, 2, 3a, 3b, 3c, and 4) based on expressed patterns (Figure 2.3, Table 2.2). DEG's with bolded numbers to the right were identified with at least a GO term or other functional annotation. Group 1 had one DEG for which the annotation suggested protein transport and signal transduction proteins. Group 2 had no DEG's that were able to be annotated. Group 3a had a one DEG involved in orexin reception and others involved in viral replication. Group 3b contained 6 annotated DEG's involved in various metabolic processes, including nitrogen and sulfur metabolism, cell structuring, and transport, among other functions (see Table 2.2 for long list of gene ontology terms in these DEG's). Group 3c contained DEG's relating to peptidase activity and signal transduction. Group 4 had five annotated DEG's for which the functions were all related to membrane transport.

Gene Prediction with Augustus

Of the 19 DEG's present in Group 1, 13 were successfully mapped to the Red Abalone genome. Out of these 13, Augustus was able to predict neighboring sequences, introns, or overlapping sequences for eight fragments. Four of those eight Augustus predictions had

matches in BLAST. These four genes included the one annotated DEG from the Trinotate search which agreed with that finding. Of the remaining three sequences with Augustus findings and BLAST matches, one neighboring gene was a 60S ribosomal protein (L13-like), one overlapping sequence matched the sperm lysin precursor in *Haliotis*, and the third overlapped with a STAT5 (signal transducer and activator of transcription) gene in *Haliotis*. (Table 2.3)

Of the 16 DEG's present in Group 3a, six were successfully mapped to the Red Abalone genome. Augustus predicted neighboring sequences, introns, or overlapping sequences for these six fragments. Four of those six Augustus predictions had matches in BLAST. These four genes were all unique sequences compared to those identified with Trinotate methods described above. Of the four sequences with Augustus findings and BLAST matches, one overlapping sequence was a putative microsatellite. Another overlapping sequence matched an ATP-binding cassette transporter G family member 22 protein in *Haliotis gigantea*. A third DEG was identified as a neighboring sequence to genes that were similar to C1q domain containing protein, peptidoglycan recognition protein, hemocyanin, and tyrosine phosphatase genes in various *Haliotis* species. The fourth was a neighboring sequence to a 16s ribosomal protein. (Table 2.3). Thus, there were no consistent metabolic pathway or scaffold patterns in the newly annotated DEGs using this more detailed method.

DISCUSSION

Pinto Abalone showed differential patterns of gene expression throughout the 7-month infection experiment. At both 3 and 7 months, all animals included in DEG analysis that were exposed to withering syndrome tested positive for WS-RLO and RLOv gene copies (Table 2.1, Figure 2.2), confirming that all Pinto Abalone using in transcriptome analysis in the infected

group were indeed infected with the RLO (both the WS-RLO and RLOv forms). These animals also showed RLO loads in histological preparations (Carolyn Friedman, pers. comm.). The infected animals, especially those at 7-months post-infection, also exhibited distinct patterns of gene expression compared to their 7-month control counterparts. During heatmap analysis, the DEGs were divided into 4 main groups, based on similarities in their expression patterns as demonstrated by dendrogram grouping (Table 2.2).

DEG's: Group 1

In Group 1 (Figure 2.3, Table 2.2), relative downregulation of DEGs occurred in pre-exposure animals and exposed 7-month animals. Upregulation of these DEGs occurred in 24-hour exposed, 3-month exposed, and 7-month control animals. A possible explanation for this pattern is the genes are downregulated in healthy animals, but throughout the experiment, both infected and uninfected animals exhibited upregulation in these genes, perhaps due to experimental/handling stress, or other conditions from living in captivity. However, at 7-months post-infection, exposed animals show a unique downregulation in these DEGs, similar to the pre-exposure animals. If these genes, for example, were responsible for a normal stress response in the animals, perhaps animals that are already fighting off a WS infection and have been for 7 months, are not exhibiting appropriate stress responses that they would otherwise be able to exhibit without the additional burden of WS infection. Alternatively, some of these genes may be downregulated similarly to the downregulation of ribonuclease inhibitors in infected oysters (He et al. 2015; Guo and Ford 2016). In this case, perhaps the Pinto Abalone genes are being downregulated in 7-month infected animals because those genes normally inhibit immune or other disease-related responses.

One of the DEGs in this first group (labelled #3 in Figure 2.3 and Table 2.2) was identified as either ADP-ribosylation factor 1-like 2, a GTP-binding protein. In humans, this protein is involved in Golgi vesicle budding, and it's downregulation in the 7-month exposed animals (compared to 7-month control animals) could result in less protein transport and changes to Golgi protein trafficking (https://www.uniprot.org/uniprot/P84077, Table 2.2). In mammal models, Golgi disassembly is a response to stress and can lead to cell death (Machamer 2015), but this appears to be understudied or not examined in mollusks. Although only one gene was annotated and assigned any functional gene ontology information, this group of DEGs is an interesting target area for further exploration, as this downregulation may be a result of advanced WS disease state. The Augustus results suggest that there is downregulation in the region of the genome where a 60S ribosomal protein gene is located (Table 2.3). Understanding which genes in the Pinto DEGs were nearby this 60S ribosomal gene could be important for understanding the physiological processes downregulated during advanced disease state. Interestingly, an Augustus-predicted gene that overlaps with a downregulated DEG in this group was identified as a sperm lysin gene, a gene involved in reproduction (Vacquier and Lee 1993), indicating that reproduction may be hindered in animals after a 7-month infection. The sheer number of unnamed genes also leads us to call for more genomic resources in mollusks, especially in aquaculture contexts where selective breeding would be enhanced by this knowledge (Hollenbeck and Johnston 2018).

DEG's: Group 2

The Group 2 DEGs feature 13 genes that show greater variation in up- or down-regulation of DEGs within groups. However, the overall pattern is that these Group 2 DEGs are all downregulated in the 7-month infected animals compared to all other groups. The DEGs in

this group may be downregulated as a result of 7-month infections and may reflect gene expression changes at advanced stages of the disease. This group of genes is also an interesting target group for understanding genetic response to WS in Pinto Abalone. The difference between Group 1 and Group 2 DEGs is that Group 2 genes are not also downregulated in the pre-exposure animals. Whereas Group 1 genes may emphasize genes that extremely WS-impacted animals are unable to express, Group 2 genes may be genes that are unique targets of WS infection in all animals, regardless of other stress responses (such as those to living in captivity). Unfortunately, none of the 13 DEGs in this group were able to be annotated or assigned any functional terms, such as gene ontology labels. Thus, future work should focus on identifying what these genes are and in what metabolic pathways they are integrated.

DEG's: Group 3

The Group 3 DEGs are all downregulated in the pre-exposure animals and 24-hour infected animals. However, Subgroup 3a genes (Figure 2.3) are upregulated in the 7-month exposed animals, and to a lesser extent in the one 3-month exposed animal. These genes are an interesting area for further exploration for understanding Pinto Abalone response to WS because they are uniquely upregulated only in long-term exposed/infected animals. These genes, therefore, may be activated in response to infection and demonstrate which genes are upregulated in response to long-term infection.

Of the four DEGs that have annotations in subgroup 3a, two are of viral origin, one being a replicase polyprotein, which is associated with the biological process of viral replication, and the other a structural polyprotein. An NCBI BLAST query for both sequences yielded no matches. As the genome of the phage that infects the RLOv has been sequenced (Closek et al. 2016), it is not likely that these viral sequences then are from the phage hyperparasite. Thus, they

may be from a yet undescribed hyperparasite of the RLO or a viral parasite of the abalone that opportunistically impacts animals already stressed by withering syndrome (since it only appears upregulated in the 7-month exposed animals). Alternatively, these genes could be of viral origin but now integrated into the abalone genome. In humans, the estimate is that 5-8% of our genetic content is of viral origin retrotransposed into the genome (Lander et al. 2001; Belshaw et al. 2004).

Of the other two DEGs with annotation in this subgroup, orexin receptor type 2 and uncharacterized protein ORF91 were upregulated only in the 7-month exposed animals relative to the controls. The biological processes associated with orexin receptor type 2 include feeding behavior and cellular responses to hormones, among other processes (See Table 2.2 for full list). Orexin in mammalian systems regulate hunger and stimulate food consumption (Sakurai et al. 1998). In advanced stages of withering syndrome, Pinto Abalone are starving from lack of digestive capacity, so this upregulation of an orexin receptor is likely an attempt to stimulate feeding behavior. However, with impaired digestive function from WS, animals are unable to get nutrients from their food. Uncharacterized protein ORF91 is a protein found in chloroplasts, with no biological process attributed as of yet, and very little is known about it (https://www.uniprot.org/uniprot/Q3BAI2). It is likely that this protein being found here is the result of contamination from food in the digestive system of the sample animals. It may show upregulation in the 7-month exposed animals because they are unable to digest food as their digestive systems were impaired by the WS-RLO and RLOv.

Augustus found genes that overlapped the un-annotated DEGs in this group, as well (Table 2.3). Notably, one DEG overlap of the comp87279 sequence most closely matched a C1q domain containing protein or a peptidoglycan recognition protein in *Haliotis discus*. These

proteins are associated with immune and antigen function in animals, including mollusks (Dziarski and Gupta 2006; Arivalagan et al. 2017). As Group 3a DEGs were all upregulated in the 7-month infected animals, this indicates that the animals had some immune response to infection.

The DEGs in the other Subgroups 3b and 3c (Figure 2.3) are upregulated in 7-month exposed and control animals. These DEGs may be involved in the long-term response to life in captivity, such as a response to living in recirculating seawater or remaining on a consistent diet for months. Cysteine sulfinic acid decarboxylase is upregulated in all animals at 7 months and is associated with a variety of catabolic and metabolic processes, according to biological process gene ontology results (Table 2.2, #9). It is has been demonstrated that captivity can have wide-reaching affects on metabolic processes in other animals (Palme et al. 2005). Mussels held in captivity experience metabolic changes similar to mussels held in captivity and being fasted (Roznere et al. 2014), and similar stress responses may apply to abalone. The metallopeptidases upregulated in all 7-month animals (Table 2.2, #12 and #14) are associated with the inflammatory response and cell migration, and have been shown to be upregulated in other animals exposed to stress, such as a biocide exposure (Jia et al. 2011) but also in oysters in disease resistant lines exposed to diseases (McDowell et al. 2014). The protein associated with cartilage (Table 2.2, #13) has multiple possible identities, and all are related to growth and cell-cell organization with cartilage. The biological process assigned to this DEG is related to chitin metabolism. As the molluscan radula is composed largely of chitin on a cartilaginous base, it is likely that this upregulation found in all 7-month animals is related to stress on the radula from scraping manmade surfaces in captivity. A nonspecific neurotrypsin or protease is also upregulated in 7-month animals and is associated with exocytosis and proteolysis (Table 2.2,

#16). A viral structural polyprotein, similar to those upregulated in Subgroup 3a was also found upregulated in both 7-month groups here (Table 2.2, #17). As this viral protein did not match any other BLAST results as well, the same discussion above may explain the presence of this gene here. Lastly, the peptidase (Table 2.2, #1) upregulated mostly in the 7-month exposed and in some of the 7-month control animals may be a bacterial protein, but it is poorly characterized (https://www.uniprot.org/uniprot/R4SR89) and is therefore unremarkable here.

DEG's: Group 4

The Group 4 DEGs show mixed upregulation and downregulation in pre-exposure and 24-hour infected animals, but downregulation in the 3-month exposed individual and both 7-month groups. These DEGs do not, therefore, elucidate any response to WS in Pinto Abalone. According to the gene ontology for biological processes, all of the DEGs with annotations in this group are related to transmembrane transport. There are no strong patterns, however, between treatment groups for differential expression direction.

Conclusion & Significance

This study shows distinct patterns of differential gene expression involved in the long-term exposed to the WS-RLO and RLOv in Pinto Abalone. Different groups of transcripts show distinct regulation patterns, with some associated with life in captivity and others associated with long-term exposure to the disease WS. A few genes of particular interest function in hunger regulation and possible immune response. This work represents the first transcriptomic response to WS in Pinto Abalone, and highlights many areas for further exploration to understand this disease process. Deeper annotation and characterization of the Pinto Abalone genome and transcriptome would help elucidate functional differences in exposed and control animals. Future studies may consider comparing Pinto Abalone response to closely related species with higher

WS-resistance, such as Pink or Green Abalone (Álvarez Tinajero et al. 2002; Moore et al. 2009). This study has identified at least 68 gene responses that show differential expression between exposed and control animals that should be further studied.

Because different species of abalone show differences in their susceptibility to withering syndrome (Crosson et al. 2014), transcriptomic analysis would be particularly useful if it could differentiate host species responses to bacterial challenges among different abalone taxa. Indeed, a case study on a bacterial pathogen of American oysters demonstrates how transcriptomics can be used to better understand resistance pathways in mollusks with severe diseases (Box 1, (McDowell et al. 2014)). Studies like this one highlight the importance of understanding the molecular pathways that lead to disease states in marine organisms, and lead to a fervent call for better annotated molluscan genomes. In study systems with varying susceptibility levels to a disease (like the *Haliotis* species in the northeastern Pacific with varying susceptibility to WS (Crosson and Friedman 2018)), understanding the differences in molecular responses to disease leads to an understanding of why and how closely related species are differentially susceptible to diseases. However, to come to an understanding of differential resistance, the response to the disease itself in a susceptible species must be characterized before comparing with other, more resistant species. This study is the essential first step filling this knowledge gap of the gene expression response to WS-RLO in abalone.

BOX 1: Transcriptomic Analysis as a Tool for Understanding Disease Resistance Differences

Study: Transcriptome of American Oysters, *Crassostrea virginica*, in Response to Bacterial Challenge: Insights into Potential Mechanisms of Disease Resistance (McDowell et al. 2014)
Parasite: *Roseovarius crassostreae* (gram-negative bacteria)
Host: *Crassostrea virginica* (American Oyster)
Disease: Roseovarius Oyster Disease (ROD)
Symptoms: Slow and reduced growth, mortality, unequal shell growth, cupping of left valve, shell checks and conchiolin rings ("brown rings") on the internal surface of the shells

Like abalone responses to WS, oysters vary in their susceptibility to ROD. Within the species *Crassostrea virginica*, different lines of oysters show different levels of resistance to *Roseovarius crassostreae*. After 3 months of exposure to the pathogen, mortality in a susceptible line can reach up to 3x that in the resistant line, whose mortality rates are similar to animals never exposed to the pathogen. Researchers used transcriptomics to determine the underlying molecular mechanisms that can explain these differences.

They discovered that 24% of the variation in gene expression patterns between the resistant and susceptible groups exposed to the pathogen could be explained by genetic differences between the lines. This means that evolutionary (or more specifically, breeding) history explained a quarter of the variation in molecular responses to the pathogen in different lines of the same species of oyster. They also identified specific contigs, or gene fragments, that were upregulated or downregulated significantly in the exposed susceptible line. Some of the highly upregulated genes are involved in processes like detoxification, which indicates ongoing negative impacts of infection in susceptible animals. Additionally, the upregulated metabolic process genes support the hypothesis that a failed immune response against ROD places a large metabolic demand on the oysters, leading to their eventual death. In the resistant line, upregulated genes included those involved in extracellular matrix modification, ligand-binding proteins, stress proteins, and signaling proteins. In short, inflammatory response and immune function genes were differentially upregulated in the resistant line, supporting the hypothesis that resistance to this pathogen has a molecular underpinning. Understanding the molecular pathways that lead to these differences in resistance and susceptibility, and in the response to infection in general, is essential for understanding how closely related organisms respond differently to diseases in the wild. It also lends insight into the mechanisms employed by resistant animals to resist diseases.

Table 2.1: qPCR copy numbers of WS-RLO and RLOv
Copies/reaction of DNA for the WS-RLO and RLOv for 7 samples, including control and experimental (exposed) animals. Data provided are mean copies/reaction ± standard deviation.

Animal ID	Time	Treatment	WS-RLO	RLOv
C-7mo-1	7 month	Control	0 ± 0	0 ± 0
C-7mo-2	7 month	Control	0 ± 0	0 ± 0
E-3mo-1	3 month	Exposed	13 ± 1.53	7.21 ± 1.92
E-7mo-1	7 month	Exposed	335 ± 5.54	2950000 ± 95500
E-7mo-2	7 month	Exposed	23400 ± 3230	6130000 ± 347000
E-7mo-3	7 month	Exposed	6.38 ± 0.819	3390 ± 474
E-7mo-4	7 month	Exposed	97.2 ± 10.9	648 ± 18.5

Figure 2.1: Experimental design for Pinto Abalone infection with WS
Pinot Abalone were held in two separate tank systems with a head tank containing red abalone. In the control treatment, red abalone were healthy, uninfected animals. In the experimental treatment (bottom), Red Abalone was infected with WS-RLO. In the control treatment (top), Red Abalone in the head tank were healthy, uninfected individuals.

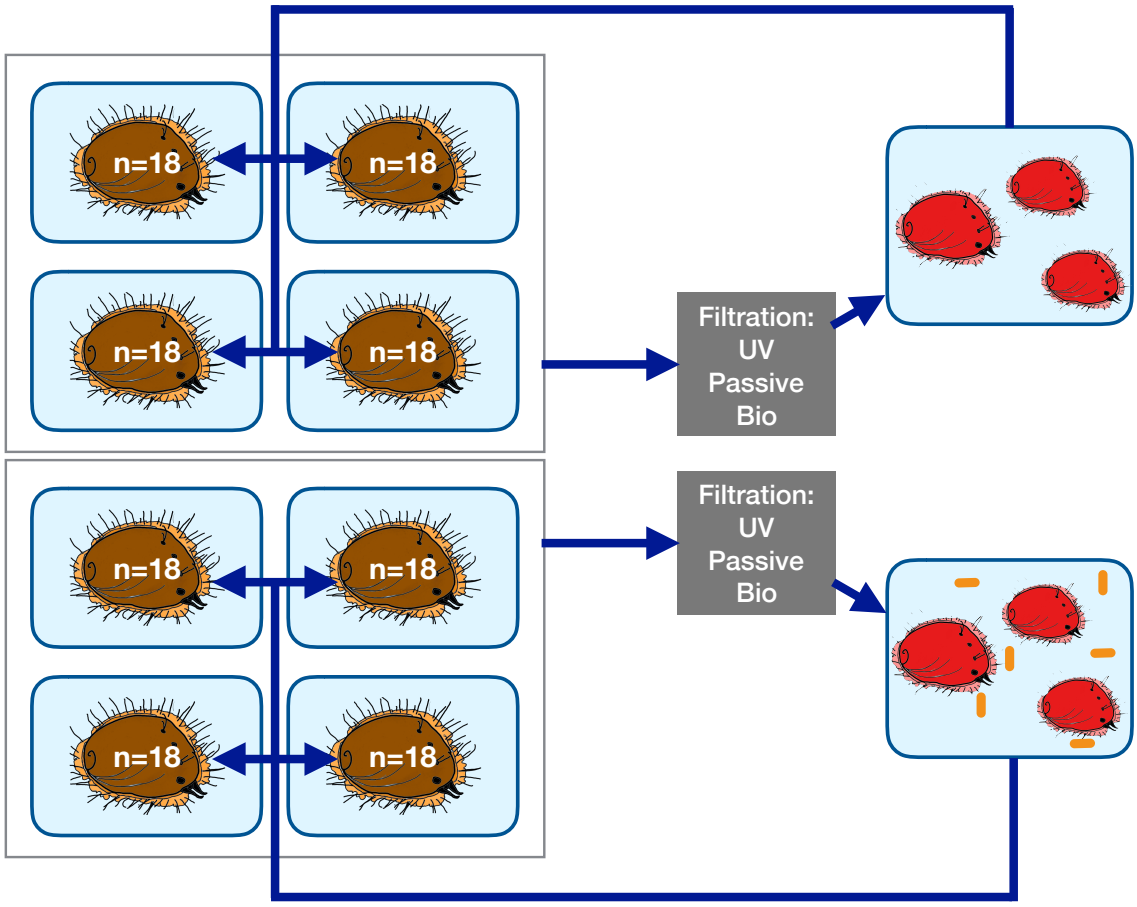

Figure 2.2: Infection intensity of WS-RLO and RLOv in 3-month and 7-month exposed animals.
qPCR copy/reaction averages of the RLO and RLOv DNA fragments. Data is plotted on a logarithmic scale. See Table 1 for control infection values, which were all zero. Only exposed animals (one at 3 months and 4 at 7 months) are shown. Control animals all had zero copies of DNA in both categories.

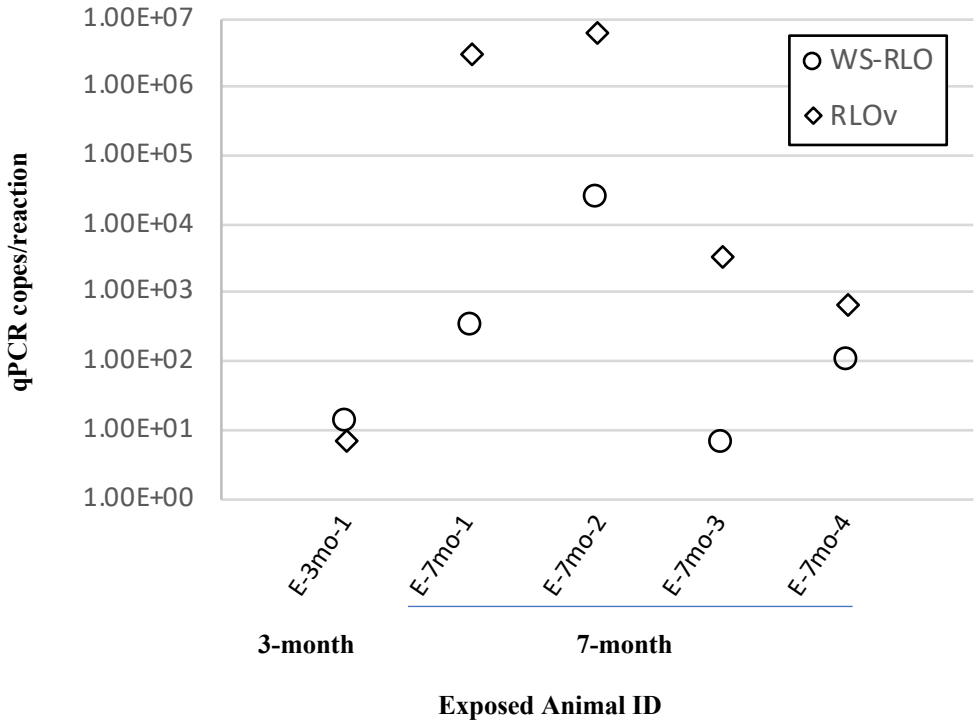

Figure 2.3: Heatmap of differentially expressed transcripts in naïve (control) Pinto Abalone and abalone exposed to WS-RLO over a 7-month experimental course.
Four main clusters of differentially expressed genes (DEGs) were found among the n=17 animals using in heatmap analysis, and annotated along the clustering dendrogram, which shows similarities in expression patterns between individuals. 18 DEGs were annotated and/or had GO terms attributed to them, and are labelled on the right by their gene ID # (See Table 2). Purple colors represent relative downregulation. Black represents neutral regulation relative to other animals. Yellow represents relative upregulation relative to other individuals. Animals are labelled as either C or E for control or exposed, respectively. The middle portion of their IDs is the time they were sampled (e.g. 0 for t=0 and 24h for t=24h, etc.).

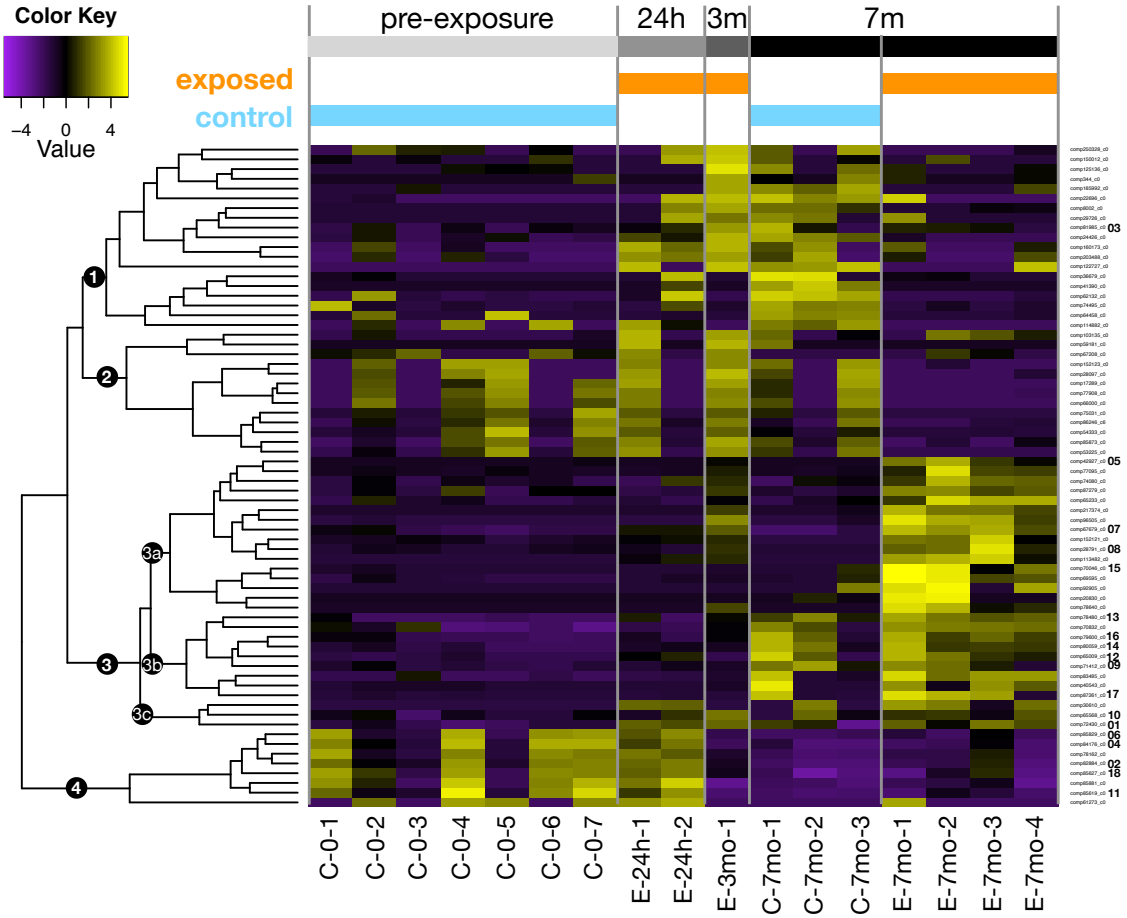

Table 2.2: Gene annotation and biological process gene ontology terms for 18 differentially expressed genes. 18 DEGs, labelled on the heat map in Figure 3, had gene annotations or gene ontology terms attributed to them. The table summarizes the direction of differential expression for each DEG, the annotations from NCBI BlastX/BlastP and EMBL EggNOG, as well as gene ontology assignments from NCBI Blast and EMBL pfam. Where direction of differential expression is expressed as "up/down," individuals in each group were split roughly evenly between upregulation and downregulation of that particular gene.

Gene ID	Gene ID #	Heat Map Group	type of DE (C-0)	type of DE (C-7mo)	type of DE (E-7mo)	Annotation	GO: Biological Process
lcl|comp81985_c0	3	1	down	up	down	ADP-ribosylation factor 1-like2; GTP-binding protein	protein transport, small GTPase mediated signal transduction, vesicle-mediated transport
lcl|comp82884_c0	2	4	up/down	down	down	organic cation transporter 1; solute carrier family 2	carnitine transmembrane transport, determination of adult lifespan, organic cation transport
lcl|comp84176_c0	4	4	up/down	down	down	solute carrier family 22 member 15	ion transport, transmembrane transport
lcl|comp85829_c0	6	4	up/down	down	down	solute carrier family 22 member 6-A	transmembrane transport
lcl|comp85619_c0	11	4	up/down	down	down	monocarboxylate transporter 3	plasma membrane lactate transport, transmembrane transport
lcl|comp85627_c0	18	4	up/down	down	down	monocarboxylate transporter 6; major facilitator superfamily	plasma membrane lactate transport, transmembrane transport
lcl|comp42927_c0	5	3a	down	down	up	orexin receptor type 2	cellular response to hormone stimulus, circadian sleep/wake cycle process, feeding behavior, neuropeptide signaling pathway, phospholipase C-activating G-protein coupled receptor signaling pathway, regulation of circadian sleep/wake cycle, response to peptide, synaptic transmission, G-coupled receptor signaling pathway
lcl|comp67679_c0	7	3a	down	down	up	viral replicase polyprotein	DNA-templated transcription, viral genome replication
lcl|comp28791_c0	8	3a	down	down	up	viral structural polyprotein	-
lcl|comp70046_c0	15	3a	down	down	up	uncharacterized protein ORF91	-
lcl|comp71412_c0	9	3b	down	up	up	cysteine sulfinic acid decarboxylase	cellular nitrogen compound metabolic process, small molecular metabolic process, sulfur amino acid catabolic process, sulfur amino acid metabolic process, taurine biosynthetic process, carboxylic acid metabolism, cellular amino acid metabolic process
lcl|comp65009_c0	12	3b	down	up	up	A disintegrin and metalloproteinase with thrombospondin motifs; metallopeptidase with thrombospondin type 1 motif	cell migration, cell-matrix adhesion, cellular response to BMP stimulus, cellular response to interleukin-1, cellular response to tumor necrosis factor, negative regulation of cellular response to hepatocyte growth factor stimulus, negative regulation of cellular response to vascular endothelial growth factor stimulus, negative regulation of hepatocyte growth factor receptor signaling pathway, negative regulation of chondrocyte differentiation, proteoglycan catabolic process, proteolysis involved in cellular protein catabolic process, regulation of endothelial tube morphogenesis, regulation of inflammatory response, proteolysis
lcl|comp78480_c0	13	3b	down	up	up	collagen alpha-1(XIV) chain; cartilage matrix protein; growth plate cartilage chondrocyte morphogenesis	chitin metabolic process
lcl|comp80059_c0	14	3b	down	up	up	A disintegrin and metalloproteinase with thrombospondin motifs gon-1	cell migration, ER to Golgi vesicle-mediated transport, gonad development, protein transport
lcl|comp79600_c0	16	3b	down	up	up	Neurotrypsin; protease	exocytosis, proteolysis
lcl|comp87261_c0	17	3b	down	up	up	viral structural polyprotein	DNA-templated transcription
lcl|comp72430_c0	1	3c	down	up/down	up	glutamyl endopeptidase; peptidase s1 and s6 chymotrypsin hap	-
lcl|comp65568_c0	10	3c	down	up/down	up	-	signal transduction

Table 2.3: Augustus results for gene finding in DEGs from Groups 1 and 3a.
DEGs from Groups 1 and 3a were mapped to the Red Abalone genome, and corresponding Scaffold sequences are summarized. In sequences where more than one match was found within the same Red Abalone scaffold, the highest percent identity is shown in the table. Where the Pinto Abalone DEG did not map to the Red Abalone genome, "none" is indicated. Augustus gene tool (Stanke et al. 2008) findings are summarized as either overlapping sequences with the Scaffold and/or cDNA DEG sequence, neighboring sequences, or introns. In multiple DEGs, Augustus was unable to predict gene locations. Even where Augustus found results, the Augustus output did not always correspond to a match in the NCBI BLAST database.

DEG GROUP	DEG ID	Red Ab Scaffold	% ID	Augustus finding	BLAST results
1	comp250328	83	95.56	neighboring sequence	none found
1	comp150012	none	none	x	x
1	comp125136	1064	97.94	no match	none found
1	comp344	none	none	x	x
1	comp185992	none	none	x	x
1	comp22696	37	97.06	neighboring sequence	60S ribosomal protein L13-like; partial mRNA for ribosomal protein L13-like
1	comp8002	98	90.85	no match	x
1	comp29726	167	73.46	neighboring sequence	none found
1	comp81985	953	highest 99.26	overlapping sequence	ADP ribosylation factor
1	comp24426	42	98.17	intron	none found
1	comp160173	1216	highest 91.43	no match	none found
1	comp203488	1216	99.76	no match	none found
1	comp122727	none	none	x	x
1	comp36679	202	highest 100	overlapping sequence	sperm lysin precursor Haliotis
1	comp41390	99	highest 98.8	overlapping sequence	STAT5 (signal trasnducer and activator of transcription) in Haliotis, microsatellite
1	comp62132	64	highest 97.5	no match	none found
1	comp74495	221	97.63	neighboring sequence	none found
1	comp64458	none	none	x	x
1	comp114822	none	none	x	x
3a	comp42927	693	highest 99.27	overlapping sequence	none found
3a	comp77095	1149	highest 100	overlapping and introns	microsatellites (H. discus)
3a	comp74080	159	highest 95.86	overlapping sequence	Haliotis gigantea ATP-binding cassette transporter G family member 22;
3a	comp87279	63	highest 98.86	overlapping sequence	H. discus: C1q domain containing protein 1; peptidoglycan recognition protein gene; H. diversicolor: hemocyanin isoform 1 (h1)' H. corrugata: tyrosine phosphatase like gene
3a	comp65233	188	highest 100	overlapping and introns	none found
3a	comp217374	none	none	x	x
3a	comp96505	none	none	x	x
3a	comp67679	none	none	x	x
3a	comp152121	none	none	x	x
3a	comp28791	none	none	x	x
3a	comp113482	none	none	x	x
3a	comp70046	none	none	x	x
3a	comp69595	224	highest 77.83	neighboring sequence	16S ribosomal protein
3a	comp92905	none	none	x	x
3a	comp20830	none	none	x	x
3a	comp78640	none	none	x	x

Chapter 3

Comparative digestive physiology and the effect of temperature stress on abalone across the Pacific

INTRODUCTION

Many marine host-pathogen systems are poorly understood, and even less is known about how climate change will affect the dynamics of these systems (Burge et al. 2014). Of particular interest is the abalone (genus *Haliotis*) and *Rickettsiales*-like organism (RLO) system. The RLO is a bacterial parasite that infects abalone digestive tissues, which leads to starvation and a characteristic degradation of the gastropod foot (a disease called withering syndrome, or WS) (Crosson et al. 2014). First identified in black abalone following an El Niño event (Vanblaricom et al. 1993), WS has since been detected in all abalone species on the northeastern Pacific. Abalone guts often harbor a Rickettsiales-like organism, a bacteria that causes withering syndrome (WS-RLO) and causes distinct morphological changes in the abalone gut (Friedman et al. 2000). WS-RLO infected abalone experience reduction in growth, food intake, and metabolism (Gonzalez et al. 2012). Apart from these macro-level observations, the critical digestive functional changes that occur during WS-RLO infection and high temperature conditions (see Chapter 2 for more details), especially during sub-lethal stages of the disease, have not been studied.

Curiously, not all species express WS at environmentally relevant temperatures (Crosson et al. 2014). For instance, WS affected Black Abalone (*Haliotis cracherodii*) so severely that this disease is listed as a main contributing factor to the federal classification of Black Abalone as "Endangered." Red Abalone (*H. rufescens*) is also quite susceptible to WS (Moore et al. 2000),

whereas Green Abalone (*H. fulgens*) and Pink Abalone (*H. corrugata*) are more resistant to WS infection and associated mortality. Green and Pink Abalone are each relatively highly resistant to the disease in the wild (Álvarez Tinajero et al. 2002; Moore et al. 2009), yet experimentally high temperatures can increase disease severity in *H. fulgens* held in captivity (Garcia-Esquivel et al. 2007). WS, therefore, appears to be modulated, in part by temperature, wherein we see abalone exposed to high temperatures generally showing marked increases in infection intensity and disease (Moore et al. 2000; Braid et al. 2005; Moore et al. 2009; Rogers-Bennett et al. 2010; Moore et al. 2011; Crosson et al. 2014). Black Abalone declines have been linked to increases in withering syndrome (WS) correlated with these extreme warm water events (Raimondi et al. 2002), and high temperature anomalies are an ongoing threat to the recovery of this Endangered species (Butler et al. 2009).

High temperature alone is also known to also cause stress in other, non-WS infected species. Heat stress is a defined threat to farmed abalone species worldwide (Hooper et al. 2014), even in species that are not exposed to WS. Critical thermal maxima for adult abalone have only been measured in adults of five species, and limited to Black and Red Abalone from the northeastern Pacific ((Diaz et al. 2000), reviewed in (Morash and Alter 2015)). Furthermore, New Zealand's abalone (*H. iris*, known locally as Pāua,) are smaller at the northern (and warmest) end of their biogeographic range (Dr. Norman Ragg, pers. comm.). Red Abalone and Pāua are commercially farmed and there is some evidence that temperature impacts gut function of at least some abalone species (Hooper et al. 2014). However, the mechanisms linking heat stress to a reduction in abalone digestive performance, especially specific digestive enzyme activity levels and algal digestibility, all of which matter for successful aquaculture, remain unclear. As expected in ectotherms, feeding rate is impacted by temperature; Red Abalone

increase their feeding rates progressively as temperatures increase to the highest they normally experience in the wild (about 18°C) but then decline sharply at higher temperatures (Leighton 2000). There is also clear evidence of physiological stress at temperatures >18°C (Rogers-Bennett et al. 2010; Morash and Alter 2015).

Increasing temperature can impact gut morphology and lead to overall declines in digestive functions. For example, Red Abalone that experience heat stress, starvation, or WS exposure (and combinations of the three) undergo digestive gland glycogen depletion over long periods of time (Braid et al. 2005). Haemocyte infiltration in the digestive gland, an indicator of physiological stress, is impacted by high temperature stress in Red Abalone (Hooper et al. 2014). There are no studies, however, detailing the effect of heat stress on other individual aspects of digestive physiology, such as digestive enzyme function and digestive efficiency, which is surprising given the centrality of these processes in digestive tract function. Abalone are able to alter their metabolism by increasing oxygen consumption during periods of stress (Reviewed in (Morash and Alter 2015)), but it is unknown whether abalone can alter digestive strategies to keep pace with the higher energetic demands of heat stress.

Understanding how heat stress, disease, and the combination of the two impact abalone digestion is difficult because the fundamental, basic knowledge of how abalone guts function is limited. The known morphology suggests that abalone guts consist of a mouth, esophagus, digestion gland/stomach complex, and intestine (Mclean 1970; Morton 1979; Bevelander 1988; Nybakken 1996). However, even the basic function and anatomy of the stomach and intestine are unclear, with crude drawings and data making it difficult to discern organs and function.

Functional digestion and physiology of abalone guts is also poorly studied. For example, digestive enzyme activities have been assayed but with critical methodological errors that

prevent application of the data to whole organisms physiology. For instance, the gut is often homogenized as if it is a single organ without compartmentalized function (Bansemer et al. 2016a; Bansemer et al. 2016b), even though there is likely compartmentalization of abalone gut function based on the morphology (Figure 3.1). Furthermore, digestive enzyme activity levels, which indicate an animal's ability to digest specific substrates, are often measured at temperatures (e.g., 37°C) irrelevant to any abalone species (Picos-Garcia et al. 2000; Garcia-Carreno et al. 2003; Garcia-Esquivel and Felbeck 2006) because the methodology is adapted from studies on humans, rather than adjusting for physiologically-relevant conditions for the species of interest. Moreover, to my knowledge, there are no detailed comparative investigations of gut physiology in wild abalone and no detailed studies of their gut physiology on natural diets. This knowledge of healthy abalone gut function is critical for understanding the impact of stressors, such as disease and temperature, on abalone digestive physiology.

This study has two main goals:

Goal 1: Determine whether and, if so, how abalone digestive function changes with increased metabolic demand at the highest temperatures they experience in the wild.

Goal 2: Compare the impact of high temperature and resultant ramped up metabolism on digestive tract function between two distantly related *Haliotis* species, one of which doesn't experience WS.

To address the goals of this study, metabolic rates, digestibility, and digestive enzyme activities were compared between Pāua (*Haliotis iris*) and Red Abalone (*H. rufescens*). Both species experience stress and limited growth at higher temperatures (details above), yet Pāua has never been exposed to the WS-RLO, as the disease is not found in New Zealand. Metabolic rates of each species were measured at both an ambient temperature (i.e., a temperature common in

the species' normal range) and a species-relevant "stressful" temperature 5°C above that ambient temperature and which is approximately the maximum stressful temperatures these animals experience in the wild. These "stressful" temperatures were used to determine the impact of high temperature on the energy demands of the two species. To examine digestive tract function, I measured organic matter and individual nutrient (protein, carbohydrate, and lipid) digestibilities of algae at the two temperatures in each species. Finally, to investigate any mechanisms of altered digestion, I measured the activity levels of amylase, maltase, and trypsin in the digestive gland of the abalone, and compared them among the two species, both, at the ambient and elevated "stressful" temperatures (Karasov and Douglas 2013). Amylase breaks polysaccharides into glucose and maltose, the latter is broken down by maltase into glucose. Trypsin breaks polypeptides into small peptide molecules, so these three enzymes can provide a broad overview of the beginnings of enzymatic digestion in these animals of both carbohydrates (the main component of their diet) and proteins. Overall, this study addresses some basic questions about abalone digestion in the face of temperature stress that may exacerbate disease in the wild and in cultured populations of these important animals.

METHODS

Animal collection and husbandry – Red Abalone

Twenty Red Abalone, approximately 190 grams each, were purchased from The Cultured Abalone aquaculture facility (Goleta, CA, USA). They were transferred to the UCI animal care facility and acclimated to a recirculating filtered seawater system at 12.5°C for approximately 2 months and fed *Macrocystis pyrifera* daily. Animals were divided into two identical tank systems, each with shared sump and UV filtration amongst the tanks that were in series with the sump (Figure 3.2.). The difference between the systems is that one had heaters in the sump to

raise the temperature of the water in that system to 17.5°C (5°C above the ambient system). Before the experiment started, the water temperature in the heated system was warmed by approximately 1°C/day until it reached 17.5°C, which took about one week. Animals were acclimated to their respective temperature treatments (ambient or heated) for approximately one month before starting fecal collections.

Animal collection and husbandry – Pāua

Nine Pāua were collected from Breaker Bay and eleven Pāua were collected from Princess Bay (Wellington, New Zealand) during the first week of March, 2018, and housed in the Victoria University Coastal Ecology Lab. They were housed in a runway of flow-through filtered seawater for 10 days, then transferred to individual buckets with the same flow-through seawater (14°C, which was the ambient temperature of the seawater pumped into the facility). Pāua were allowed to acclimate to their individual containers for another week, and were fed *Ecklonia radiata* and *Lessonia variegata* (collected from the same bays) *ad libitum*. After one week, a combined head tank and bath system was used to raise the water temperature in half of the animals to 5°C above ambient by approximately to 1°C/day (Figure 3.2). After one week, a heat treatment of 5°C above ambient temperature (19°C) was achieved. The animals were acclimated to their temperature treatments for an additional two weeks before fecal collections began.

Both Red Abalone and Pāua were fed *ad libitum* during that acclimation periods. Before beginning the experiment, animals were not fed for 24 hours and all feces were removed from treatment buckets to ensure any fecal material collected during the experiment was from the experimental diet only. All ambient treatment Pāua (*H. iris,* n=10) survived throughout the experiment, and ate every day. Due to an irrigation blockage, one of the heat treatment Pāua died. Furthermore, one heat treatment Pāua was removed from analysis because its metabolic

rate measured an order of magnitude above any other animal measured and it rarely ate, making it not useful for a feeding trial. Thus, the heated Pāua used for analysis had a sample size of n=8. Red Abalone (*H. rufescens*) had no survival issues and all animals (n=10) were included in analysis for ambient and heated treatments.

Experimental Design

Animals were weighed and shell length and width were measured at the start of the feeding trials, and at the end during dissections. Animals were housed individually in 3L containers in flowing seawater, with turnover rate at least once per hour. Every day, animals were fed brown algae, of a species they would encounter in their respective natural habitats. Red Abalone were fed *Macrocystis pyrifera*, and Pāua were fed *Ecklonia radiata* and *Lessonia variegata*. Animals were fed *ad libitum*, and always offered more than they would eat within the day. After 24 hours, the remaining food was removed and replaced with a new piece of dried algae. Algae was dried prior to use to help reduce the presence of any other organisms on the algae, and to measure the approximate amount of algal mass offered to each animal. Fecal material was removed with a siphon. Saltwater was decanted off and the feces were rinsed once with deionized water, and dried at 60°C overnight. Dried feces each day were combined with previous days' collections for each abalone, and approximately 1-3g of dried fecal material was collected per animal by the end of the experiment. Feeding trials lasted 4 weeks for each species. At the end of 4 weeks, animals were held for less than a week longer at their respective temperatures, and continued to be fed ad libitum their respective diets. During this final week, metabolic rate measurements, final mass and lengths, and tissue samples were taken.

Metabolic rate measurements

After the 4-week long feeding trial, respiration rates were recorded for each experimental animal during daylight hours following methods in Connor, et al. (2016). All measurements were performed at the treatment temperature that an individual had experienced during the feeding trial. Animals were sealed in a chamber of known seawater volume (approximately 1.1-2.3L, depending on the size and shape of the animal) with a stir bar to ensure homogeneity of oxygen saturation in the chamber. An optical dissolved oxygen probe (Neofox, Ocean Optics, Dunedin, FL) measured the decline in dissolved oxygen over time (measuring every 30s) in the chamber. The sensor was calibrated with aerated (100% O_2) and anaerobic (achieved by bubbling N_2 gas into the water within a sealed container) seawater. For each animal, measurements were taken until the oxygen concentration declined by 10%, at which time the chamber was reopened and flooded with oxygen-saturated seawater before beginning another measurement on the same animal, with each animal measured in triplicate. The mass of each animal was recorded, and later corrected by removing the mass of the shell (as the shell has no metabolically active tissue). Metabolic rate in mg-O_2/min g was calculated using Eq. 1, where $V_{respirometer}$ is the volume of the chamber in liters, $V_{abalone}$ is the volume of the entire abalone (L), V_{shell} is the volume of the shell (L), ΔCwO_2 is the change in dissolved oxygen (mg-O_2), Δt is the change in time in minutes, $M_{abalone}$ is the mass of the abalone (g), and M_{shell} is the mass of the shell (g). Metabolic rate in oxygen consumption was converted to calories/min/g using Eq. 2 where the conversion factor is 0.35 cal/mg-O_2. Average Q_{10} per treatment, which measures the sensitivity of metabolic rate to an increase in 10°C, was calculated using Eq. 3.

(Eq. 1) $$M\text{-}O_2 \text{ (mg-}O_2\text{/min g)} = \frac{(V_{respirometer} - V_{abalone} - V_{shell}) \times \Delta CwO_2}{\Delta t \times (M_{abalone} - M_{shell})}$$

(Eq. 2) $$M\text{-}O_2 \text{ (cal/min/g)} = M\text{-}O_2 \text{ (mg-}O_2\text{/min/g)} * 0.35$$

(Eq. 3) $$Q_{10} = \left(\frac{\text{M-O}_2\ \text{Cold}}{\text{M-O}_2\ \text{Heat}}\right)^{\left(\frac{10}{(T_{Heat} - T_{Cold})}\right)}$$

Dissections and tissue sample preparation for biochemical assays

After metabolic measurements were performed, animals were returned to their enclosures to reduce stress and allow them to eat for at least 48 hours before dissections were performed. Animals were placed in ice until unresponsive, then removed from their shell by severing the foot muscle attachment (Figure 3.1). Dissections were performed on a metal tray filled with ice. The digestive organs were removed and separated into different regions (German et al. 2015): radula, esophagus, post-esophagus, stomach, digestive gland (further subdivided into proximal, mid, and distal segments), intestine, and distal intestine (Figure 3.1). The pH of each gut region was measured with litmus paper to determine appropriate pH for later homogenization buffers. Gut contents were squeezed from the esophagus, stomach, digestive gland, intestine, and distal intestine if present (Santos et al. 2018). All gut tissue and contents samples were immediately frozen in 1.5mL vials, either in liquid nitrogen for Red Abalone or at -80°C for Pāua. Pāua samples were transported to UCI on dry ice, and immediately stored at -80°C.

Gut tissue samples were homogenized in ice-cold buffers using a Polytron homogenizer (Brinkman Instruments; Westbury, New York) in 30-second pulses. The digestive gland samples were homogenized in citric acid sodium citrate buffer pH 5.6. Homogenized samples were centrifuged at 9400g for 2 minutes at 4°C, then the supernatant was stored in 100-130 µl aliquots at -80°C until used in assays (German et al. 2015).

Nutrient content sample homogenate preparation

The algal diets for each abalone species were prepared separately. Algae and feces samples were rinsed in DI water, and dried at 60°C for 24-48 hours. Dried algal samples were

ground with liquid nitrogen and a mortar and pestle. They were then homogenized on ice in 25mM Tris-HCl pH 7.0. Samples were centrifuged for 2 minutes at 4°C, then the supernatant was stored in 50-200 µl aliquots at -80°C until used in assays.

Organic matter and protein content assays

Organic content of fecal and algal samples was measured using an ash-corrected digestibility measurement to determine the proportion of organic matter and protein that were digested by each animal. Total fecal collections (as opposed to this ash-corrected measurement) were impossible given the way that abalone scrape algae, producing tiny particles. Hence, small amounts of feces were lost during the experiment no matter which method of fecal collection was used. In this method, ash, the leftover product of combustion, is used as an indigestible marker for the amount of material consumed and excreted (German 2011). To determine the percentage of fecal or algal material that is organic content, samples were dried thoroughly at 105°C, and weighed intermittently to ensure that all water content has evaporated. Samples were combusted on ceramic crucibles at 550°C for 3 hours, cooled to 105°C, and the mass of leftover indigestible mark, ash, was recorded. Apparent organic matter digestibility was calculated using Eq. 4 where a_d and a_f are the mass (g) of indigestible ash in the diet and feces, and m_d and m_f are the organic matter (total matter-ash) mass (g) in the diet and feces, respectively (German 2011). Apparent organic matter (OM) digestibility was calculated, as opposed to total organic matter, because waste may be lost in other ways (e.g. kidney filtration) and because it was impossible to collect all fecal material as in a closed system (see the experimental design above). Nutrient content assays were performed on algal and fecal homogenates following the methods used in (Santos et al. 2018). Protein content was measured using the bicinchoninic acid assay (Smith et al. 1985).

(Eq. 4) $$\text{Apparent Organic Matter Digestibility (\%)} = \left[1 - \left(\frac{a_d}{a_f} \times \frac{m_f}{m_d}\right)\right] \times 100$$

Digestive enzyme assays

The biochemical activity levels of three digestive enzymes (amylase, maltase, and trypsin) were measured at the experimental treatment temperatures using the gut-tissue homogenates from digestive glands, following the methods of (German et al. 2004; Horn et al. 2006; German et al. 2015). Due to assay difficulties, a subset of individuals were used in amylase assays (see legend of figure 3.6).

Statistical analysis

Metabolic rates, apparent organic matter digestibility percentages, and enzyme activities were compared within each species, between the temperature treatments. Species were also compared to one another, but only within similar treatment groups (either ambient or heated treatment) for metabolic rate and apparent organic matter digestibility. Prior to all parametric tests, a Bartlett's test for homogeneity of variance was performed on the data, and a Shapiro-Wilk test for normality was performed on the residuals of all models. Where necessary (comparing within Pāua samples for organic digestibility), a box-cox transformation was used before analysis. Ambient organic digestibility data failed normality tests with multiple transformations, so a non-parametric Kruskal-Wallis ANOVA was used. Individual two-way comparisons were conducted with an ANOVA fitting a linear model in R Studio (R version 3.6.0).

RESULTS

Metabolic rate

Ambient treatment Pāua metabolic rate was 0.0023±0.0004 cal/min/g (mean ± standard error), which trended lower than the heated treatment Pāua metabolic rate at 0.0036±0.0006

cal/min/g ($F_{1,16}$ = 3.22, p = 0.092; Table 3.1; Figure 3.3). Metabolic rate was 56% higher in the heat treatment. Similarly, ambient treatment Red Abalone metabolic rate was 0.0053±0.0005 cal/min/g, which was significantly lower than the heated treatment *H. rufescens* metabolic rate at 0.0070±0.0004 cal/min/g ($F_{1,18}$ = 7.22, p = 0.02; Table 3.1; Figure 3.3). Metabolic rate was 32% higher in the heat treatment.

At both species-relevant ambient treatment ($F_{1,18}$ = 24.6, p = 0.0001; Table 3.1) and heated ($F_{1,16}$ = 22.3, p = 0.0002; Table 3.1) temperatures, Red Abalone had a significantly higher metabolic rate compared with *H. iris* (Table 3.1). Q_{10}, a measurement of sensitivity of metabolic rate to an increase in temperature, was 2.46 for Pāua and 1.73 for Red Abalone.

Apparent organic matter digestibility

Ambient treatment Pāua organic matter (OM) digestibility was 45.49 ± 6.12% (mean ± standard deviation), which was not significantly higher than heated Pāua OM digestibility at 37.92% ± 13.47% ($F_{1,16}$ = 2.16, p = 0.16; Table 3.2; Figure 3.4). Ambient treatment Red Abalone OM digestibility was 68.03% ± 4.64%, which was not significantly higher than the heated Red Abalone OM digestibility at 62.93% ± 8.12% ($F_{1,18}$ = 2.98, p = 0.10; Table 3.2; Figure 3.4). At both species-relevant ambient (χ^2 = 14.29, d.f. = 1, p = 0.00016; Table 3.2) and heated ($F_{1,16}$ = 21.6, p = 0.003; Table 3.2) temperatures, Red Abalone digested a higher proportion of organic matter compared with Pāua (Table 3.2).

Nutrient digestibility

Ambient treatment Pāua protein digestibility was 79.64% ± 3.38% (mean ± standard deviation), which was not significantly different from heated Pāua organic digestibility at 76.41% ± 5.96% ($F_{1,16}$ = 0.327, p = 0.58; Table 3.3; Figure 3.5). Ambient treatment Red Abalone protein digestibility was 70.31% ± 9.58%, which was not significantly different from the heated

Red Abalone protein digestibility at 66.51% ± 15.11% ($F_{1,18} = 0.452$, $p = 0.51$; Table 3.3; Figure 3.5).

Digestive enzyme activities

There were no significant differences between treatments within each species ($p = 0.085$ for Pāua and $p = 0.521$ for Red Abalone; Figure 3.6, Table 3.4) for **amylase** activity. Heated treatment Red Abalone **maltase** activity was significantly higher than the level of maltase activity in ambient treatment Red Abalone ($p = 0.006$; Figure 3.7, Table 3.4). Heated treatment Red Abalone **trypsin** activity was significantly higher than the level of trypsin activity in ambient treatment Red Abalone ($p = 0.029$; Figure 3.8, Table 3.4).

DISCUSSION

This study's two main goals were to (1) Determine whether and, if so, how abalone digestive function changes with increased metabolic demand at the highest temperatures they experience in the wild; and (2) Compare the impact of high temperature and resultant ramped up metabolism on digestive tract function between two distantly related *Haliotis* species, one from California, where animals are always exposed to a gut-disease-causing bacteria, and one in New Zealand, where that bacteria and disease are absent. Metabolic rates increased during the heat treatment, digestibility was not significantly changed, and enzyme activities followed individual patterns, with some increases and decreases in the heat treatment.

Metabolic rate

Metabolic rate in heated treatment Pāua was marginally significantly higher than those individuals in the ambient treatment. Similarly, metabolic rate was 32% higher in the heat treatment Red Abalone, compared to individuals in the ambient treatment (Table 3.1, Figure 3.3).

These results confirm that the high temperature treatment group is experiencing metabolic changes compared with animals at ambient temperatures. Similar temperatures in at least one previous study showed marked differences in metabolomic profiles that indicated stressful conditions for Red Abalone (Rosenblum et al. 2005). These results also demonstrate that each species of abalone can respond differently to the same effective increase in temperature over their ambient conditions, which has been shown in *H. rufescens*, *H. fulgens*, and *H. corrugata* (Red, Green, and Pink Abalone, resp.) with respect to respiration (Dahlhoff and Somero 1993a). This study (although the comparison can only be made qualitatively) shows similar patterns in increased metabolic rates in invertebrate species from cooler habitats, wherein the Red Abalone (with a colder ambient temperature) have higher metabolic rates, even at ambient temperatures, than Pāua (Figure 3.3) (Addo-Bediako et al. 2002; Vorhees et al. 2013).

Q_{10}, a measurement of sensitivity of metabolic rate to an increase in temperature, was 2.46 for Pāua and 1.73 for Red Abalone. Q_{10} differences can be explained by thermal stability of the natural environment, as has been shown in mosquitoes (Vorhees et al. 2013), where higher environmental variability leads to less sensitivity (lower metabolic rate-temperature slope) in metabolic rate. Applying this logic, Red Abalone having a lower metabolic sensitivity to temperature compared to Pāua may be explained by the higher variability in environmental temperatures experienced by Red Abalone. Indeed, there have been declines in Red Abalone reproductive success at aquaculture facilities as well as in wild populations (Catton et al. 2016a) in recent years during thermal anomalies like the Pacific warm "Blob,", suggesting that these animals, which can live for decades, are exposed to variable environments during their lifetimes. Pāua are exposed to more stable environments, and thermal events are just starting to impact

wild harvests, and these differences in environmental stability may explain why Q_{10} (metabolic sensitivity to temperature) is higher in Pāua than in Red Abalone.

As reviewed by Somero (2010), other marine intertidal snails show an interesting pattern with thermal tolerance and survival. Animals found highest in the tidal zone (so experiencing the hottest and more variable temperatures) are the most heat tolerant, but because the hotter environmental temperatures closely align with the highest temperatures that these animals can tolerate, they experience higher mortality than nearby species (Somero 2010). This may explain why Pāua, at least within the population sampled for this experiment, have a higher Q_{10} than Red Abalone – they live at higher temperatures in the very shallow (1-4m) intertidal zone. Perhaps they are closer to their thermal maximum already. Measuring metabolic rate across a broader temperature regime would help clarify where on the metabolic rate-temperature curve these samples were taken.

Digestibility

In this study, both total organic matter digestibility and individual nutrient digestibility were examined in two species at ambient and heated temperatures. Within each species, organic matter (OM) digestibility and protein digestibility were lower, albeit not significantly so, in the heated treatments (Figure 3.4, Table 3.2). Additionally, OM digestibility and protein digestibility are more variable at the higher temperatures, indicating that each individual responds slightly differently to this increase in temperature. OM digestibility was not significantly impacted by the temperatures used in this experiment, but this is partly due to high variability in this measurement. Looking at higher temperature stress *may* be important in determining whether digestibility is impacted by thermal stress. However, we do see a similar pattern wherein the OM digestibility at the higher temperatures is 16% lower (effect size, not absolute change in OM

digestibility) in the heat treatment Pāua, and there is a similar decline in Red Abalone, with heat treatment animals having 7% lower OM digestibility than ambient animals. Larger sample sizes may help resolve these patterns, although, interestingly, one other study has demonstrated stable patterns in digestibility of *Haliotis laevigata* across a 12°C gradient. Despite having a faster transit time of digesta at 26°C vs 14°C, the animals maintained the same digestibility of their diet (Currie et al. 2015). This suggests that, to maintain digestibility with higher metabolic rate, digestion was in some way ramped up. The length of the gut (which was not measured in this experiment) could have increased to allow more time for digestion, or enzyme activity could have increased. Maltase activity did increase during heat treatment for Red Abalone (see discussion below), but for a complete picture on how these animals maintained digestibility during increased metabolic rates, other enzymatic data should be explored.

Although transit time was not measured in this experiment, if we assume the same pattern would follow in these species, we can hypothesize changes what may be happening in Red Abalone and Pāua that would serve as important hypotheses for future experiments. If transit time decreases at higher temperatures, this means that more food is transiting through the gut in the same amount of time. If the apparent digestibility (which is a proportion of the food digested and assimilated) in those animals remains constant, and we assume animals are constantly eating (this was observed in the lab), then the total amount of organic material being digested by the animals will have increased in the animals in the heated treatment. This could mean that Red Abalone and Pāua (and possibly all other species of *Haliotis*) are able to extract more organic matter from their diets during periods of physiological stress. Other measurements on the impact of temperature stress on digestive glands have been studied, but they focus more on stress metrics than digestive function. For example, haemocyte infiltration in the digestive gland, an

indicator of physiological stress, increases during high temperature stress in *H. rufescens* (Hooper et al. 2014). More experiments measuring assimilation directly would be an excellent follow-up to determine how these animals alter their digestive strategies during temperature stress beyond that to which I exposed the animals. Additionally, understanding the transition in response from temperature stress to WS stress (and the combination of the two) are key questions to study.

Enzyme activity

Neither species had significantly different amylase activity levels between the ambient and heated treatments (Figure 3.6, Table 3.4). In a previous study, amylase (in addition to lipase) was found to have increased in *Haliotis laevigata* as temperature was increased (Bansemer et al. 2016b). However, it is noteworthy that a very small subsample of animals was analyzed for amylase activity (n=2 for Red Abalone heat treatment) in this study. Additionally, in Bansemer et al. (2016b), there is no specification about which digestive tissue was used. Therefore, analyzing more specified gut samples from this experiment may yield different patterns of amylase activity.

Maltase and trypsin activities were only compared within Red Abalone treatment groups. With both enzymes, treatment had a significant effect on enzyme activity level. Maltase activity was significantly higher in in the heat treatment ($p = 0.006$; Figure 3.7, Table 3.4), as where trypsin activity was significantly lower in the heat treatment ($p = 0.029$; Figure 3.8, Table 3.4). Despite the finding of lower trypsin activity in heated treatment Red Abalone (Figure 3.8), protein digestibility was not different between heat and ambient treatments. This suggests the animals are becoming less efficient at digesting protein at higher temperatures, despite having more trypsin present. Interestingly, the trypsin activity results again contrast with the findings of

(Bansemer et al. 2016b), which found that temperature had no impact on trypsin activity. One way to increase understanding these results is to use biochemical and molecular techniques to determine which tissues are actually producing enzymes, and where they are most active. With this information, target enzymes pinpointed to specific gut regions could be determined for future studies on the impact of temperature stress on the gut.

No strong patterns of enzyme activity changes with temperature emerge from these results, which may be due to the limited species data (Red Abalone being the only species for which we can compare all 3 enzymes) and limited gut tissue information (all samples in this chapter are from proximal digestive gland samples). Further sampling of the digestive organs is needed, as there is strong evidence that digestive enzymes will vary among region within these species (Garcia-Esquivel and Felbeck 2006).

To put these enzyme assays into a broader physiological context, abalone consume marine red, green, and brown algae (Leighton 2000), but they may be digesting only some components of this food, including the biofilms on their surfaces. The refractory components of this diet are carrageenan, cellulose, and alginic acid. The less refractory ones are starch, laminarin, and chrysolaminarin, in addition to other essential nutrients like proteins and lipids (Karasov and Douglas 2013). Although digestive enzyme assays are not commonly optimized for abalone guts, some investigations have found evidence for endogenous production of cellulases (Enriquez et al. 2001; Lo et al. 2003; Suzuki et al. 2003), which would aide in digestion of the cell walls of green macroalgae, and terrestrially derived detritus that may be incidentally consumed in their coastal habitats. There is also evidence of exogenous (microbially-derived) alginase production (Sawabe et al. 1995), which would break down alginic acid in cell walls of brown algae, but no evidence of endogenous production of this enzyme. In

Haliotis midae, antibiotic treated abalone still had functional cellulase, alginate lyase, laminarinase, agarase, and carrageenase activity, indicating that these enzymes may be endogenously produced by the animals and that the activity of carbohydrases differ significantly in animals fed different algal diets (Erasmus et al. 1997). Other studies have focused on detecting the basic presence or absence of enzymes in abalone guts, and others conducted feeding trials comparing growth and digestibility of artificial feeds (Britz et al. 1996; Knauer et al. 1996; Hernandez-Santoyo et al. 1998; Picos-Garcia et al. 2000; Garcia-Esquivel and Felbeck 2009). Most of the available literature that considers comparative digestive physiology of abalone is concerned with the efficacy of different commercial feeds for growth in farmed animals. While this may be useful for aquaculture's immediate needs to grow larger animals for human consumption, it does little to improve our understanding of the nutritional physiology of abalone, and particularly what they do in nature. To better capture the full impact of thermal stress on digestive function, these enzymes in each gut region should be analyzed in future studies of heat stress impacts.

Figure 3.1: *H. iris* and *H. rufescens* were removed from shells and dissected on metal trays filled with ice to maintain enzymatic integrity. This image shows *H. iris* cleanly removed from its shell. The digestive system runs along the lower portion of the body, with the large digestive gland housed inside the green horn-shaped ovary on the right of the image.

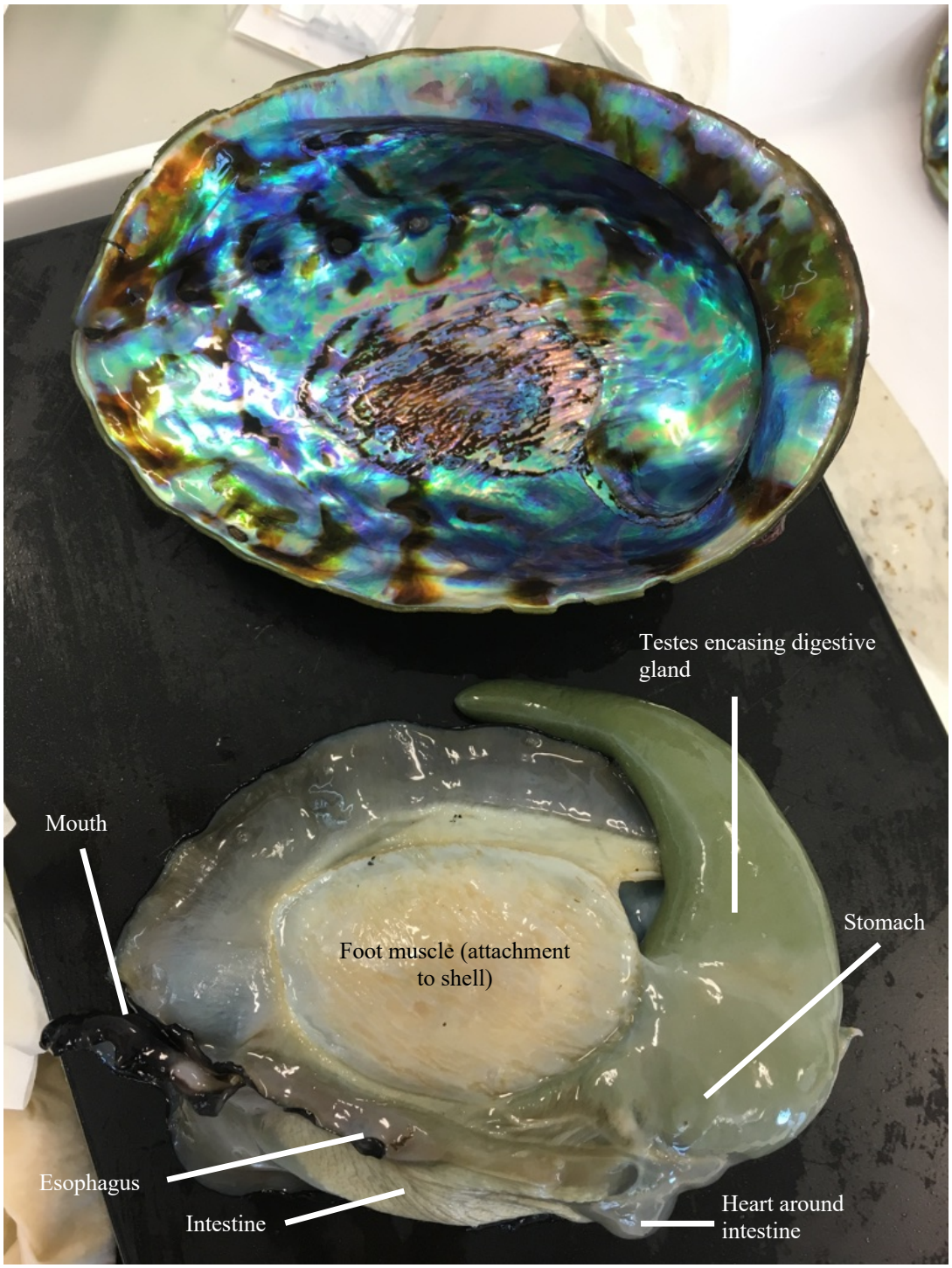

Figure 3.2: Experimental tank set-up for *H. iris*. Animals were housed in flow-through, filtered seawater in individual bucket enclosures. Half of the animals received ambient water (below) and the other have received water that was first passed through a bath with heaters. For *H. rufescens*, an identical system was used except that each of the two treatments had its own closed, recirculating system. The heaters for the *H. rufescens* experimental group were placed in the sump tank to evenly heat all aquaria.

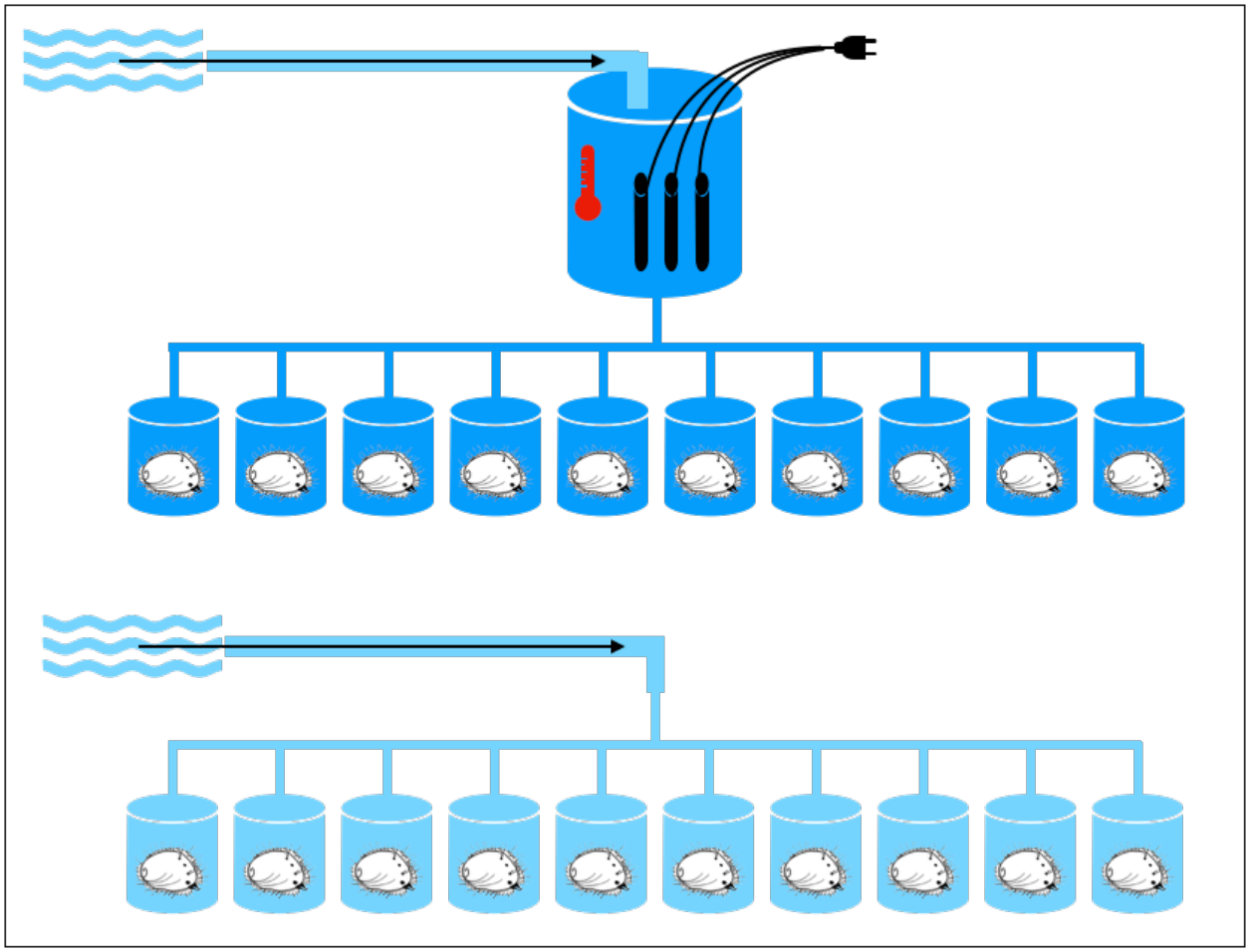

Figure 3.3: Average metabolic rates in all four treatments (mean ± standard error). Ambient treatment Pāua (*H. iris*) metabolic rate was 0.0023±0.0004 cal/min/g. Heated treatment *H. iris* metabolic rate was 0.0036±0.0006 cal/min/g. Ambient treatment Red Abalone (*H. rufescens*) metabolic rate was 0.0053±0.0005 cal/min/g. Heated treatment *H. rufescens* metabolic rate was 0.0070±0.0004 cal/min/g. Q10 for *H. iris* was 2.46, and 1.73 for *H. rufescens*. Statistical test values are provided within species only, and comparisons within treatment are available in Table 3.1.

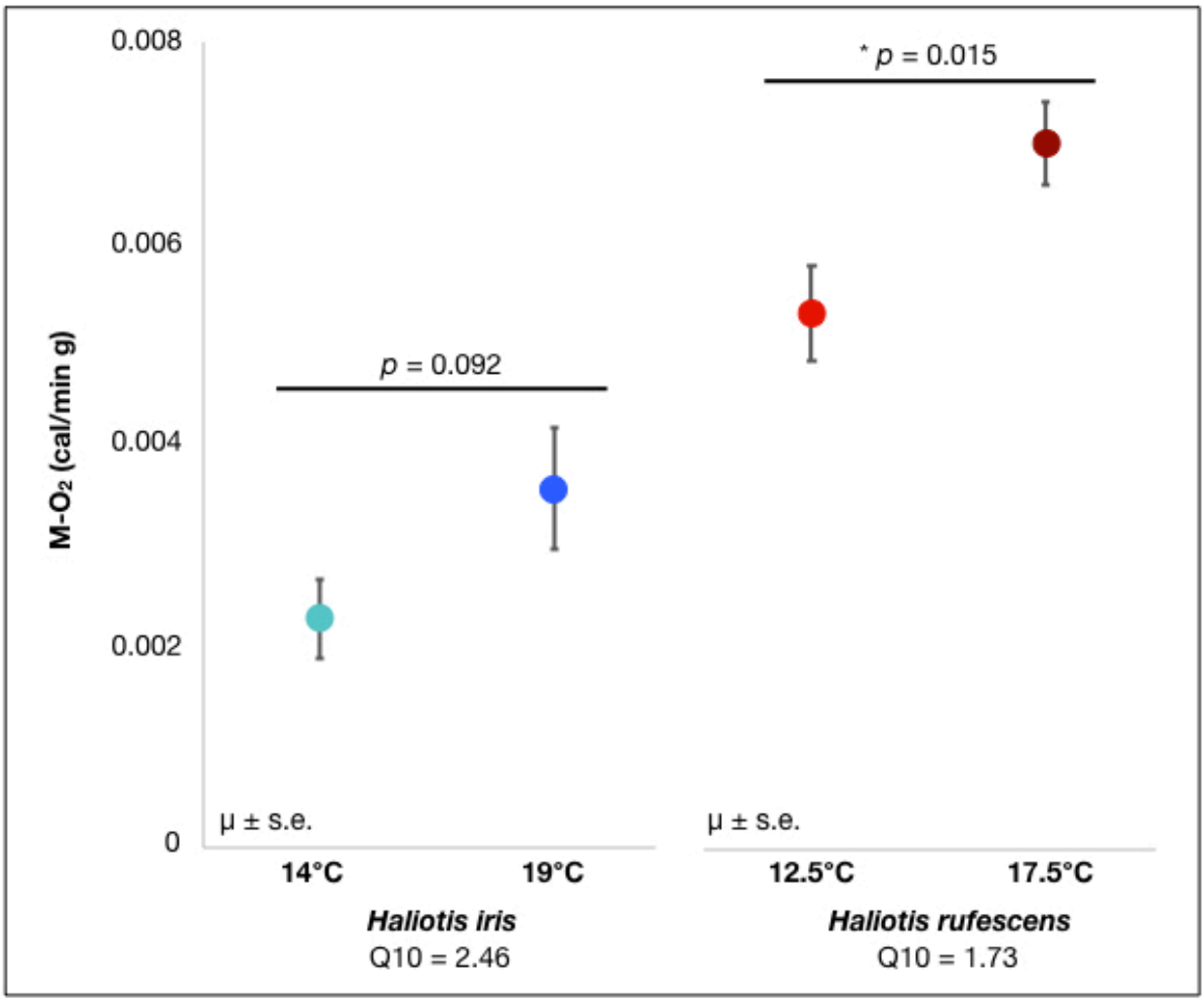

Table 3.1: Statistical analysis values for Metabolic Rates. Bartlett's tests for equal variances and Shapiro-Wilk normality tests were used to test the assumptions before running an ANOVA. For all metabolic comparisons, ANOVA's without any transformations were used.

				Bartlett's, homoscedascity			Shapiro-Wilk normality		ANOVA		
Metabolic rates	**Transformation**	**Group 1**	**Group 2**	**K^2**	**d.f.**	***p***	**W**	***p***	**d.f.**	**F**	***p***
pāua	-	pāua, 14°C	pāua, 19°C	1.148	1	0.284	0.904	0.067	1,16	3.219	0.0917
red	-	red, 12.5°C	red, 17.5°C	0.225	1	0.635	0.960	0.538	1,18	7.223	0.0150
ambient	-	pāua, 14°C	red, 12.5°C	0.366	1	0.545	0.958	0.505	1,18	24.560	0.0001
heated	-	pāua, 19°C	red, 17.5°C	0.902	1	0.342	0.930	0.194	1,16	22.28	0.0002

Figure 3.4: Average apparent organic matter (OM) digestibility in all four treatments (mean ± standard deviation). Ambient treatment Pāua (*H. iris*) organic digestibility was 45.49% ± 6.12%. Heated treatment *H. iris* organic digestibility was 37.92% ± 13.47%. Ambient treatment Red Abalone (*H. rufescens*) organic digestibility was 68.03% ± 4.64%. Heated treatment *H. rufescens* organic digestibility was 62.93% ± 8.12%. Statistical test values are provided within species only, comparisons within treatment are available in Table 3.2.

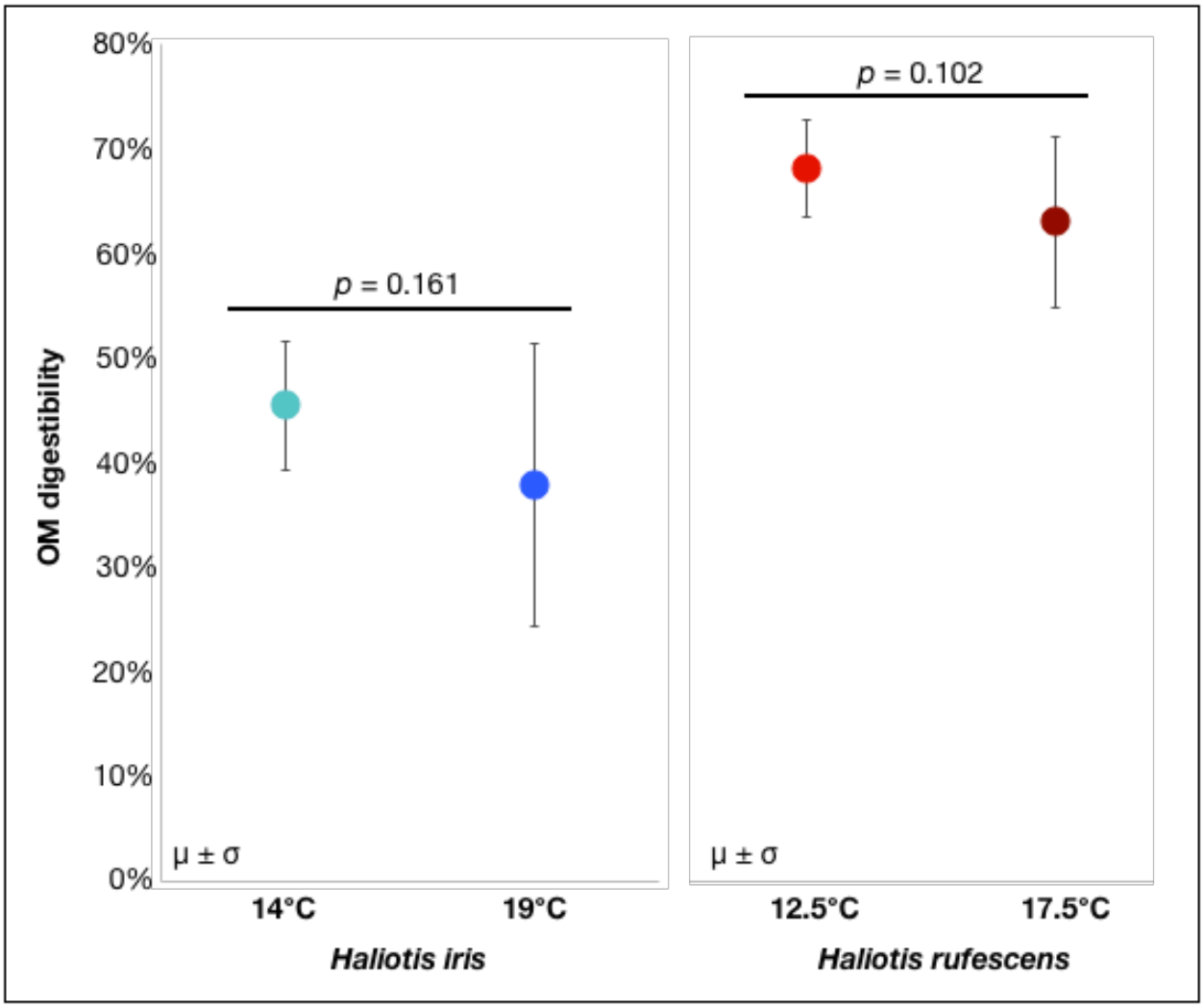

Table 3.2: Statistical analysis values for Apparent Organic Matter Digestibility Bartlett's tests for equal variances and Shapiro-Wilk normality tests were used to test the assumptions before running an ANOVA. A box-cox transformation was used to achieve normality and homoscedascity for comparing ambient and heated treatment groups within Pāua, *H. iris*. Box-cox and log transformations were unsuccessful in achieving homoscedascity and normality for ambient treatment groups in both species, so a Kruskal-Wallis non-parametric test was used to compare species are ambient temperatures.

Organic				Bartlett's, homoscedascity			Shapiro-Wilk normality		ANOVA		
digestibility	Transformation	Group 1	Group 2	K^2	d.f.	*p*	W	*p*	d.f.	F	*p*
pāua	power, ^1.4	pāua, 14°C	pāua, 19°C	3.676	1	0.055	0.911	0.089	1,16	2.164	0.161
red	-	red, 12.5°C	red, 17.5°C	2.546	1	0.111	0.972	0.800	1,18	2.975	0.102
heated	-	pāua, 19°C	red, 17.5°C	0.447	1	0.504	0.955	0.515	1,16	21.6	0.00268
									d.f.	χ^2 *	*p*
ambient	*	pāua, 14°C	red, 12.5°C	6.722	1	0.010	0.899	0.040	1	14.286	0.000157
										*Kruskal-Wallis	

Figure 3.5: Average protein digestibility in all four treatments (with error bars representing standard deviation). Ambient treatment Pāua (*H. iris*) protein digestibility was 79.64% ± 1.07%. Heated treatment *H. iris* protein digestibility was 76.41% ± 2.11%. Ambient treatment Red Abalone (*H. rufescens*) protein digestibility was 70.31% ± 3.03%. Heated treatment *H. rufescens* protein digestibility was 66.51% ± 4.78%. Statistical test values are provided within species only (Table 3.3).

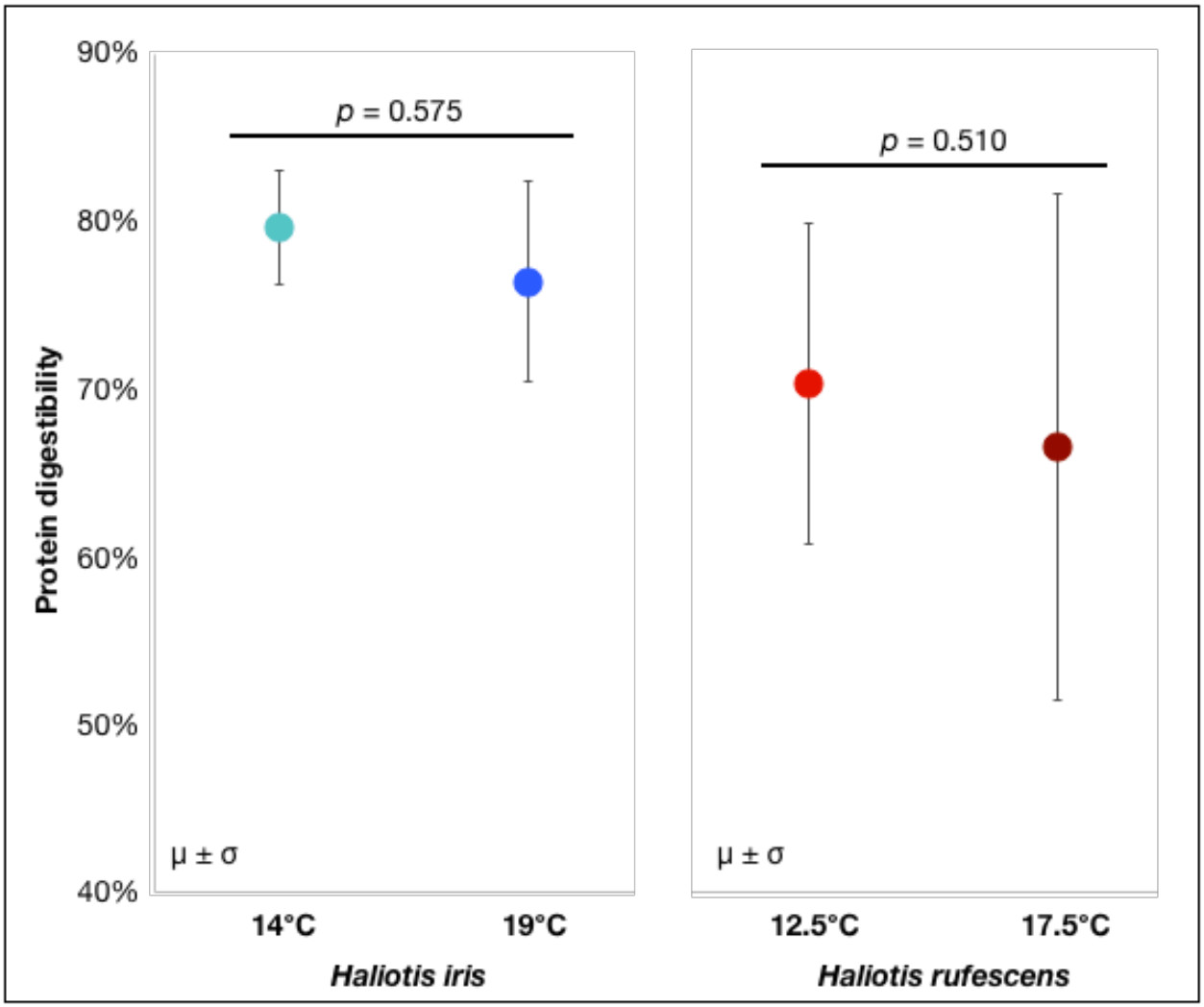

Table 3.3: Statistical analysis values for Protein Digestibility. Bartlett's tests for equal variances and Shapiro-Wilk normality tests were used to test the assumptions before running an ANOVA. For all protein digestibility comparisons, ANOVA's without any transformations were used.

Protein digestibility	Transformation	Group 1	Group 2	Bartlett's, homoscedascity			Shapiro-Wilk normality		ANOVA		
				K^2	d.f.	*p*	W	*p*	d.f.	F	*p*
pāua	-	pāua, 14°C	pāua, 19°C	2.292	1	0.130	0.964	0.680	1,16	0.327	0.575
red	-	red, 12.5°C	red, 17.5°C	1.710	1	0.191	0.907	0.056	1,18	0.452	0.510

Figure 3.6: Average proximal digestive gland amylase activity (µmol min^{-1} g^{-1}) in all four treatments (with error bars representing standard deviation). Ambient treatment Pāua (*H. iris*, n=7) amylase activity was 3.98 ± 1.60 µmol min^{-1} g^{-1}. Heated treatment *H. iris* (n=8) amylase activity was 2.81 ± 0.74 µmol min^{-1} g^{-1}. Ambient treatment Red Abalone (*H. rufescens,* n=6) amylase activity was 1.54 ± 0.60 µmol min^{-1} g^{-1}. Heated treatment *H. rufescens* (n=2) amylase activity was 1.84 ± 0.17 µmol min^{-1} g^{-1}. Statistical test values are provided within species only (Table 3.4).

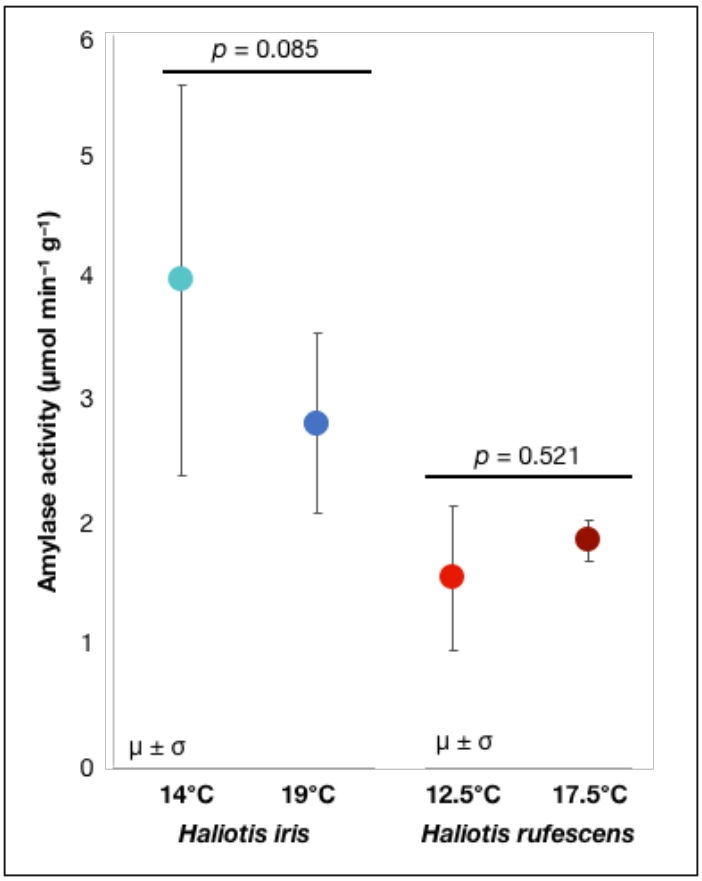

Table 3.4: Statistical analysis values for amylase, maltase, and trypsin activities within species. Bartlett's tests for equal variances and Shapiro-Wilk normality tests were used to test the assumptions before running an ANOVA. A box-cox transformation was used to achieve normality and homoscedascity for comparing ambient and heated treatment groups Red Abalone for maltase and trypsin only.

				Bartlett's, homoscedascity			Shapiro-Wilk normality		ANOVA		
Enzymes	**Transformation**	**Group 1**	**Group 2**	**K^2**	**d.f.**	***p***	**W**	***p***	**d.f.**	**F**	***p***
red, amylase	-	red, 12.5°C	red, 17.5°C	1.154	1	0.283	0.878	0.179	1,6	0.464	0.521
red, maltase	power, ^-0.7	red, 12.5°C	red, 17.5°C	3.324	1	0.068	0.933	0.176	1,18	9.631	0.006
red, trypsin	power, ^-0.4	red, 12.5°C	red, 17.5°C	2.077	1	0.150	0.952	0.392	1,18	5.630	0.029
pāua, amylase	-	pāua, 14°C	pāua, 19°C	3.358	1	0.067	0.887	0.061	1,13	3.488	0.085

Figure 3.7: Average proximal digestive gland maltase activity (µmol min^{-1} g^{-1}) in ambient Pāua and both treatments in Red Abalone (with error bars representing standard deviation). Ambient treatment Pāua (*H. iris*, n=10) maltase activity was 1.97 ± 0.55 µmol min^{-1} g^{-1}. Ambient treatment Red Abalone (*H. rufescens,* n=10) maltase activity was 2.04 ± 0.31 µmol min^{-1} g^{-1}. Heated treatment *H. rufescens* (n=10) maltase activity was 3.28 ± 1.15 µmol min^{-1} g^{-1}. Statistical test values are provided within Red Abalone only (Table 3.4.)

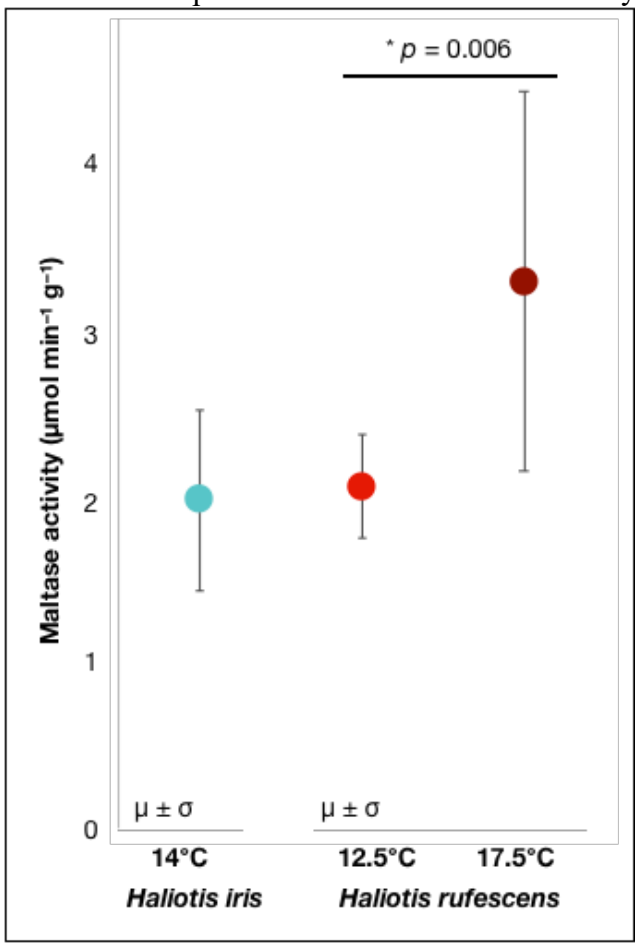

Figure 3.8: Average proximal digestive gland trypsin activity (µmol min^{-1} g^{-1}) in ambient Pāua and both treatments in Red Abalone (with error bars representing standard deviation). Ambient treatment Pāua (*H. iris*, n=9) trypsin activity was 8.04 ± 4.55 µmol min^{-1} g^{-1}. Ambient treatment Red Abalone (*H. rufescens,* n=10) trypsin activity was 5.19 ± 1.88 µmol min^{-1} g^{-1}. Heated treatment *H. rufescens* (n=10) trypsin activity was 3.05 ± 0.77 µmol min^{-1} g^{-1}. Statistical test values are provided within Red Abalone only (Table 3.4).

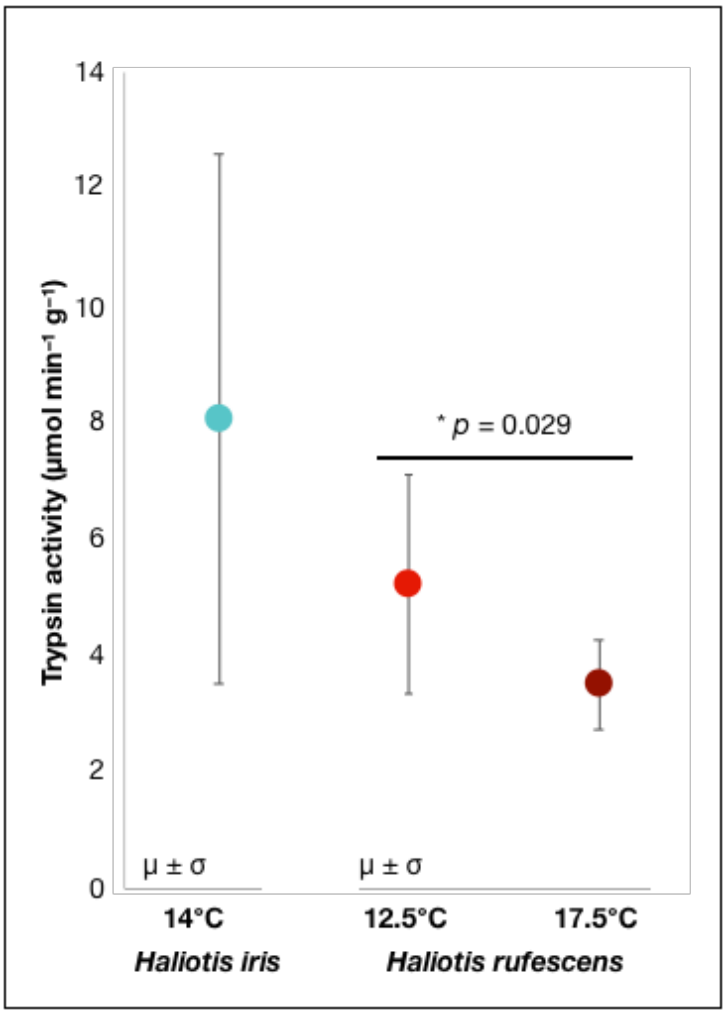

DISCUSSION

The ultimate goal of this work was to better understand the evolutionary history of withering syndrome resistance and susceptibility, and the impacts of withering syndrome and stressful temperatures on abalone physiology. I took a genetic, transcriptomic, and physiological approach to answering these questions. This work has uncovered potential evolutionary lineages of abalone that are more susceptible to withering syndrome (WS), gene expression patterns of infected animals, and functional changes in abalone physiology during heat stress.

In Chapter 1, the most susceptible species (*H. cracherodii, H. rufescens, H. walallensis, H. sorenseni,* and *H. kamtschatkana*), form a monophyletic grouping apart from the other northeastern Pacific taxa. This implies that WS susceptibility could be considered a derived trait that traces back to the last common ancestor of this hypothesized clade, and supports the hypothesis that patterns of WS resistance and susceptibility have a quite deep evolutionary basis. This phylogenetic hypothesis these Haliotids would be improved with more genes and taxon sampling. If there is an evolutionary component to WS susceptibility (and these results suggest that there is), identifying genetic differences between susceptible and resistant species may reveal why physiological response differences between these two groups occurs. We know that heat stress and temperature variability play a role in mediation of WS disease state (Ben-Horin et al. 2013), and that understanding the mechanisms of physiological change under heat and disease stress is critical for making climate change predictions (Bay et al. 2017) and management decisions (Tracy et al. 2006; Rohr et al. 2013). A phylogenetic analysis of taxa allows for the placement of these physiological studies into an evolutionary context. Given that abalone have tremendous cultural importance in California, and a substantial contribution to fisheries revenue,

it is essential that any studies investigating mechanisms of disease resistance should include both evolutionary and physiological contexts.

The work in chapters 2 and 3 is designed to better understand the impact of disease and temperature (which exacerbates WS (Moore et al. 2000; Braid et al. 2005; Moore et al. 2009; Rogers-Bennett et al. 2010; Moore et al. 2011; Crosson et al. 2014)) in that physiological context. The Pinto Abalone transcriptome comparison between infected and naïve animals allows us to see how infection impacts gene expression patterns. The real use of these data will be in future studies, comparing a species like Pinto Abalone to the response of a more resistance species, such as Pink or Green Abalone (Álvarez Tinajero et al. 2002; Moore et al. 2009). If we are able to determine what genetic pathways are absent or present only in susceptible animals, we can identify the mechanism for susceptibility in these animals. Likewise, we can understand specific pathways for resistance in Pink or Green Abalone. Further examination of these differences during heat stress, which exacerbates WS, is particularly relevant to outplanting efforts for recovery of these species.

Lastly, Chapter 3 allows for the comparison of heat stress on the digestive physiology of abalone species that have been exposed to WS (Red Abalone) and a completely naïve species (Pāua). Withering syndrome, a severe disease which has depleted much of the abalone stocks in the northeast Pacific, is impacted by temperature. Abalone exposed to high temperatures generally showing marked increases in infection intensity and disease (Moore et al. 2000; Braid et al. 2005; Moore et al. 2009; Rogers-Bennett et al. 2010; Moore et al. 2011; Crosson et al. 2014). Heat stress alone is a defined threat to farmed abalone species worldwide (Morash and Alter 2015), even in species that are not exposed to WS. This study examined the effects of heat stress on metabolic rate, digestibility, and digestive enzyme activities in two species of abalone.

Metabolic rates were significantly elevated in heat treatment animals. Digestibility did not significantly change, but this may be balanced by changes in transit time and total intake, measurements which need to be assessed in future experiments. Digestive enzyme activities followed no clear pattern, with one (amylase) remaining the same, one (maltase) increasing, and one (trypsin) decreasing with heat stress. These changes may be the result of physiological response to heat stress, but a full understanding of how these animals adjust their physiology requires further gut tissue and enzyme type analysis.

Understanding digestive changes caused by temperature stress is important for aquaculture (Morash and Alter 2015). Food intake, fecal production, and oxygen consumption have been shown to decline during withering syndrome infections (Gonzalez et al. 2012). Importantly, high temperature anomalies are also an ongoing threat to the recovery of Endangered and threatened abalone species, as well as their intertidal and subtidal neighbors (Butler et al. 2009). Further understanding of these anomalies' impacts on digestive and whole animal physiology, and the interaction with disease impacts, is essential to their conservation. Lastly, these need to be tested in each species of concern. Because each species occurs at slightly different depths and ranges, their exposure to pathogens and temperature stressors or anomalies may be unique. An expansion of these studies, especially comparing closely related species within the same experiments, is critical to informing management. Understanding the sublethal physiological changes (as in Chapter 3) on other organ systems like reproductive potential and readiness would also be of the utmost importance for understanding how to manage disease and climate change in restoration work.

REFERENCES

Aagaard J.E., Vacquier V.D., MacCoss M.J., Swanson W.J. (2010) ZP Domain Proteins in the Abalone Egg Coat Include a Paralog of VERL under Positive Selection That Binds Lysin and 18-kDa Sperm Proteins. *Mol Biol Evol* **27**: 193-203.

Addo-Bediako A., Chown S.L., Gaston K.J. (2002) Metabolic cold adaptation in insects: a large-scale perspective. *Funct Ecol* **16**: 332-338.

Ai B., Kang M. (2015) How Many Genes are Needed to Resolve Phylogenetic Incongruence? *Evol Bioinform Online* **11**: 185-188.

Altstatt J.M., Ambrose R.F., Engle J.M., Haaker P.L., Lafferty K.D., Raimondi P.T. (1996) Recent declines of black abalone Haliotis cracherodii on the mainland coast of central California. *Mar Ecol Prog Ser* **142**: 185-192.

Álvarez Tinajero M.d.C., Cáceres-Martínez J., Gonzáles Avilés J.G. (2002) Histopathological evaluation of the yellow abalone Haliotis corrugata and the blue abalone Haliotis fulgens from Baja California, México. *J Shellfish Res* **21**: 825-830.

An H.S., Jee Y.J., Min K.S., Kim B.L., Han S.J. (2005) Phylogenetic analysis of six species of Pacific abalone (Haliotidae) based on DNA sequences of 16s rRNA and cytochrome c oxidase subunit I mitochondrial genes. *Mar Biotechnol* **7**: 373-380.

Arivalagan J., Yarra T., Marie B., Sleight V.A., Duvernois-Berthet E., Clark M.S., Marie A., Berland S. (2017) Insights from the Shell Proteome: Biomineralization to Adaptation. *Mol Biol Evol* **34**: 66-77.

Bansemer M.S., Qin J.G., Harris J.O., Duong D., Currie K.L., Howarth G.S., Stone D.A.J. (2016a) Dietary inclusions of dried macroalgae meal in formulated diets improve the growth of greenlip abalone (Haliotis laevigata). *J Appl Phycol* **28**: 3645-3658.

Bansemer M.S., Qin J.G., Harris J.O., Schaefer E.N., Wang H.R., Mercer G.J., Howarth G.S., Stone D.A.J. (2016b) Age-dependent response of digestive enzyme activities to dietary protein level and water temperature in greenlip abalone (Haliotis laevigata). *Aquaculture* **451**: 451-456.

Barber A.H., Lu D., Pugno N.M. (2015) Extreme strength observed in limpet teeth. *J R Soc Interface* **12**.

Bay R.A., Rose N.H., Logan C.A., Palumbi S.R. (2017) Genomic models predict successful coral adaptation if future ocean warming rates are reduced. *Science Advances* **3**.

Belshaw R., Pereira V., Katzourakis A., Talbot G., Paces J., Burt A., Tristem M. (2004) Long-term reinfection of the human genome by endogenous retroviruses. *P Natl Acad Sci USA* **101**: 4894-4899.

Ben-Horin T., Lenihan H.S., Lafferty K.D. (2013) Variable intertidal temperature explains why disease endangers black abalone. *Ecology* **94**: 161-168.

Bevelander G. (1988) Abalone: Gross and Fine Structure. Boxwood Press

Boots M., Bowers R.G. (1999) Three mechanisms of host resistance to microparasites - Avoidance, recovery and tolerance - Show different evolutionary dynamics. *J Theor Biol* **201**: 13-23.

Braid B.A., Moore J.D., Robbins T.T., Hedrick R.P., Tjeerdema R.S., Friedman C.S. (2005) Health and survival of red abalone, Haliotis rufescens, under varying temperature, food supply, and exposure to the agent of withering syndrome. *J Invertebr Pathol* **89**: 219-231.

Briscoe A.D., Macias-Munoz A., Kozak K.M., Walters J.R., Yuan F.R., Jamie G.A., Martin S.H., Dasmahapatra K.K., Ferguson L.C., Mallet J., Jacquin-Joly E., Jiggins C.D. (2013)

Female Behaviour Drives Expression and Evolution of Gustatory Receptors in Butterflies. *Plos Genet* **9**.
Britz P.J., Hecht T., Knauer J. (1996) Gastric evacuation time and digestive enzyme activity in abalone Haliotis midae fed a formulated diet. *South African Journal of Marine Science-Suid-Afrikaanse Tydskrif Vir Seewetenskap* **17**: 297-303.
Brown L.D. (1993) Biochemical Genetics and Species Relationships within the Genus Haliotis (Gastropoda, Haliotidae). *J Mollus Stud* **59**: 429-443.
Burge C.A., Eakin C.M., Friedman C.S., Froelich B., Hershberger P.K., Hofmann E.E., Petes L.E., Prager K.C., Weil E., Willis B.L., Ford S.E., Harvell C.D. (2014) Climate Change Influences on Marine Infectious Diseases: Implications for Management and Society. *Annual Review of Marine Science* **6**: 249-280.
Butler J., DeVogelaere A., Gustafson C.M., Mobley C., Neuman M., Richards D., Rumsey S., Taylor B., VanBlaricom G. (2009) Status Review for Black Abalone (*Haliotis cracherodii* Leach, 1814). In: Commerce D.o. (ed)
Carson H.S., Ulrich M. (2019) Status report for the pinto abalone in Washington, Olympia, WA.
Catton C., Rogers-Bennett L., Amrhein A. (2016a) "Perfect Storm" Decimates Northern California Kelp Forests
Catton C.A., Stierhoff K.L., Rogers-Bennett L. (2016b) Population Status Assessment and Restoration Modeling of White Abalone Haliotis Sorenseni in California. *J Shellfish Res* **35**: 593-599.
CDFW (2019) Red Abalone Fishery Management Plan. In: Wildlife C.D.o.F.a. (ed)
Closek C.J., Langevin S., Burge C.A., Crosson L., White S., Friedman C.S. (2016) Genomic Characterization of a Novel Phage Found in Black Abalone (Haliotis cracherodii) Infected with Withering Syndrome, pp ME44C-0875.
Coleman A.W., Vacquier V.D. (2002) Exploring the phylogenetic utility of ITS sequences for animals: A test case for abalone (Haliotis). *J Mol Evol* **54**: 246-257.
Colgan D.J., Ponder W.F., Eggler P.E. (2000) Gastropod evolutionary rates and phylogenetic relationships assessed using partial 28S rDNA and histone H3 sequences. *Zoologica Scripta* **29**: 29-63.
Connor K.M., Sung A., Garcia N.S., Gracey A.Y., German D.P. (2016) Modulation of digestive physiology and biochemistry in Mytilus californianus in response to feeding level acclimation and microhabitat. *Biol Open* **5**: 1200-1210.
Crosson L.M., Friedman C.S. (2018) Withering syndrome susceptibility of northeastern Pacific abalones: A complex relationship with phylogeny and thermal experience. *J Invertebr Pathol* **151**: 91-101.
Crosson L.M., Wight N., VanBlaricom G.R., Kiryu I., Moore J.D., Friedman C.S. (2014) Abalone withering syndrome: distribution, impacts, current diagnostic methods and new findings. *Dis Aquat Organ* **108**: 261-270.
Currie K.L., Lange B., Herbert E.W., Harris J.O., Stone D.A.J. (2015) Gastrointestinal evacuation time, but not nutrient digestibility, of greenlip abalone, Haliotis laevigata Donovan, is affected by water temperature and age. *Aquaculture* **448**: 219-228.
Dahlhoff E., Somero G.N. (1993a) Effects of Temperature on Mitochondria from Abalone (Genus Haliotis) - Adaptive Plasticity and Its Limits. *Journal of Experimental Biology* **185**: 151-168.
Dahlhoff E., Somero G.N. (1993b) Kinetic and structural adaptations of cytoplasmic malate dehydrogenases of eastern Pacific abalone (genus *Haliotis*) from different thermal

habitats: biochemical correlates of biogeographical patterning. *Journal of Experimental Biology* **185**: 137-150.
De Wit P., Palumbi S.R. (2013) Transcriptome-wide polymorphisms of red abalone (Haliotis rufescens) reveal patterns of gene flow and local adaptation. *Mol Ecol* **22**: 2884-2897.
Degliesposti M., Devries S., Crimi M., Ghelli A., Patarnello T., Meyer A. (1993) Mitochondrial Cytochrome-B - Evolution and Structure of the Protein. *Biochim Biophys Acta* **1143**: 243-271.
Degnan B.M., Groppe J.C., Morse D.E. (1995) Chymotrypsin mRNA expression in digestive gland amoebocytes: cell specification occurs prior to metamorphosis and gut morphogenesis in the gastropod, Haliotis rufescens. *Roux's archives of developmental biology* **205**: 97-101.
Degnan S.A., Imron, Geiger D.L., Degnan B.M. (2006) Evolution in temperate and tropical seas: Disparate patterns in southern hemisphere abalone (Mollusca : Vetigastropoda : Haliotidae). *Mol Phylogenet Evol* **41**: 249-256.
Diaz F., del Rio-Portilla M.A., Sierra E., Aguilar M., Re-Araujo A.D. (2000) Preferred temperature and critical thermal maxima of red abalone Haliotis rufescens. *J Therm Biol* **25**: 257-261.
Dziarski R., Gupta D. (2006) The peptidoglycan recognition proteins (PGRPs). *Genome Biol* **7**: 232.
Enriquez A., Viana M.T., Vasquez C., Shimada A. (2001) Digestion of cellulose by stomach homogenates of green abalone (Haliotis fulgens). *J Shellfish Res* **20**: 297-300.
Erasmus J.H., Cook P.A., Coyne V.E. (1997) The role of bacteria in the digestion of seaweed by the abalone Haliotis midae. *Aquaculture* **155**: 377-386.
Estes J.A., Lindberg D.R., Wray C. (2005) Evolution of large body size in abalones (Haliotis): patterns and implications. *Paleobiology* **31**: 591-606.
Estes J.A., Steinberg P.D. (1988) Predation, Herbivory, and Kelp Evolution. *Paleobiology* **14**: 19-36.
Friedman C.S., Andree K.B., Beauchamp K.A., Moore J.D., Robbins T.T., Shields J.D., Hedrick R.P. (2000) 'Candidatus Xenohaliotis californiensis', a newly described pathogen of abalone, Haliotis spp., along the west coast of North America. *Int J Syst Evol Micr* **50**: 847-855.
Friedman C.S., Crosson L.M. (2012) Putative Phage Hyperparasite in the Rickettsial Pathogen of Abalone, "Candidatus Xenohaliotis californiensis". *Microbial Ecology* **64**: 1064-1072.
Friedman C.S., Trevelyan G., Robbins T.T., Mulder E.P., Fields R. (2003) Development of an oral administration of oxytetracycline to control losses due to withering syndrome in cultured red abalone Haliotis rufescens. *Aquaculture* **224**: 1-23.
Friedman C.S., Wight N., Crosson L.M., VanBlaricom G.R., Lafferty K.D. (2014a) Reduced disease in black abalone following mass mortality: phage therapy and natural selection. *Front Microbiol* **5**.
Friedman C.S., Wight N., Crosson L.M., White S.J., Strenge R.M. (2014b) Validation of a quantitative PCR assay for detection and quantification of ‘Candidatus Xenohaliotis californiensis’. *Dis Aquat Organ* **108**: 251-259.
Galindo B.E., Moy G.W., Swanson W.J., Vacquier V.D. (2002) Full-length sequence of VERL, the egg vitelline envelope receptor for abalone sperm lysin. *Gene* **288**: 111-117.
Galindo B.E., Vacquier V.D., Swanson W.J. (2003) Positive selection in the egg receptor for abalone sperm lysin. *P Natl Acad Sci USA* **100**: 4639-4643.

Garcia T.I., Shen Y.J., Crawford D., Oleksiak M.F., Whitehead A., Walter R.B. (2012) RNA-Seq reveals complex genetic response to deepwater horizon oil release in Fundulus grandis. *Bmc Genomics* **13**.

Garcia-Carreno F.L., del Toro M.A.N., Serviere-Zaragoza E. (2003) Digestive enzymes in juvenile green abalone, Haliotis fulgens, fed natural food. *Comp Biochem Phys B* **134**: 143-150.

Garcia-Esquivel Z., Felbeck H. (2006) Activity of digestive enzymes along the gut of juvenile red abalone, Haliotis rufescens, fed natural and balanced diets. *Aquaculture* **261**: 615-625.

Garcia-Esquivel Z., Felbeck H. (2009) Comparative performance of juvenile red abalone, Haliotis rufescens, reared in laboratory with fresh kelp and balanced diets. *Aquacult Nutr* **15**: 209-217.

Garcia-Esquivel Z., Montes-Magallon S., Gonzalez-Gomez M.A. (2007) Effect of temperature and photoperiod on the growth, feed consumption, and biochemical content of juvenile green abalone, Haliotis fulgens, fed on a balanced diet. *Aquaculture* **262**: 129-141.

Gardner G.R., Harshbarger J.C., Lake J.L., Sawyer T.K., Price K.L., Stephenson M.D., Haaker P.L., Togstad H.A. (1995) Association of Prokaryotes with Symptomatic Appearance of Withering Syndrome in Black Abalone Haliotis cracherodii. *J Invertebr Pathol* **66**: 111-120.

Geiger D.L., Groves L.T. (1999) Review of fossil abalone (Gastropoda : Vetigastropoda : Haliotidae) with comparison to Recent species. *J Paleontol* **73**: 872-885.

Geiger D.L., Owen B. (2012) Abalone: World-Wide Haliotidae. Conchbooks, Hackenheim, Germany.

George W.C. (1952) The Digestion and Absorption of Fat in Lamellibranchs. *Biol Bull* **102**: 118-127.

German D.P. (2011) Digestive efficiency. In: Farrell A.P. J.J.C., J.G. Richards, and E.D. Stevens (ed) Encyclopedia of Fish Physiology, From Genome to Environment. Elsevier, San Diego, CA

German D.P., Horn M.H., Gawlicka A. (2004) Digestive enzyme activities in herbivorous and carnivorous prickleback fishes (Teleostei: Stichaeidae): ontogenetic, dietary, and phylogenetic effects. *Physiol Biochem Zool* **77**: 789-804.

German D.P., Sung A., Jhaveri P., Agnihotri R. (2015) More than one way to be an herbivore: convergent evolution of herbivory using different digestive strategies in prickleback fishes (Stichaeidae). *Zoology (Jena, Germany)* **118**: 161-170.

Gilbert G.S., Parker I.M. (2016) The Evolutionary Ecology of Plant Disease: A Phylogenetic Perspective. *Annu Rev Phytopathol* **54**: 549-578.

Gomez-Chiarri M., Guo X.M., Tanguy A., He Y., Proestou D. (2015) The use of -omic tools in the study of disease processes in marine bivalve mollusks. *J Invertebr Pathol* **131**: 137-154.

Gonzalez R.C., Brokordt K., Lohrmann K.B. (2012) Physiological performance of juvenile Haliotis rufescens and Haliotis discus hannai abalone exposed to the withering syndrome agent. *J Invertebr Pathol* **111**: 20-26.

Gruenthal K.M., Burton R.S. (2005) Genetic diversity and species identification in the endangered white abalone (Haliotis sorenseni). *Conserv Genet* **6**: 929-939.

Guo X.M., Ford S.E. (2016) Infectious diseases of marine molluscs and host responses as revealed by genomic tools. *Philos T R Soc B* **371**.

He Y., Jouaux A., Ford S.E., Lelong C., Sourdaine P., Mathieu M., Guo X. (2015) Transcriptome analysis reveals strong and complex antiviral response in a mollusc. *Fish Shellfish Immun* **46**: 131-144.

Hernandez-Santoyo A., Hernandez-Arana A., Arreguin-Espinosa R., Rodriguez-Romero A. (1998) Purification and characterization of several digestive proteases from the blue abalone, Haliotis fulgens. *Aquaculture* **159**: 203-216.

Hobday A.J., Tegner M.J. (2000) Status review of white abalone (*Haliotis sorenseni*) throughout its range in California and Mexico. In: Commerce D.o. (ed). NOAA Technical Memorandum NMFS

Hollenbeck C.M., Johnston I.A. (2018) Genomic Tools and Selective Breeding in Molluscs. *Frontiers in Genetics* **9**.

Hooper C., Day R., Slocombe R., Benkendorff K., Handlinger J., Goulias J. (2014) Effects of severe heat stress on immune function, biochemistry and histopathology in farmed Australian abalone (hybrid Haliotis laevigata x Haliotis rubra). *Aquaculture* **432**: 26-37.

Horn M.H., Gawlicka A.K., German D.P., Logothetis E.A., Cavanagh J.W., Boyle K.S. (2006) Structure and function of the stomachless digestive system in three related species of New World silverside fishes (Atherinopsidae) representing herbivory, omnivory, and carnivory. *Mar Biol* **149**: 1237-1245.

Jia X., Zou Z., Wang G., Wang S., Wang Y., Zhang Z. (2011) Gene expression profiling in respond to TBT exposure in small abalone Haliotis diversicolor. *Fish Shellfish Immun* **31**: 557-563.

Kajtoch Ł., Kolasa M., Kubisz D., Gutowski J.M., Ścibior R., Mazur M.A., Holecová M. (2019) Using host species traits to understand the Wolbachia infection distribution across terrestrial beetles. *Sci Rep-Uk* **9**: 847.

Karasov W.H., Douglas A.E. (2013) Comparative Digestive Physiology. *Compr Physiol* **3**: 741-783.

Kim K.H., Horn M.H., Sosa A.E., German D.P. (2014) Sequence and expression of an alpha-amylase gene in four related species of prickleback fishes (Teleostei: Stichaeidae): ontogenetic, dietary, and species-level effects. *J Comp Physiol B* **184**: 221-234.

Knauer J., Britz P.J., Hecht T. (1996) Comparative growth performance and digestive enzyme activity of juvenile South African abalone, Haliotis midae, fed on diatoms and a practical diet. *Aquaculture* **140**: 75-85.

Lafferty K.D., Kuris A.M. (1993) Mass mortality of abalone Haliotis cracherodii on the California Channel Islands: tests of epidemiological hypotheses. *Mar Ecol-Prog Ser* **96**: 239-239.

Lander E.S., Linton L.M., Birren B., Nusbaum C., Zody M.C., Baldwin J., Devon K., Dewar K., Doyle M., FitzHugh W., Funke R., Gage D., et al. (2001) Initial sequencing and analysis of the human genome. *Nature* **409**: 860-921.

Lee Y., Vacquier V.D. (1992) The Divergence of Species-Specific Abalone Sperm Lysins Is Promoted by Positive Darwinian Selection. *Biol Bull* **182**: 97-104.

Lee Y.H., Ota T., Vacquier V.D. (1995) Positive Selection Is a General Phenomenon in the Evolution of Abalone Sperm Lysin. *Mol Biol Evol* **12**: 231-238.

Lee Y.H., Vacquier V.D. (1995) Evolution and systematics in Haliotidae (Mollusca: Gastropoda): Inferences from DNA sequences of sperm lysin. *Mar Biol* **124**: 267-278.

Leighton D.L. (2000) The Biology and culture of California Abalones. Dorrance Publishing Co., Inc., Pittsburgh, PA.

Lo N., Watanabe H., Sugimura M. (2003) Evidence for the presence of a cellulase gene in the last common ancestor of bilaterian animals. *P R Soc B* **270**: S69-S72.
Lobo-da-Cunha A., Oliveira E., Alves A., Coelho R., Calado G. (2010) Light and electron microscopic study of the anterior oesophagus of Bulla striata (Mollusca, Opisthobranchia). *Acta Zool-Stockholm* **91**: 125-138.
Machamer C.E. (2015) The Golgi complex in stress and death. *Front Neurosci* **9**: 421-421.
Martin G.G., Bessette T., Martin A., Cotero R., Vumbaco K., Oakes C. (2010) Morphology of Epithelial Cells Lining the Digestive Tract of the Giant Keyhole Limpet, Megathura crenulata (Mollusca; Vetigastropoda). *J Morphol* **271**: 1134-1151.
Martin G.G., Martin A., Tsai W., Hafner J.C. (2011) Production of digestive enzymes along the gut of the giant keyhole limpet Megathura crenulata (Mollusca: Vetigastropoda). *Comparative Biochemistry and Physiology a-Molecular & Integrative Physiology* **160**: 365-373.
Masonbrink R.E., Purcell C.M., Boles S.E., Whitehead A., Hyde J.R., Seetharam A.S., Severin A.J. (2019) An Annotated Genome for Haliotis rufescens (Red Abalone) and Resequenced Green, Pink, Pinto, Black, and White Abalone Species. *Genome Biology and Evolution* **11**: 431-438.
McDowell I.C., Nikapitiya C., Aguiar D., Lane C.E., Istrail S., Gomez-Chiarri M. (2014) Transcriptome of American Oysters, Crassostrea virginica, in Response to Bacterial Challenge: Insights into Potential Mechanisms of Disease Resistance. *Plos One* **9**: e105097.
Mclean N. (1970) Digestion in Haliotis-Rufescens Swainson (Gastropoda-Prosobranchia). *J Exp Zool* **173**: 303-&.
Moore J.D., Juhasz C.I., Robbins T.T., Vilchis L.I. (2009) Green abalone, Haliotis fulgens infected with the agent of withering syndrome do not express disease signs under a temperature regime permissive for red abalone, Haliotis rufescens. *Mar Biol* **156**: 2325-2330.
Moore J.D., Marshman B.C., Chun C.S.Y. (2011) Health and Survival of Red Abalone Haliotis rufescens from San Miguel Island, California, USA, in a Laboratory Simulation of La Nina and El Nino Conditions. *J Aquat Anim Health* **23**: 78-84.
Moore J.D., Robbins T.T., Friedman C.S. (2000) Withering syndrome in farmed red abalone Haliotis rufescens: Thermal induction and association with a gastrointestinal Rickettsiales-like prokaryote. *J Aquat Anim Health* **12**: 26-34.
Morash A.J., Alter K. (2015) Effects of environmental and farm stress on abalone physiology: perspectives for abalone aquaculture in the face of global climate change. *Reviews in Aquaculture*: n/a-n/a.
Morton B. (1982) Amoebocytes. In: Wilbur K.M., Saleuddin A.S.M. (eds) The Mollusca: Physiology: Part 2. Academic Press, New York, pp 65-148.
Morton J. (1952) The role of the crystalline style. *J Mollus Stud* **29**: 85-92.
Morton J.E. (1951) The Ecology and Digestive System of the Struthiolariidae (Gastropoda). *J Cell Sci* **s3-92**: 1-25.
Morton J.E. (1979) Feeding and digestion Molluscs. Hutchinson & Co., Ltd, London, pp 97-123.
Nam B.H., Kwak W., Kim Y.O., Kim D.G., Kong H.J., Kim W.J., Kang J.H., Park J.Y., An C.M., Moon J.Y., Park C.J., Yu J.W., et al. (2017) Genome sequence of pacific abalone (Haliotis discus hannai): the first draft genome in family Haliotidae. *Gigascience* **6**.

Neuman M., Tissot B., Vanblaricom G. (2010) Overall Status and Threats Assessment of Black Abalone (Haliotis Cracherodii Leach, 1814) Populations in California. *J Shellfish Res* **29**: 577-586.
Nybakken J.W. (1996) Diversity of the Invertebrates: A Laboratory Manual. Wm. C. Brown Publishers
Owen B., Raffety A. (2017) *Haliotis kamtschatkana* Jonas, 1845 - a Single Species, not a Pair of Subspecies. *The Festivus* **49**: 18-32.
Page R.D.M., Charleston M.A. (1997) From gene to organismal phylogeny: Reconciled trees and the gene tree species tree problem. *Mol Phylogenet Evol* **7**: 231-240.
Palme R., Rettenbacher S., Touma C., El-Bahr S.M., Möstl E. (2005) Stress Hormones in Mammals and Birds: Comparative Aspects Regarding Metabolism, Excretion, and Noninvasive Measurement in Fecal Samples. *Annals of the New York Academy of Sciences* **1040**: 162-171.
Penry D.L., Jumars P.A. (1987) Modeling Animal Guts as Chemical Reactors. *Am Nat* **129**: 69-96.
Picos-Garcia C., Garcia-Carreno F.L., Serviere-Zaragoza E. (2000) Digestive proteases in juvenile Mexican green abalone, Haliotis fulgens. *Aquaculture* **181**: 157-170.
Raimondi P.T., Wilson C.M., Ambrose R.F., Engle J.M., Minchinton T.E. (2002) Continued declines of black abalone along the coast of California: are mass mortalities related to El Nino events? *Mar Ecol Prog Ser* **242**: 143-152.
Register F. (2009) Endangered and Threatened Wildlife and Plants; Endangered Status for Black Abalone. In: Commerce D.o. (ed)
Rogers-Bennett L., Dondanville R.F., Moore J.D., Vilchis L.I. (2010) Response of Red Abalone Reproduction to Warm Water, Starvation, and Disease Stressors: Implications of Ocean Warming. *J Shellfish Res* **29**: 599-611.
Rohr J.R., Raffel T.R., Blaustein A.R., Johnson P.T.J., Paull S.H., Young S. (2013) Using physiology to understand climate-driven changes in disease and their implications for conservation. *Conservation Physiology* **1**.
Ronquist F., Teslenko M., van der Mark P., Ayres D.L., Darling A., Hohna S., Larget B., Liu L., Suchard M.A., Huelsenbeck J.P. (2012) MrBayes 3.2: Efficient Bayesian Phylogenetic Inference and Model Choice Across a Large Model Space. *Syst Biol* **61**: 539-542.
Rosenblum E.S., Viant M.R., Braid B.M., Moore J.D., Friedman C.S., Tjeerdema R.S. (2005) Characterizing the metabolic actions of natural stresses in the California red abalone, Haliotis rufescens using H-1 NMR metabolomics. *Metabolomics* **1**: 199-209.
Roznere I., Watters G.T., Wolfe B.A., Daly M. (2014) Nontargeted metabolomics reveals biochemical pathways altered in response to captivity and food limitation in the freshwater mussel Amblema plicata. *Comparative Biochemistry and Physiology Part D: Genomics and Proteomics* **12**: 53-60.
Sakurai T., Amemiya A., Ishii M., Matsuzaki I., Chemelli R.M., Tanaka H., Williams S.C., Richardson J.A., Kozlowski G.P., Wilson S., Arch J.R.S., Buckingham R.E., et al. (1998) Orexins and Orexin Receptors: A Family of Hypothalamic Neuropeptides and G Protein-Coupled Receptors that Regulate Feeding Behavior. *Cell* **92**: 573-585.
Santos A.J., Frederick A.R., Higgins B.A., Carrillo A., Carter A.L., Dickson K.A., German D.P., Horn M.H. (2018) The beach-spawning California grunion Leuresthes tenuis eats and digests conspecific eggs. *J Fish Biol* **93**: 282-289.

Sawabe T., Oda Y., Shiomi Y., Ezura Y. (1995) Alginate Degradation by Bacteria Isolated from the Gut of Sea-Urchins and Abalones. *Microbial Ecology* **30**: 193-202.
Schulz M.H., Zerbino D.R., Vingron M., Birney E. (2012) Oases: robust de novo RNA-seq assembly across the dynamic range of expression levels. *Bioinformatics* **28**: 1086-1092.
Smith P.K., Krohn R.I., Hermanson G.T., Mallia A.K., Gartner F.H., Provenzano M.D., Fujimoto E.K., Goeke N.M., Olson B.J., Klenk D.C. (1985) Measurement of Protein Using Bicinchoninic Acid. *Anal Biochem* **150**: 76-85.
Somero G.N. (2010) The physiology of climate change: how potentials for acclimatization and genetic adaptation will determine 'winners' and 'losers'. *Journal of Experimental Biology* **213**: 912-920.
Song X., Hu X., Sun B., Bo Y., Wu K., Xiao L., Gong C. (2017) A transcriptome analysis focusing on inflammation-related genes of grass carp intestines following infection with Aeromonas hydrophila. *Sci Rep-Uk* **7**: 40777.
Stanke M., Diekhans M., Baertsch R., Haussler D. (2008) Using native and syntenically mapped cDNA alignments to improve de novo gene finding. *Bioinformatics* **24**: 637-644.
Steinberg P.D. (1989) Biogeographical Variation in Brown Algal Polyphenolics and Other Secondary Metabolites - Comparison between Temperate Australasia and North-America. *Oecologia* **78**: 373-382.
Streit K., Geiger D.L., Lieb B. (2006) Molecular phylogeny and the geographic origin of Haliotidae traced by haemocyanin sequences. *J Mollus Stud* **72**: 105-110.
Stumpp M., Hu M., Casties I., Saborowski R., Bleich M., Melzner F., Dupont S. (2013) Digestion in sea urchin larvae impaired under ocean acidification. *Nat Clim Change* **3**: 1044.
Suzuki K., Ojima T., Nishita K. (2003) Purification and cDNA cloning of a cellulase from abalone Haliotis discus hannai. *Eur J Biochem* **270**: 771-778.
Swanson W.J., Aquadro C.F., Vacquier V.D. (2001) Polymorphism in abalone fertilization proteins is consistent with the neutral evolution of the egg's receptor for lysin (VERL) and positive Darwinian selection of sperm lysin. *Mol Biol Evol* **18**: 376-383.
Tracy C.R., Nussear K.E., Esque T.C., Dean-Bradley K., Tracy C.R., DeFalco L.A., Castle K.T., Zimmerman L.C., Espinoza R.E., Barber A.M. (2006) The importance of physiological ecology in conservation biology. *Integr Comp Biol* **46**: 1191-1205.
Vacquier V.D., Lee Y.H. (1993) Abalone sperm lysin: unusual mode of evolution of a gamete recognition protein. *Zygote* **1**: 181-196.
Vanblaricom G.R., Ruediger J.L., Friedman C.S., Woodard D.D., Hedrick R.P. (1993) Discovery of Withering Syndrome among Black Abalone Haliotis-Cracherodii Leach, 1814, Populations at San-Nicolas Island, California. *J Shellfish Res* **12**: 185-188.
Vilchis L.I., Tegner M.J., Moore J.D., Friedman C.S., Riser K.L., Robbins T.T., Dayton P.K. (2005) Ocean warming effects on growth, reproduction, and survivorship of Southern California abalone. *Ecological Applications* **15**: 469-480.
Vorhees A.S., Gray E.M., Bradley T.J. (2013) Thermal resistance and performance correlate with climate in populations of a widespread mosquito. *Physiological and biochemical zoology : PBZ* **86**: 73.
Wang Y., Zhang H., Lu Y., Wang F., Liu L., Liu J., Liu X. (2017) Comparative transcriptome analysis of zebrafish (Danio rerio) brain and spleen infected with spring viremia of carp virus (SVCV). *Fish Shellfish Immun* **69**: 35-45.

Wildlife C.D.o.F.a. (2016-2017) Life History Information for Selected California Marine Invertebrates and Plants: Invertebrates

Yang Z.H., Swanson W.J., Vacquier V.D. (2000) Maximum-likelihood analysis of molecular adaptation in abalone sperm lysin reveals variable selective pressures among lineages and sites. *Mol Biol Evol* **17**: 1446-1455.

Zerbino D.R., Birney E. (2008) Velvet: Algorithms for de novo short read assembly using de Bruijn graphs. *Genome Res* **18**: 821-829.